

AD-A207 845

NAVAL POSTGRADUATE SCHOOL

Monterey, California



THESIS

CONSIDERATION OF GRAVITY GRADIENT
STABILIZATION FOR ORION

by

Frank W. Boyd

March 1989

Thesis Advisor:

Harold A. Titus

Approved for public release; distribution is unlimited.

DTIC
ELECTE
MAY 18 1989
S H D
Cb

63 0 13 040

Unclassified

security classification of this page

REPORT DOCUMENTATION PAGE

1a Report Security Classification Unclassified			1b Restrictive Markings		
2a Security Classification Authority			3 Distribution Availability of Report		
2b Declassification Downgrading Schedule			Approved for public release; distribution is unlimited.		
4 Performing Organization Report Number(s)			5 Monitoring Organization Report Number(s)		
6a Name of Performing Organization Naval Postgraduate School		6b Office Symbol (if applicable) 32	7a Name of Monitoring Organization Naval Postgraduate School		
6c Address (city, state, and ZIP code) Monterey, CA 93943-5000			7b Address (city, state, and ZIP code) Monterey, CA 93943-5000		
8a Name of Funding Sponsoring Organization		8b Office Symbol (if applicable)	9 Procurement Instrument Identification Number		
8c Address (city, state, and ZIP code)			10 Source of Funding Numbers		
			Program Element No	Project No	Task No
			Work Unit Accession No		
11 Title (include security classification) CONSIDERATION OF GRAVITY GRADIENT STABILIZATION FOR ORION					
12 Personal Author(s) Frank W. Boyd					
13a Type of Report Master's Thesis		13b Time Covered From To		14 Date of Report (year, month, day) March 1989	
				15 Page Count 99	
16 Supplementary Notation The views expressed in this thesis are those of the author and do not reflect the official policy or position of the Department of Defense or the U.S. Government.					
17 Cosati Codes			18 Subject Terms (continue on reverse if necessary and identify by block number)		
Field	Group	Subgroup	ORION, Attitude control, gravity gradient.		
19 Abstract (continue on reverse if necessary and identify by block number)					
<p>Certain ORION missions may require three axis stabilization. Since ORION's physical size severely limits its onboard fuel storage capability, passive stabilization techniques warrant investigation. This paper shows the development of linearized equations of motion and regions of stability with respect to gravity gradient stabilization. Gravity gradient stabilization by itself provides little yaw restoring torque; therefore, additional torque generating devices are necessary to augment the gravity gradient effect. Control moment gyros, reaction wheels, and magnetic torquers will be investigated as to their suitability for ORION.</p>					
20 Distribution Availability of Abstract			21 Abstract Security Classification		
<input checked="" type="checkbox"/> unclassified unlimited <input type="checkbox"/> same as report <input type="checkbox"/> DTIC users			Unclassified		
22a Name of Responsible Individual Harold A. Titus			22b Telephone (include Area code) (408) 646-2768		22c Office Symbol 62Ts

DD FORM 1473,84 MAR

83 APR edition may be used until exhausted
All other editions are obsolete

security classification of this page

Unclassified

Approved for public release; distribution is unlimited.

Consideration of Gravity Gradient Stabilization for ORION

by

Frank W. Boyd
Lieutenant, United States Navy
B.A., University of California, Los Angeles, 1982

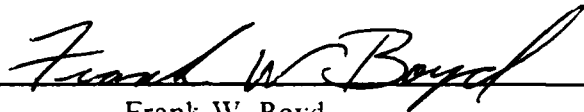
Submitted in partial fulfillment of the
requirements for the degree of

MASTER OF SCIENCE IN ELECTRICAL ENGINEERING

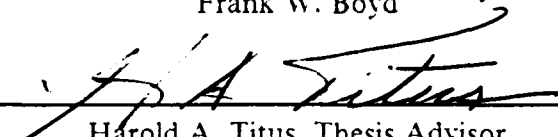
from the

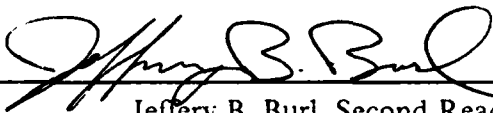
NAVAL POSTGRADUATE SCHOOL
March 1989


Author:



Frank W. Boyd

Approved by:


Harold A. Titus, Thesis Advisor


Jeffery B. Burl, Second Reader


John P. Powers, Chairman,
Department of Electrical Engineering


Gordon E. Schacher,
Dean of Science and Engineering

ABSTRACT

Certain ORION missions may require three axis stabilization. Since ORION's physical size severely limits its onboard fuel storage capability, passive stabilization techniques warrant investigation. This paper shows the development of linearized equations of motion and regions of stability with respect to gravity gradient stabilization. Gravity gradient stabilization by itself provides little yaw restoring torque; therefore, additional torque generating devices are necessary to augment the gravity gradient effect. Control moment gyros, reaction wheels, and magnetic torquers will be investigated as to their suitability for ORION.



Accession For	
NTIS GRA&I	<input checked="" type="checkbox"/>
DTIC TAB	<input type="checkbox"/>
Unannounced	<input type="checkbox"/>
Justification	
By _____	
Distribution/	
Availability Codes	
Dist	Avail and/or Special
A-1	

TABLE OF CONTENTS

I. INTRODUCTION	1
A. BACKGROUND ON ORION	1
1. Background on attitude control	2
II. GRAVITY GRADIENT STABILIZATION THEORY	5
A. COORDINATE DEFINITION	5
B. COORDINATE TRANSFORMATION	6
1. Direction cosines method	6
2. Quaternions	7
3. Euler angles method	9
C. RIGID BODY EQUATIONS	13
1. Derivative of a Vector in a Rotating Coordinate System	13
2. General Particle Motion	14
3. Momentum of a Rigid Body	15
4. Equations of motion/Euler's Moment Equations	17
D. GRAVITY GRADIENT EFFECT	20
E. DESIGN FOR STABILITY	23
1. Stability and Frequency Analysis	23
III. ENVIRONMENTAL DISTURBANCES AND RESTORING TORQUES ..	27
A. ENVIRONMENTAL DISTURBANCES/TORQUES	27
1. Aerodynamic disturbance	27
a. Drag	27
b. Aerodynamic torque	27
2. Rigid Body Solar Pressure Torque	30
B. RESTORING TORQUES	31
1. Thrusters	31
2. Momentum Exchange Devices	32
a. Reaction wheels	33
3. CMG(s)	35
4. Magnetic torquers	35

IV. CHAPTER 4	39
A. GRAVITY GRADIENT STABILIZATION RESULTS	39
1. Attitude Control	39
2. Various results based on different configurations	39
a. Effects of extending booms	39
b. Gravity gradient effect alone	39
c. Effects of Reaction Wheel(s)	42
d. Effects of Magnetic torquers	58
3. Gravity Gradient capture (from tumbling mode)	79
V. CHAPTER 5	81
A. CONCLUSIONS	81
1. Gravity gradient stabilization (only)	81
2. Gravity gradient with 3 reaction wheels	81
a. Advantages	81
b. Disadvantages	81
3. Control moment gyro (CMG)	81
a. Advantages	81
b. Disadvantages	81
4. Gravity gradient with three magnetic torquers	82
a. Advantages	82
b. Disadvantages	82
5. Thrusters	82
a. Advantages	82
b. Disadvantages	82
6. Overview	82
APPENDIX GRADIENT STABILIZATION PROGRAM	84
LIST OF REFERENCES	89
INITIAL DISTRIBUTION LIST	90

LIST OF FIGURES

Figure 1. Nasa Get-Away-Special (GAS) Cannister [Ref. 1, p. 30]	1
Figure 2. Cross section of GAS Cannister [Ref. 1, p. 42]	2
Figure 3. Summary of typical Navy STP payload requirements	3
Figure 4. Passive Stabilization Methods [Ref. 4, p. 19]	4
Figure 5. Active Stabilization Methods [Ref. 4, p. 19]	4
Figure 6. Coordinate Definition for Gravity Gradient Systems	5
Figure 7. Coordinate Transformation Methods [Ref. 4, p. 412]	6
Figure 8. Rotation about the Euler Axis	7
Figure 9. Euler Angles	10
Figure 10. Rotation about the Z axis through the Angle	10
Figure 11. Table of Euler angle combinations [Ref. 4, p. 764]	12
Figure 12. Vector in a rotating system [Ref. 6, p. 107]	13
Figure 13. Translational motion of a particle [Ref. 6, p. 107]	14
Figure 14. Gravity gradient torque [Ref. 6, p. 113]	21
Figure 15. Gravity Gradient torque Magnitudes vs Altitude [Ref. 3, p. 58]	23
Figure 16. Gravity Gradient Stability Regions	26
Figure 17. Environmental Disturbance Torques [Ref. 4, p. 17]	27
Figure 18. Aerodynamic effects for cylindrical satellite [Ref. 3, p. 58]	28
Figure 19. Aerodynamic pressure as a function of altitude [Ref. 8, p. 456]	29
Figure 20. Aerodynamic torque for a 1 inch offset as a function of altitude.	30
Figure 21. Rigid body solar pressure torques [Ref. 3, p. 61]	31
Figure 22. Fuel required for orbit transfer based on a 250lb satellite. [Ref 2, p. 23]	32
Figure 23. 3 axis reaction wheel control scheme [Ref. 6, p. 149]	34
Figure 24. Twin gyro controller with one drive motor [Ref. 8, p. 415]	35
Figure 25. Magnetic Moment Due to a Current Loop [Ref. 4, p. 204]	36
Figure 26. Some existing magnetic moment schemes [Ref. 3, p. 205]	37
Figure 27. Earth's magnetic field modeled as a tilted dipole [Ref. 6, p. 148]	37
Figure 28. Effect of extending boom on moments of inertia	40
Figure 29. Gravity gradient effect only $I_x = 15$, $I_y = 18$, $I_z = 3$	41
Figure 30. Gravity gradient effect only $I_x = 95$, $I_y = 98$, $I_z = 3$	42
Figure 31. Teldrix Reaction Wheel Technical Data	43

Figure 32. Bendix Aerospace Reaction Wheel Technical Data.	44
Figure 33. Gravity gradient effect with 3 RW (X axis) $I_x = 15$, $I_y = 18$, $I_z = 3$	45
Figure 34. Gravity gradient effect with 3 RW (Y axis) $I_x = 15$, $I_y = 18$, $I_z = 3$	46
Figure 35. Gravity gradient effect with 3 RW (Z axis) $I_x = 15$, $I_y = 18$, $I_z = 3$	47
Figure 36. Gravity gradient effect with 3 RW (X axis) $I_x = 95$, $I_y = 98$, $I_z = 3$	48
Figure 37. Gravity gradient effect with 3 RW (Y axis) $I_x = 95$, $I_y = 98$, $I_z = 3$	49
Figure 38. Gravity gradient effect with 3 RW (Z axis) $I_x = 95$, $I_y = 98$, $I_z = 3$	50
Figure 39. Gravity gradient effect with 3 RW (X axis) $I_x = 15$, $I_y = 18$, $I_z = 3$	52
Figure 40. Gravity gradient effect with 3 RW (Y axis) $I_x = 15$, $I_y = 18$, $I_z = 3$	53
Figure 41. Gravity gradient effect with 3 RW (Z axis) $I_x = 15$, $I_y = 18$, $I_z = 3$	54
Figure 42. Gravity gradient effect with 3 RW (X axis) $I_x = 95$, $I_y = 98$, $I_z = 3$	55
Figure 43. Gravity gradient effect with 3 (Y axis) RW $I_x = 95$, $I_y = 98$, $I_z = 3$	56
Figure 44. Gravity gradient effect with 3 RW (Z axis) $I_x = 95$, $I_y = 98$, $I_z = 3$	57
Figure 45. Gravity gradient with magnetic torquing (X axis)	60
Figure 46. Gravity gradient with magnetic torquing (Y axis)	61
Figure 47. Gravity gradient with magnetic torquing (Z axis)	62
Figure 48. Gravity gradient with magnetic torquing (X axis)	63
Figure 49. Gravity gradient with magnetic torquing (Y axis)	64
Figure 50. Gravity gradient with magnetic torquing (Z axis)	65
Figure 51. Gravity gradient with magnetic torquing (X axis)	67
Figure 52. Gravity gradient with magnetic torquing (Y axis)	68
Figure 53. Gravity gradient with magnetic torquing (Z axis)	69
Figure 54. Gravity gradient with magnetic torquing (X axis)	70
Figure 55. Gravity gradient with magnetic torquing (Y axis)	71
Figure 56. Gravity gradient with magnetic torquing (Z axis)	72
Figure 57. Gravity gradient with magnetic torquing (X axis)	73
Figure 58. Gravity gradient with magnetic torquing (Y axis)	74
Figure 59. Gravity gradient with magnetic torquing (Z axis)	75
Figure 60. Gravity gradient with magnetic torquing (X AXIS)	76
Figure 61. Gravity gradient with magnetic torquing (Y AXIS)	77
Figure 62. Gravity gradient with magnetic torquing (Z AXIS)	78
Figure 63. Gravity gradient capture by extension of boom	80

I. INTRODUCTION

A. BACKGROUND ON ORION

The philosophy behind the design and development of the Orion satellite is being driven in part by economic considerations. Small, affordable, general purpose satellites must be developed without sacrificing reliability. The preliminary groundwork on the feasibility of the ORION concept and design is detailed in [Ref. 1].

Orion is currently being designed to be launched from a Get Away Special (GAS) cannister aboard the Space Shuttle. The GAS cannister physically limits the size of ORION to approximately 35" in height and 19" in diameter. Figure 1 shows the Get-Away Special Cannister attached to the side of the shuttle bay.

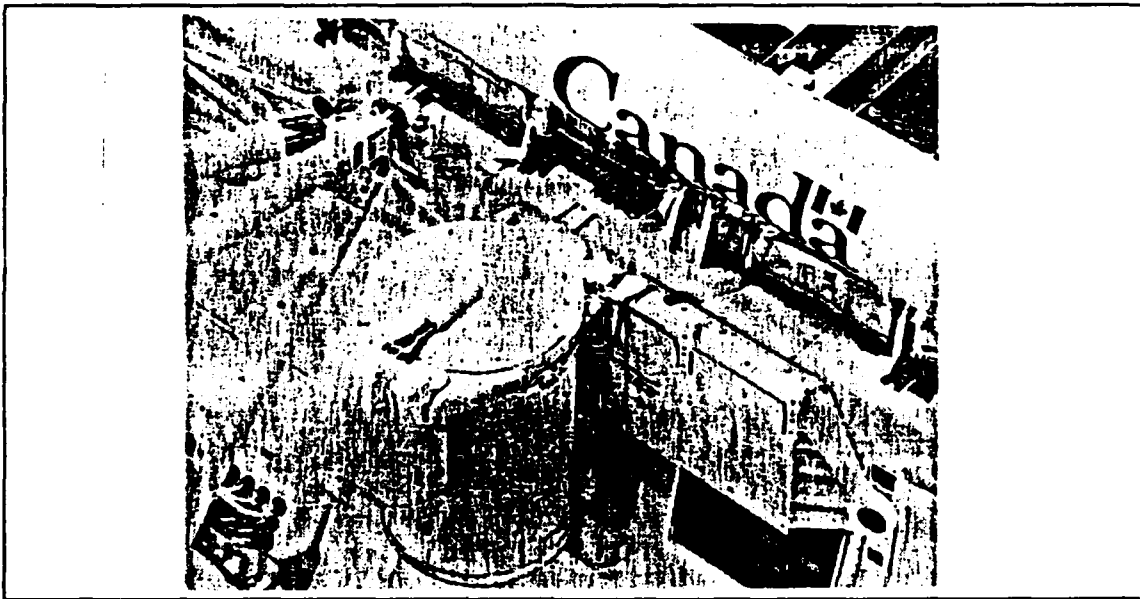


Figure 1. NASA Get-Away-Special (GAS) Cannister [Ref. 1, p. 30]

The Get-Away-Special (GAS) Cannister is designed to launch its satellite autonomously on command. A cross sectional view of the (GAS) Cannister is shown in Figure 2 on page 2.

ORION should be able to meet the requirements of standard or typical payloads. Some of these requirements are listed by Reference 2 and given in Figure 3 on page 3.

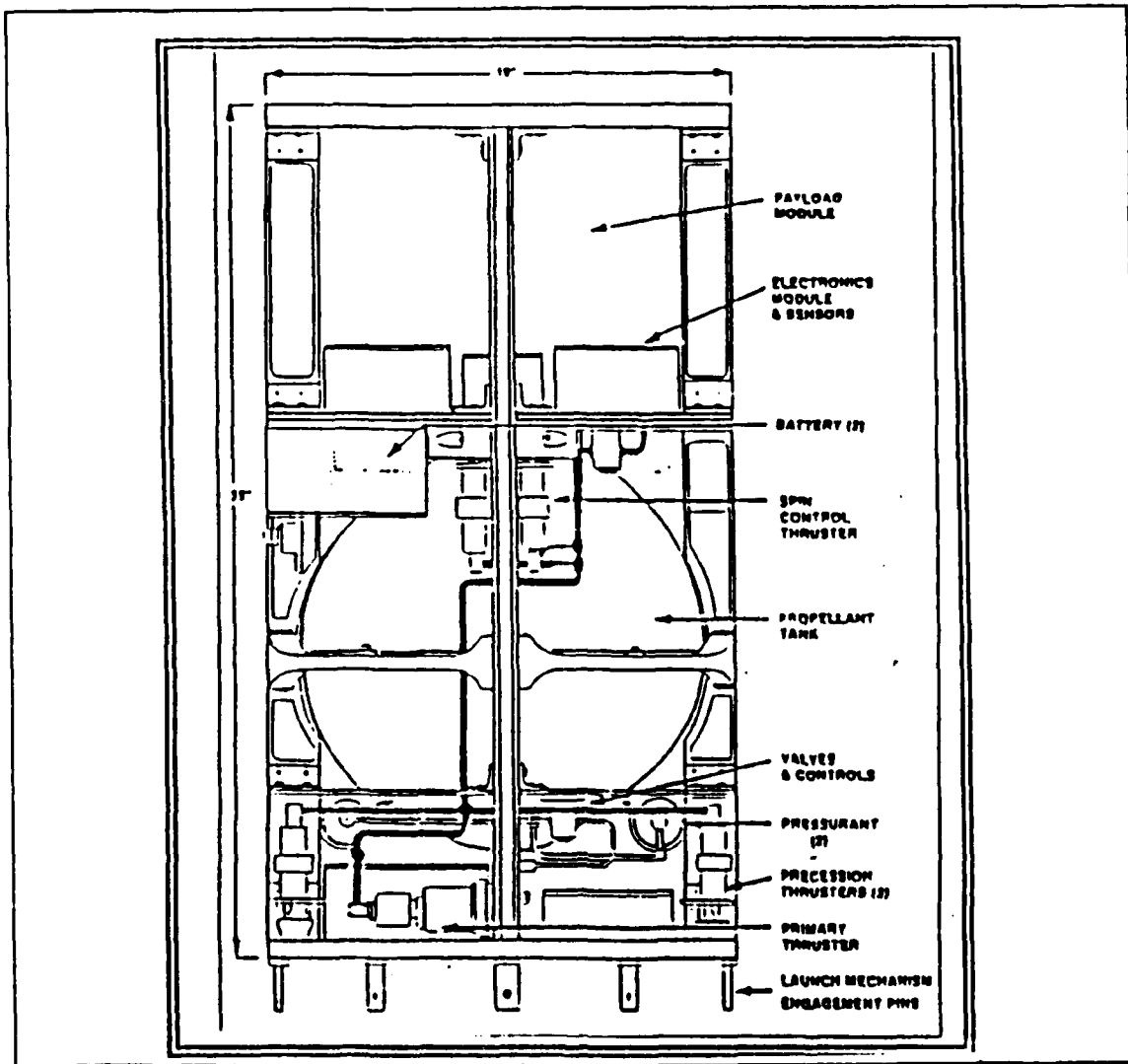


Figure 2. Cross section of GAS Cannister [Ref. 1, p. 42]

1. Background on attitude control

The success of any satellite is dependent on its attitude control system. To be mission capable, the vehicle must first acquire a desired or specified orientation in space, and then maintain this orientation within mission limits given such external factors as magnetic fields, aerodynamic drag, solar pressure, gravitational effects, and other disturbances. Deviations from desired orientations are detected through the use of sensors.

Considerations for an attitude control system include:

- (1) pointing accuracy
- (2) fuel consumption
- (3) thermal
- (4) power constraints
- (5) satellite lifetime
- (6) response time

Mass	32 lbm
Volume	2.36 ft ³
Power	34 watts
DataRate	5000 bits/sec
Orbit	200-800 nm circular
Inclination	0°-30° or 60°-120°
Instruments	Particle counter or Lens

Figure 3. Summary of typical Navy/STP payload requirements

The weight given to each of these considerations ultimately lies in the specific mission requirements designated for each satellite. The direction of this thesis will be to investigate the feasibility of achieving sufficient performance utilizing a gravity gradient control system. The standard of ± 1 degree for each axis will be used. This criteria is sufficient to enable ORION to satisfy most STP (space test program) mission requirements.[Ref. 1, p. 93]

To achieve stabilization, many methods of generating controlling torques have been developed. These methods are divided into either active or passive categories. Each of these categories has their relative advantages and disadvantages [Figure 4 on page 4 and Figure 5 on page 4].

In this study, the primary focus is on a gravity gradient stabilization augmented by other torque generating devices to achieve the desired ± 1 degree goal for each axis. A discussion of the equations of motion and gravity gradient stabilization theory is presented in Chapter 2. Disturbance torques and other torque generating devices are discussed in Chapter 3. Chapter 4 presents the results of stabilization schemes derived in Chapters 2 and 3. Observations and conclusions are discussed in Chapter 5.

METHOD	ADVANTAGES	DISADVANTAGES
SPIN STABILIZED	SIMPLE, EFFECTIVE NEARLY ANYWHERE IN ANY ORIENTATION, MAINTAINS ORIENTATION IN INERTIAL SPACE	CENTRIFUGAL FORCE REQUIRES STRUCTURAL STABILITY AND SOME RIGIDITY. SENSORS AND ANTENNAS CANNOT GENERALLY REMAIN POINTED AT A SPECIFIC INERTIAL TARGET. Wobble (NUTATION) IF NOT PROPERLY BALANCED. DRIFT DUE TO ENVIRONMENTAL TORQUES.
GRAVITY-GRADIENT STABILIZED	MAINTAINS STABLE ORIENTATION RELATIVE TO CENTRAL BODY. NOT SUBJECT TO DECAY OR DRIFT DUE TO ENVIRONMENTAL TORQUES UNLESS ENVIRONMENT CHANGES.	LIMITED TO 1 OR 2 POSSIBLE ORIENTATIONS. EFFECTIVE ONLY NEAR MASSIVE CENTRAL BODY (E.G., EARTH, MOON, ETC.). REQUIRES LONG BOOMS OR ELONGATED MASS DISTRIBUTION. SUBJECT TO Wobble (LIBRATION). CONTROL LIMITED TO ~1 DEG. PROBLEM OF THERMAL GRADIENTS ACROSS BOOM.
SOLAR RADIATION STABILIZED	CONVENIENT FOR POWER GENERATION BY SOLAR CELLS OR SOLAR STUDIES.	LIMITED TO HIGH-ALTITUDE OR INTERPLANETARY ORBITS. LIMITED ORIENTATIONS ALLOWED.
AERODYNAMIC STABILIZED MAGNETIC STABILIZED WITH PERMANENT MAGNET	{ SPECIAL PURPOSE METHODS - HIGHLY MISSION AND STRUCTURE DEPENDENT IN ALL OF THEIR CHARACTERISTICS }	

Figure 4. Passive Stabilization Methods [Ref. 4, p. 19]

METHOD	ADVANTAGES	DISADVANTAGES
GAS JETS	FLEXIBLE AND FAST. USED IN ANY ENVIRONMENT; POWERFUL.	USES CONSUMABLE (FUEL) WITH LIMITED SUPPLY AVAILABLE DUE TO FUEL WEIGHT. TOO POWERFUL FOR SOME APPLICATIONS (I.E., RELATIVELY COARSE CONTROL). COMPLEX AND EXPENSIVE PLUMBING SUBJECT TO FAILURE.
MAGNETIC (ELECTROMAGNETS)	USUALLY LOW POWER. MAY BE DONE WITHOUT USING CONSUMABLES BY USE OF SOLAR POWER.	SLOW. NEAR EARTH ONLY. APPLICABILITY LIMITED BY DIRECTION OF THE EXTERNAL MAGNETIC FIELD. COARSE CONTROL ONLY (BECAUSE OF MAGNETIC FIELD MODEL UNCERTAINTIES AND LONG TIME CONSTANTS).
REACTION WHEELS*	PARTICULARLY GOOD FOR VARIABLE SPIN RATE CONTROL. FAST, FLEXIBLE, PRECISE ATTITUDE CONTROL AND/OR STABILIZATION.	REQUIRES RAPIDLY MOVING PARTS WHICH IMPLIES PROBLEMS OF SUPPORT AND FRICTION. MAY NEED SECOND CONTROL SYSTEM TO CONTROL OVERALL ANGULAR MOMENTUM (MOMENTUM DUMPING) IN RESPONSE TO CUMULATIVE CHANGES BY ENVIRONMENTAL TORQUES. EXPENSIVE.
ALTERNATIVE THRUSTERS (ION OR ELECTRIC) ACTIVE SOLAR, AERODYNAMIC, OR GRAVITY GRADIENT	{ PRIMARILY SPECIAL PURPOSE - LESS EXPERIENCE WITH THESE THAN WITH THOSE LISTED ABOVE. CHARACTERISTICS ARE HIGHLY MISSION DEPENDENT. SOME SYSTEMS MAY SEE MORE USE IN THE FUTURE AS FURTHER EXPERIENCE IS GAINED }	

*REFERS TO ANY DEVICE THAT MAY BE USED IN A PROCESS TO EXCHANGE ANGULAR MOMENTUM WITH THE SPACECRAFT BODY

Figure 5. Active Stabilization Methods [Ref. 4, p. 19]

II. GRAVITY GRADIENT STABILIZATION THEORY

A. COORDINATE DEFINITION

Before beginning any discussion on attitude control a means of defining the coordinate system is necessary. The standardized coordinate axes for gravity gradient systems are as follows: the x axis points in the direction of satellite motion, the y axis is normal to the orbit plane, and the z axis points towards earth's geocenter. These axes correspond to the roll, pitch and yaw axes, respectively. Figure 6 from Reference 3 defines roll (ϕ), pitch (θ), and yaw (ψ) attitude errors as well as showing the standardized coordinate system.

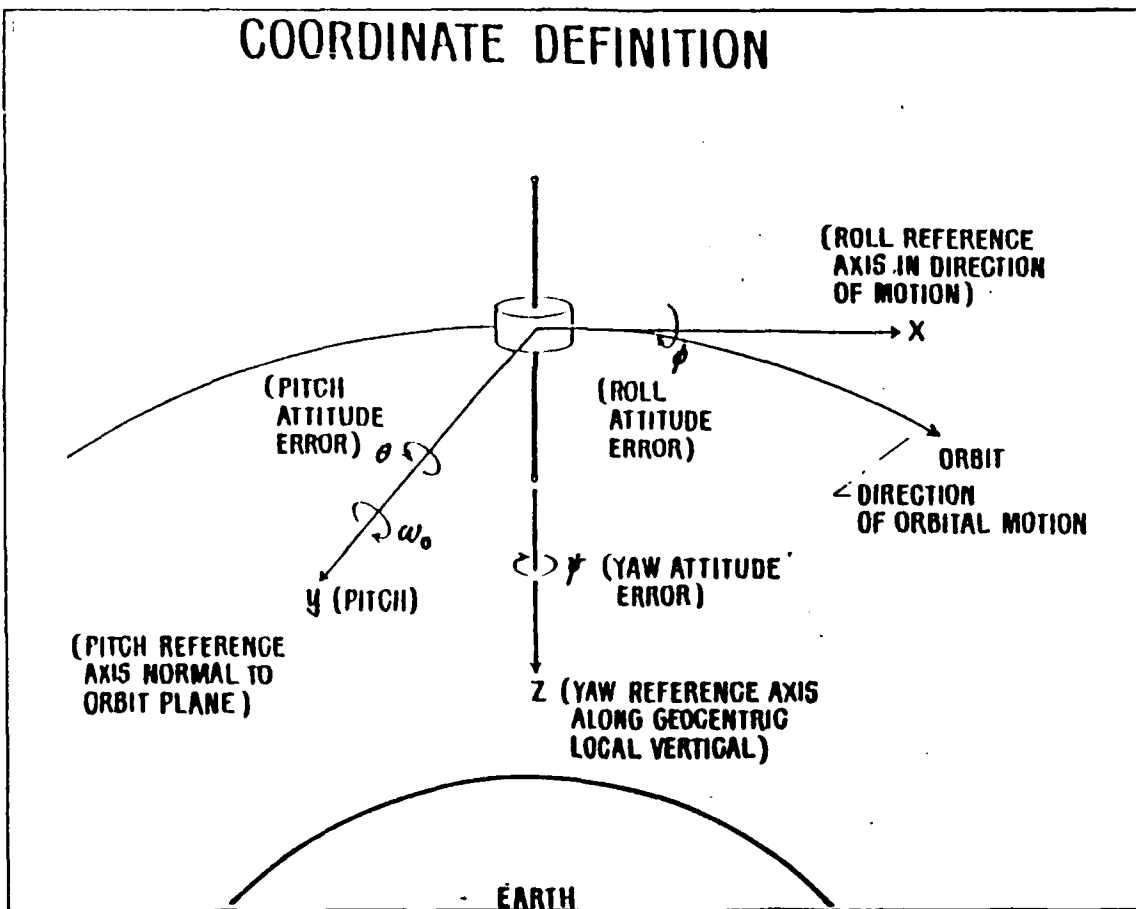


Figure 6. Coordinate Definition for Gravity Gradient Systems

B. COORDINATE TRANSFORMATION

The relationship between two coordinate systems is essential for attitude control. There are methods available to describe this relationship of which directional cosines, quaternions, and Euler angles will be briefly discussed. Figure 7 on page 6 shows various methods of coordinate transformations along with their respective advantages and disadvantages.

PARAMETERIZATION	NOTATION	ADVANTAGES	DISADVANTAGES	COMMON APPLICATIONS
DIRECTION COSINE MATRIX	$A = [A_{ij}]$	NO SINGULARITIES NO TRIGONOMETRIC FUNCTIONS CONVENIENT PRODUCT RULE FOR SUCCESSIVE ROTATIONS	SIX REDUNDANT PARAMETERS	IN ANALYSIS TO TRANSFORM VECTORS FROM ONE REFERENCE FRAME TO ANOTHER
EULER AXIS/ANGLE	α, ϕ	CLEAR PHYSICAL INTERPRETATION	ONE REDUNDANT PARAMETER AXIS UNDEFINED WHEN $\sin \phi = 0$ TRIGONOMETRIC FUNCTIONS	COMMANDING SLEW MANEUVERS
EULER SYMMETRIC PARAMETERS (QUATERNION)	q_1, q_2, q_3, q_4 (4)	NO SINGULARITIES NO TRIGONOMETRIC FUNCTIONS CONVENIENT PRODUCT RULE FOR SUCCESSIVE ROTATIONS	ONE REDUNDANT PARAMETER NO OBVIOUS PHYSICAL INTERPRETATION	ONBOARD INERTIAL NAVIGATION
GIBBS VECTOR	\mathbf{g}	NO REDUNDANT PARAMETERS NO TRIGONOMETRIC FUNCTIONS CONVENIENT PRODUCT RULE FOR SUCCESSIVE ROTATIONS	INFINITE FOR 180-DEG ROTATION	ANALYTIC STUDIES
EULER ANGLES	ϕ, θ, ψ	NO REDUNDANT PARAMETERS PHYSICAL INTERPRETATION IS CLEAR IN SOME CASES	TRIGONOMETRIC FUNCTIONS SINGULARITY AT SOME θ NO CONVENIENT PRODUCT RULE FOR SUCCESSIVE ROTATIONS	ANALYTIC STUDIES INPUT/OUTPUT ONBOARD ATTITUDE CONTROL OF 3-AXIS STABILIZED SPACECRAFT

Figure 7. Coordinate Transformation Methods [Ref. 4, p. 412]

1. Direction cosines method

The directional cosine method involves a 3×3 rotation matrix A_{ij} where

$$A_{ij} = \begin{bmatrix} A_{11} & A_{12} & A_{13} \\ A_{21} & A_{22} & A_{23} \\ A_{31} & A_{32} & A_{33} \end{bmatrix} = \begin{bmatrix} X \cdot x & X \cdot y & X \cdot z \\ Y \cdot x & Y \cdot y & Y \cdot z \\ Z \cdot x & Z \cdot y & Z \cdot z \end{bmatrix} \quad (1)$$

where

$$\begin{aligned} X \cdot x &= \cos \theta \cos \psi \\ X \cdot y &= \cos \psi \sin \theta \sin \phi + \sin \psi \cos \phi \\ X \cdot z &= \sin \psi \sin \phi - \cos \psi \sin \theta \cos \phi \\ Y \cdot x &= -\sin \psi \cos \theta \\ Y \cdot y &= \cos \phi \cos \psi - \sin \psi \sin \theta \sin \phi \\ Y \cdot z &= \sin \psi \sin \theta \cos \phi + \cos \psi \sin \phi \\ Z \cdot x &= \sin \theta \\ Z \cdot y &= -\cos \theta \sin \phi \\ Z \cdot z &= \cos \phi \cos \theta \end{aligned}$$

2. Quaternions

The quaternion method or as it is sometimes called, the Euler Symmetric Parameter method, uses the Euler axis and rotation angle (a single rotation angle α about a single axis \hat{E}) method to describe the relationship between two coordinate systems [Figure 8 on page 7].

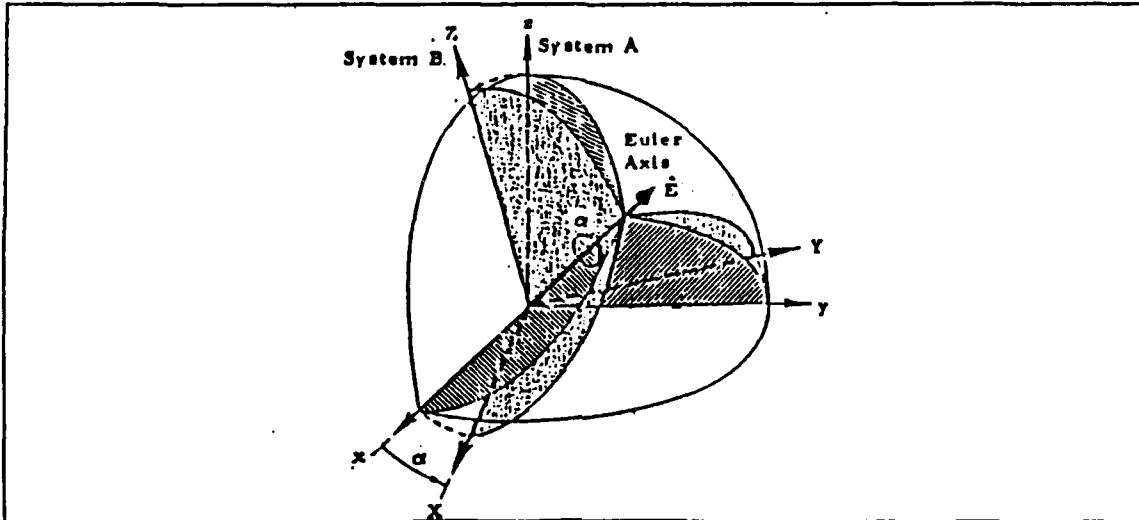


Figure 8. Rotation about the Euler Axis

The quaternion is a four component vector containing the same information as the Euler angle/axis transformation in which one coordinate axis is related to another and is of the form

$$q = [q_1 i, q_2 j, q_3 k, q_4] \quad (3)$$

where

$$\begin{aligned} q_1 &= E_x \sin \frac{\alpha}{2} \\ q_2 &= E_y \sin \frac{\alpha}{2} \\ q_3 &= E_z \sin \frac{\alpha}{2} \\ q_4 &= \cos \frac{\alpha}{2} \end{aligned}$$

The symbols i , j , and k satisfy the following conditions [Ref. 4, p. 758]

$$i^2 = j^2 = k^2 = 1$$

$$ij = -ji = k$$

$$jk = -kj = i$$

$$ki = -ik = j$$

and

$$q_1^2 + q_2^2 + q_3^2 + q_4^2 = 1$$

When used for control purposes, [Ref 5] defines the first three elements of the quaternion (q_1, q_2, q_3) as the respective roll, pitch, and yaw rotational errors:

$$\begin{aligned} [\varepsilon_{roll}, \varepsilon_{pitch}, \varepsilon_{yaw}] &= 2[q_1, q_2, q_3] \\ &= 2\left[E_x \sin \frac{\alpha}{2}, E_y \sin \frac{\alpha}{2}, E_z \sin \frac{\alpha}{2}\right] \\ &\approx [\alpha E_x, \alpha E_y, \alpha E_z] \end{aligned} \quad (7)$$

The primary advantage of the quaternion method is that the computational time can be reduced by more than 40% over the equivalent directional cosine matrix solution in operations that require successive coordinate system rotations [Ref 5]. The transformation from coordinate system A to coordinate system B can be described by the quaternion $q = [q_1i, q_2j, q_3k, q_4]$, and the second transformation from system B to C can be described by $q' = [q'_1i, q'_2j, q'_3k, q'_4]$. The transformation from system A to system C may be described by the quaternion $q'' = [q''_1i, q''_2j, q''_3k, q''_4]$ where

$$q'' = qq' = (q_1i + q_2j + q_3k + q_4)(q'_1i + q'_2j + q'_3k + q'_4) \quad (8)$$

Multiplying out and substituting in the conditions stated above, the matrix form becomes

$$\begin{bmatrix} q''_1 \\ q''_2 \\ q''_3 \\ q''_4 \end{bmatrix} = \begin{bmatrix} q'_4 & q'_3 & -q'_2 & q'_1 \\ -q'_3 & q'_4 & q'_1 & q'_2 \\ q'_2 & -q'_1 & q'_4 & q'_3 \\ -q'_1 & -q'_2 & -q'_3 & q'_4 \end{bmatrix} \begin{bmatrix} q_1 \\ q_2 \\ q_3 \\ q_4 \end{bmatrix} \quad (9)$$

Because of the quaternion property of interchangeability, a total of 16 multiplications and 12 additions are required to completely define the quaternion describing the transformation from coordinate system A to coordinate system C. To accomplish the same

transformation using directional cosines would require multiplying two 3×3 matrices, involving 27 multiplications and 18 additions. The computational time savings for successive rotations transformations becomes apparent. The major drawback for the use of quaternions is that the numbers of the quaternion do not physically represent the transformation from one system to another.

3. Euler angles method

The Euler angles utilize three different rotations (angles), defining the orientation of a body with respect to an inertial reference frame. These angles are defined as ϕ (about the x axis), θ (about the y axis), and ψ (about the z axis). These axes, by established convention, may also be referred to as 1 (for x), 2 (for y), and 3 (for z) axes, respectively.

The 321 Euler transformation described below starts with the inertial coordinate system XYZ. Figure 9 on page 10.a. shows the first rotation about the Z axis through an angle ψ , which produces x_1y_1Z . Figure 9 on page 10.b. shows the rotation of θ about y_1 , producing $x_1y_1z_1$. Figure 9 on page 10.c., showing the rotation of ϕ about x, produces xyz. The rotation described in Figure 9 on page 10.a. about the z axis produces Figure 10 on page 10. The transformation from XYZ to x_1y_1Z is

$$\begin{aligned}x_1 &= X \cos \psi + Y \sin \psi \\y_1 &= -X \sin \psi + Y \cos \psi \\Z &= Z\end{aligned}$$

or written in matrix form

$$\begin{bmatrix} x_1 \\ y_1 \\ Z \end{bmatrix} = \begin{bmatrix} \cos \psi & \sin \psi & 0 \\ -\sin \psi & \cos \psi & 0 \\ 0 & 0 & 1 \end{bmatrix} \begin{bmatrix} X \\ Y \\ Z \end{bmatrix} \quad (11)$$

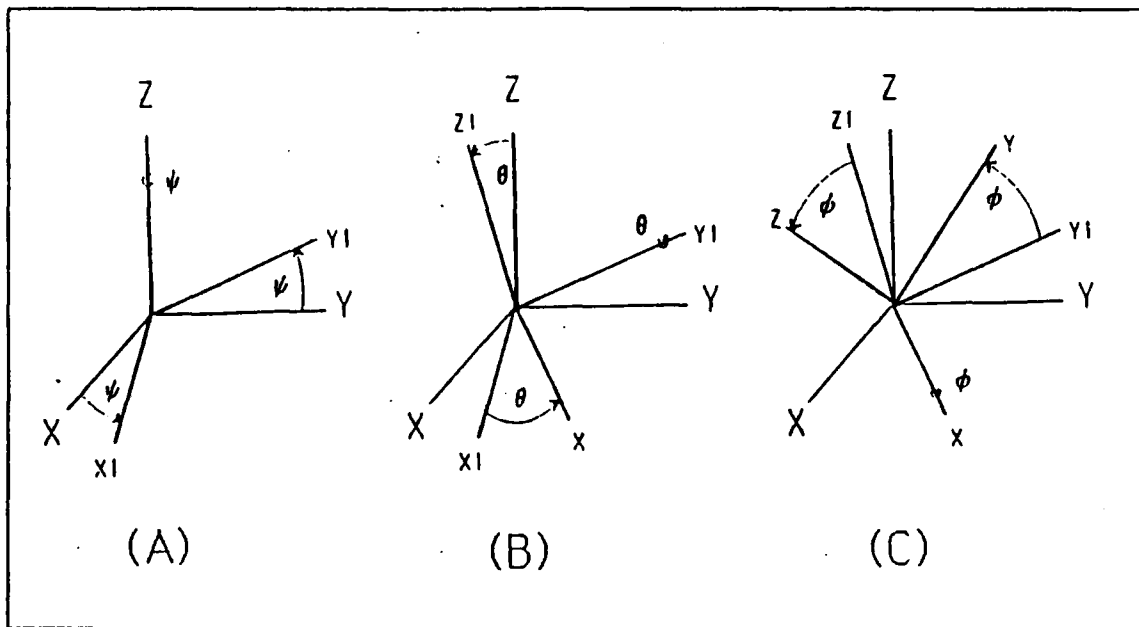


Figure 9. Euler Angles

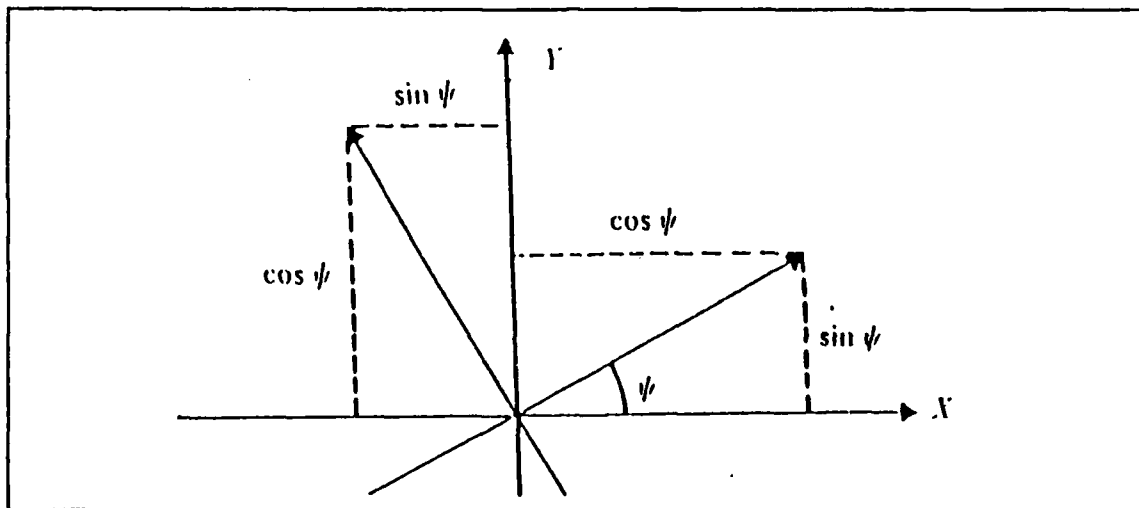


Figure 10. Rotation about the Z axis through the Angle ψ

Writing the transformations of Figures 9.b. and 9.c. in matrix form yields

$$\begin{bmatrix} x \\ y_1 \\ z_1 \end{bmatrix} = \begin{bmatrix} \cos \theta & 0 & -\sin \theta \\ 0 & 1 & 0 \\ \sin \theta & 0 & \cos \theta \end{bmatrix} \begin{bmatrix} x_1 \\ y_1 \\ Z \end{bmatrix} \quad (12)$$

and

$$\begin{bmatrix} x \\ y \\ z \end{bmatrix} = \begin{bmatrix} 1 & 0 & 0 \\ 0 & \cos \phi & \sin \phi \\ 0 & -\sin \phi & \cos \phi \end{bmatrix} \begin{bmatrix} x_1 \\ y_1 \\ z_1 \end{bmatrix} \quad (13)$$

Combining eqs(11-13) into one equation yields the complete 321 coordinate transformation from the inertial reference frame to the body reference frame

$$\begin{aligned} \begin{bmatrix} x \\ y \\ z \end{bmatrix} &= \begin{bmatrix} 1 & 0 & 0 \\ 0 & \cos \phi & \sin \phi \\ 0 & -\sin \phi & \cos \phi \end{bmatrix} \begin{bmatrix} \cos \theta & 0 & -\sin \theta \\ 0 & 1 & 0 \\ \sin \theta & 0 & \cos \theta \end{bmatrix} \begin{bmatrix} \cos \psi & \sin \psi & 0 \\ -\sin \psi & \cos \psi & 0 \\ 0 & 0 & 1 \end{bmatrix} \begin{bmatrix} I \\ J \\ K \end{bmatrix} \\ &= \begin{bmatrix} \cos \theta \cos \psi & \cos \theta \sin \psi & -\sin \theta \\ -\cos \phi \sin \phi + \sin \phi \sin \theta \cos \psi & \cos \phi \cos \psi + \sin \phi \sin \theta \sin \psi & \sin \phi \cos \theta \\ \sin \phi \sin \psi + \cos \phi \sin \theta \cos \psi & -\sin \phi \cos \psi + \cos \phi \sin \theta \sin \psi & \cos \phi \cos \theta \end{bmatrix} \begin{bmatrix} X \\ Y \\ Z \end{bmatrix} \quad (14) \end{aligned}$$

This is just one of the 12 different Euler coordinate transformations schemes available. Figure 11 on page 12 lists all possible Euler angle combinations and their resulting transformation matrices. It should be noted that eq(14) does not agree with the 321 Euler transformation matrix of Figure 11 on page 12. The 321 matrix of Figure 11 on page 12 contains a error that interchanges ϕ with ψ and ψ with ϕ .

TYPE - 1 EULER ANGLE REPRESENTATION	MATRIX A		
1-2-3	$\begin{bmatrix} C\phi C\theta & C\phi S\theta + S\phi C\theta & -C\phi S\theta + S\phi S\theta \\ -S\phi C\theta & -S\phi S\theta + C\phi C\theta & S\phi S\theta + C\phi S\theta \\ S\theta & -C\theta & C\theta \end{bmatrix}$		
1-3-2	$\begin{bmatrix} C\phi C\theta & C\phi S\theta + S\phi S\theta & C\phi S\theta - S\phi C\theta \\ -S\theta & C\theta & C\theta \\ S\phi C\theta & S\phi S\theta - C\phi S\theta & S\phi S\theta + C\phi C\theta \end{bmatrix}$		
2-3-1	$\begin{bmatrix} C\theta C\phi & S\theta & -C\theta S\phi \\ -C\phi S\theta + S\phi S\theta & C\phi C\theta & C\phi S\theta + S\phi C\theta \\ S\phi S\theta + C\phi S\theta & -S\phi C\theta & -S\phi S\theta + C\phi C\theta \end{bmatrix}$		
2-1-3	$\begin{bmatrix} C\phi C\theta + S\phi S\theta & S\phi C\theta & -C\phi S\theta + S\phi S\theta C\theta \\ -S\phi C\theta + C\phi S\theta S\theta & C\phi C\theta & S\phi S\theta + C\phi S\theta C\theta \\ C\theta S\theta & -S\theta & C\theta C\phi \end{bmatrix}$		
3-1-2	$\begin{bmatrix} C\phi C\theta - S\phi S\theta S\theta & C\phi S\theta + S\phi S\theta C\theta & -S\phi C\theta \\ -C\theta S\theta & C\theta C\phi & S\theta \\ S\phi C\theta + C\phi S\theta S\theta & S\phi S\theta - C\phi S\theta C\theta & C\phi C\theta \end{bmatrix}$		
3-2-1	$\begin{bmatrix} C\theta C\phi & C\theta S\phi & -S\theta \\ -C\phi S\theta + S\phi S\theta C\theta & C\phi C\theta + S\phi S\theta S\theta & S\phi C\theta \\ S\phi S\theta + C\phi S\theta C\theta & -S\phi C\theta + C\phi S\theta S\theta & C\phi C\theta \end{bmatrix}$		
TYPE - 2 EULER ANGLE REPRESENTATION	MATRIX A		
1-2-1	$\begin{bmatrix} C\theta & S\theta S\phi & -S\theta C\phi \\ S\phi S\theta & C\phi C\theta - S\phi C\theta S\phi & C\phi S\theta + S\phi C\theta C\phi \\ C\theta S\theta & -S\phi C\theta - C\phi C\theta S\phi & -S\phi S\theta + C\phi C\theta C\phi \end{bmatrix}$		
1-3-1	$\begin{bmatrix} C\theta & S\theta C\phi & S\theta S\phi \\ -C\phi S\theta & C\phi C\theta C\phi - S\phi S\theta & C\phi C\theta S\theta + S\phi C\theta \\ S\phi S\theta & -S\phi C\theta C\phi - C\theta S\phi & -S\phi C\theta S\theta + C\theta C\theta \end{bmatrix}$		
2-1-2	$\begin{bmatrix} C\phi C\theta - S\phi C\theta S\theta & S\phi S\theta & -C\phi S\theta - S\phi C\theta C\phi \\ S\theta S\theta & C\theta & S\theta C\phi \\ S\phi C\theta + C\phi C\theta S\theta & -C\theta S\theta & -S\phi S\theta + C\phi C\theta C\phi \end{bmatrix}$		
2-3-2	$\begin{bmatrix} C\phi C\theta C\phi - S\phi S\theta & C\theta S\theta & -C\phi C\theta S\theta - S\phi C\theta \\ -S\theta C\phi & C\theta & S\theta S\theta \\ S\phi C\theta C\phi + C\theta S\theta & S\phi S\theta & -S\phi C\theta S\theta + C\theta C\theta \end{bmatrix}$		
3-1-3	$\begin{bmatrix} C\phi C\theta - S\phi C\theta S\theta & C\phi S\theta + S\phi C\theta C\phi & S\phi S\theta \\ -S\phi C\theta - C\phi C\theta S\theta & -S\phi S\theta + C\phi C\theta C\phi & C\theta S\theta \\ S\theta S\theta & -S\theta C\phi & C\theta \end{bmatrix}$		
3-2-3	$\begin{bmatrix} C\phi C\theta C\phi - S\phi S\theta & C\phi C\theta S\theta + S\phi C\theta & -C\theta S\theta \\ -S\phi C\theta C\phi - C\theta S\theta & -S\phi C\theta S\theta + C\phi C\theta & S\phi S\theta \\ S\theta C\phi & S\theta S\theta & C\theta \end{bmatrix}$		

Figure 11. Table of Euler angle combinations [Ref. 4, p. 764]

C. RIGID BODY EQUATIONS

The general motion of a particle and its corresponding momentum have been written about extensively in various publications. A summary of the relevant derivations and equations of motion from [Ref 6] are presented here.

1. Derivative of a Vector in a Rotating Coordinate System

The time derivative of a vector in a rotating coordinate system consists of the rate of change of the vector relative to the moving axis and the rate of change due to the rotation of the axis. Figure 12 shows a vector in a rotating system where XYZ represent an inertial system and xyz are the set of axes rotating with angular velocity ω relative to XYZ. If unit vectors along the X, Y, and Z axes are i, j , and k , respectively, the vector r can be written in the form

$$r = xi + yj + zk \quad (15)$$

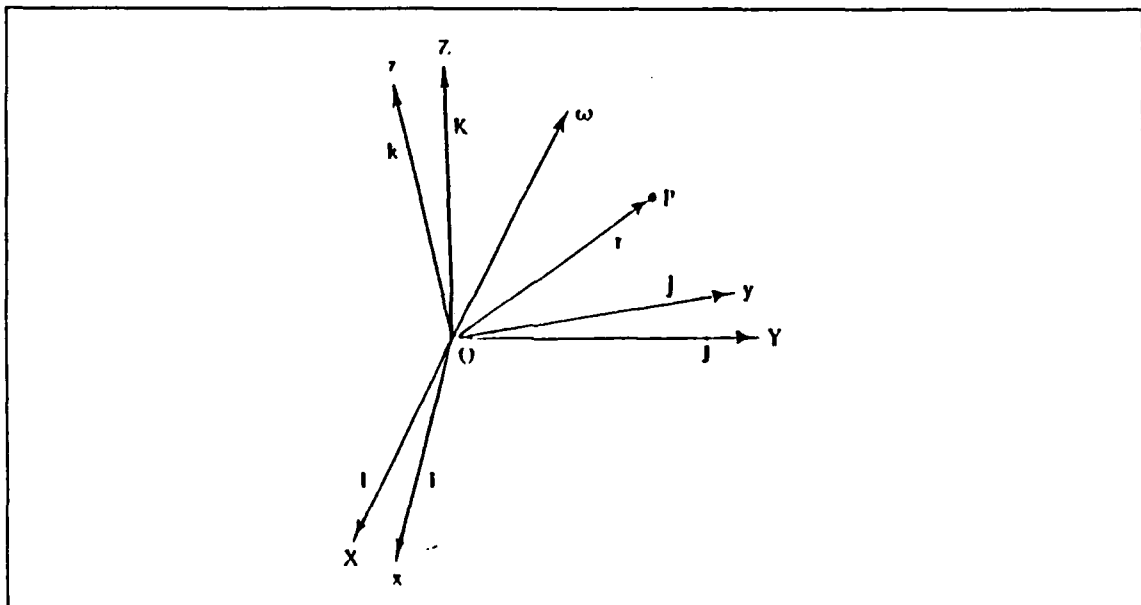


Figure 12. Vector in a rotating system [Ref. 6, p. 107]

The time derivative of r is

$$\dot{r} = \dot{x}i + x\dot{i} + \dot{y}j + y\dot{j} + \dot{z}k + z\dot{k} \quad (16)$$

From [Ref. 7], it has been shown that the time derivatives of the unit vectors are

$$\dot{i} = \omega \times i \quad (17)$$

$$\dot{j} = \omega \times j \quad (18)$$

$$\dot{k} = \omega \times k \quad (19)$$

Defining \dot{r}_{rel} as the time rate of change of r relative to xyz , eq(16) becomes

$$\dot{r} = \dot{r}_{rel} + \omega \times r \quad (20)$$

2. General Particle Motion

Translational motion of a particle with references to two coordinate systems is shown in Figure 13.

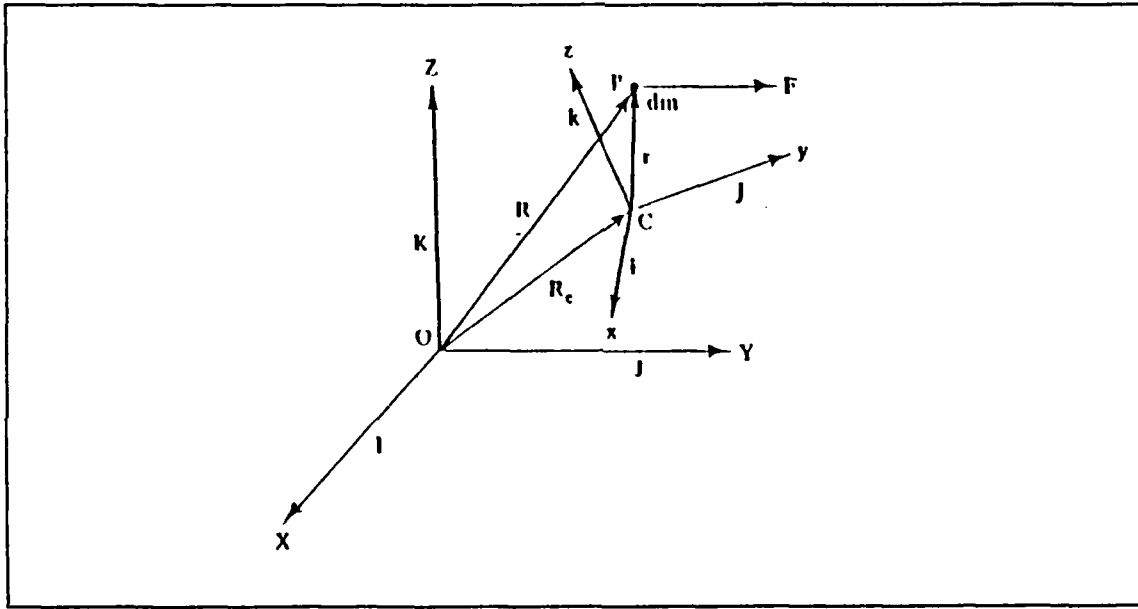


Figure 13. Translational motion of a particle [Ref. 6, p. 107]

The position vector of a particle relative to coordinate system XYZ is

$$R = R_c + r \quad (21)$$

where R_c is the vector from the axis of the XYZ coordinate frame to the xyz axis frame and r is the differential (position) vector in the xyz frame. The velocity of the particle is the derivative of eq(21) with respect to time

$$V = \dot{R} = \dot{R}_c + \dot{r} \quad (22)$$

The velocity at the origin $R_c = V_c$ combined with eq(20) yields

$$V = V_c + V_{rel} + \omega \times r \quad (23)$$

3. Momentum of a Rigid Body

A particle's momentum is the product of its velocity and mass. The linear momentum of the particle of Figure 13 on page 14 is

$$P = \int_m V dm \quad (24)$$

where V is the particle's velocity and m is its mass. Recalling that V_{rel} is the time rate of change of r relative to the xyz coordinate system, and assuming that the xyz axis is centered in the rigid body, $V_{rel} = 0$. Substituting eq(23) into eq(24) with $V_{rel} = 0$,

$$P = \int_m (V_c + \omega \times r) dm = mV_c + \omega \times \int_m r dm \quad (25)$$

By choosing the center of mass of the rigid body as the center of the rotating coordinate system, $\int_m r dm = 0$ by definition. This simplifies eq(25) to

$$P = mV_c \quad (26)$$

where P is the linear momentum of the rigid body, m is its mass, and V_c is the velocity of its center of mass.

The angular momentum of a particle dm about point C is defined as the moment about C of the linear momentum given by

$$h_c = r \times V dm \quad (27)$$

Substituting for V yields

$$H_c = \int_m r \times V dm = \int_m r \times (V_c + \omega \times r) dm \quad (28)$$

Rearranging terms

$$H_c = \left(\int_m r \, dm \right) \times V'_c + \int_m r \times (\omega \times r) \, dm \quad (29)$$

By choosing the center of mass of the rigid body as the origin of the rotating coordinate system, eq(29) reduces to

$$H_c = \int_m r \times (\omega \times r) \, dm \quad (30)$$

Reducing the angular velocity vector ω into its components

$$\omega = \omega_x i + \omega_y j + \omega_z k \quad (31)$$

Combining equations(15), (30), and (31) yields

$$\begin{aligned} H_c = & [I_{xx}\omega_x - I_{xy}\omega_y - I_{xz}\omega_z]i \\ & + [-I_{xy}\omega_x + I_{yy}\omega_y - I_{yz}\omega_z]j \\ & + [-I_{xz}\omega_x - I_{yz}\omega_y + I_{zz}\omega_z]k \end{aligned} \quad (32)$$

where

$$I_{xx} = \int_m (y^2 + z^2) \, dm \quad (33)$$

$$I_{yy} = \int_m (x^2 + z^2) \, dm \quad (34)$$

$$I_{zz} = \int_m (x^2 + y^2) \, dm \quad (35)$$

are the moments of inertia about the x,y, and z axes, respectively, and

$$I_{xy} = \int_m xy \, dm \quad (36)$$

$$I_{xz} = \int_m xz \, dm \quad (37)$$

$$I_{yz} = \int_m yz \, dm \quad (38)$$

are the products of inertia. Equation(32) written in matrix form becomes

$$\begin{bmatrix} H_x \\ H_y \\ H_z \end{bmatrix} = \begin{bmatrix} I_{xx} & -I_{xy} & -I_{xz} \\ -I_{xy} & I_{yy} & -I_{yz} \\ -I_{xz} & -I_{yz} & I_{zz} \end{bmatrix} \begin{bmatrix} \omega_x \\ \omega_y \\ \omega_z \end{bmatrix} \quad (39)$$

4. Equations of motion/Euler's Moment Equations

The derivation of the following Euler's moment equations are summarized from [Ref 6]. Recalling that angular momentum h_c relative to the point C is

$$h_c = r \times m\dot{v} \quad (40)$$

its derivative with respect to time is

$$\dot{h}_c = \dot{r} \times m\dot{v} + r \times m\ddot{v} \quad (41)$$

The moment of the force about a point C by definition is

$$M_c = r \times F \quad (42)$$

Recall Newton's second law describing force:

$$F = ma = m\ddot{v} \quad (43)$$

Substituting eqs(22) and (43) into eq(41) yields

$$\dot{h}_c = \dot{r} \times m(\dot{R}_c + \dot{r}) + r \times F \quad (44)$$

Substituting eq(42) into eq(44) and rearranging terms yields the moment equation

$$M_c = \dot{H}_c + \int_m (\dot{R}_c \times \dot{r}) dm \quad (45)$$

where H_c is the angular momentum of the rigid body about point C. From eq(20) the latter part of eq(45) can be written as

$$\int_m \dot{R}_c \times \dot{r} dm = \dot{R}_c \times \left(\dot{r}_{rel} + \left(\omega \times \int_m r dm \right) \right) \quad (46)$$

Noting that point C is the center of mass $\int_m r dm = 0$ and $r_{rel} = 0$ for a rigid body, eq(46) reduces to

$$M_c = \dot{H}_c \quad (47)$$

The moment of external forces about the center of mass of a rigid body is equal to the time rate of change of the angular momentum of the body about the center of mass [Ref. 7]. In terms of a rotating axis, the moment equation of eq(47) becomes

$$M_c = \dot{H}_{c_{rel}} + \omega \times H_c \quad (48)$$

Substituting eq(39) in for H, the components of the moment equation can be written as

$$M_x = \dot{H}_x + \omega_y H_z - \omega_z H_y \quad (49)$$

$$M_y = \dot{H}_y + \omega_z H_x - \omega_x H_z \quad (50)$$

$$M_z = \dot{H}_z + \omega_x H_y - \omega_y H_x \quad (51)$$

where $M_{x,y,z}$ are the moment equations. In this study, an assumption is made that the principle axes of the moment of inertia are the rotating axes x,y,z; therefore, the products of inertia (I_{xy} , I_{xz} , I_{yz}) are equal to zero. The angular momentum components reduce to

$$H_x = I_{xx} \omega_x \quad (52)$$

$$H_y = I_{yy}\omega_y \quad (53)$$

$$H_z = I_{zz}\omega_z \quad (54)$$

Substituting eqs(52-54) into the moment equations yields Euler's moment equations

$$M_x = I_{xx}\dot{\omega}_x + \omega_y\omega_z(I_{zz} - I_{yy}) \quad (55)$$

$$M_y = I_{yy}\dot{\omega}_y + \omega_x\omega_z(I_{xx} - I_{zz}) \quad (56)$$

$$M_z = I_{zz}\dot{\omega}_z + \omega_x\omega_y(I_{yy} - I_{xx}) \quad (57)$$

Referring to the coordinate system shown in Figure 6 on page 5, the angular velocities in terms of orbital rate ω_0 and attitude error angles pitch(θ), roll(ϕ), and yaw (ψ) from [Ref. 6, p. 130] are

$$\begin{bmatrix} \omega_x \\ \omega_y \\ \omega_z \end{bmatrix} = \begin{bmatrix} 1 & 0 & -\sin \theta \\ 0 & \cos \phi & \cos \theta \sin \phi \\ 0 & -\sin \phi & \cos \theta \cos \phi \end{bmatrix} \begin{bmatrix} \dot{\phi} \\ \dot{\theta} \\ \dot{\psi} \end{bmatrix} - \omega_0 \begin{bmatrix} \cos \theta \sin \psi \\ \cos \phi \cos \psi + \sin \phi \sin \theta \sin \psi \\ -\sin \phi \cos \psi + \cos \phi \sin \theta \sin \psi \end{bmatrix} \quad (58)$$

When using small angle approximations, eq(58) reduces to

$$\begin{bmatrix} \omega_x \\ \omega_y \\ \omega_z \end{bmatrix} = \begin{bmatrix} \dot{\phi} - \omega_0\psi \\ \dot{\theta} - \omega_0\phi \\ \dot{\psi} + \omega_0\phi \end{bmatrix} \quad (59)$$

Note that the orbital rate is defined as

$$\omega_0 = \sqrt{\frac{\mu}{R^3}} \quad (60)$$

where μ is the gravitational constant and R is the radius of the earth plus the satellite's altitude. For the purpose of station keeping, the small angle approximations are valid. Substituting eq(59) into the rigid body moment eqs(55-57) yields the linearized rigid body dynamic equations

$$M_{xRB} = I_{xx}\ddot{\phi} + \omega_0^2(I_{yy} - I_{zz})\phi - \omega_0(I_{xx} + I_{zz} - I_{yy})\dot{\psi} \quad (61)$$

$$M_{yRB} = I_{yy}\ddot{\theta} \quad (62)$$

$$M_{zRB} = I_{zz}\ddot{\psi} + \omega_0^2(I_{yy} - I_{xx})\psi - \omega_0(I_{xx} + I_{zz} - I_{yy})\dot{\phi} \quad (63)$$

D. GRAVITY GRADIENT EFFECT

Attitude control using gravity gradient stabilization works on the principle that given an object with an asymmetrically distributed mass, the object will tend to align itself with its minimum moment of inertia axis along the local vertical towards the earth.

The force due to gravity on a mass element is

$$dF = -\frac{\mu_e dm}{R^3} R \quad (64)$$

where

$$R = R_0 + r \quad (65)$$

and

$$\mu_e = GM_e = g_e R_e^2 \quad (66)$$

where G = universal gravity constant, M_e = the mass of the earth, g_e = gravity acceleration at the earth's surface, and R_e = the radius of the earth. Reference 8 shows the torque generated about the mass center of the object is

$$\begin{aligned} dM_g &= r \times dF = -\frac{\mu_e dm}{R^3} r \times R \\ &= -\frac{\mu_e dm}{R^3} r \times (R_0 + r) \\ &= -\frac{\mu_e dm}{R^3} r \times R_0 \end{aligned} \quad (67)$$

Cubing eq(65) yields

$$R^3 = R_0^3 \left[1 + \frac{3rR_0}{R_0^2} + \frac{3r^2R_0}{R_0^2} + \frac{r^3}{R_0^3} \right] \quad (68)$$

Noting that $r \ll R_0$, the higher order terms drop out. Inversion of eq(68) yields

$$\frac{1}{R^3} = \frac{1}{R_0^3} \left(1 - \frac{3r \cdot R_0}{R_0^2} \right) \quad (69)$$

Substituting eq(69) into eq(67) and integrating to find the moment yields

$$M_g = -\mu_e \int_m r \, dm \times R_0 + \frac{3\mu_e}{R_0^2} \int_m \frac{(r \times R_0)(r \cdot R_0)}{R_0^2} \, dm \quad (70)$$

Given that the center of mass is the origin of the body frame, $\int_m r \, dm = 0$, eq(70) reduces to

$$M_g = \frac{3\mu_e}{R_0^5} \int_m (r \times R_0)(r \cdot R_0) \, dm \quad (71)$$

In the reference system defined by Figure 14, the K (Z) vector is pointing towards the earth; therefore, the vector R_0 in the reference coordinate frame is

$$R_{0r} = R_0 K \quad (72)$$

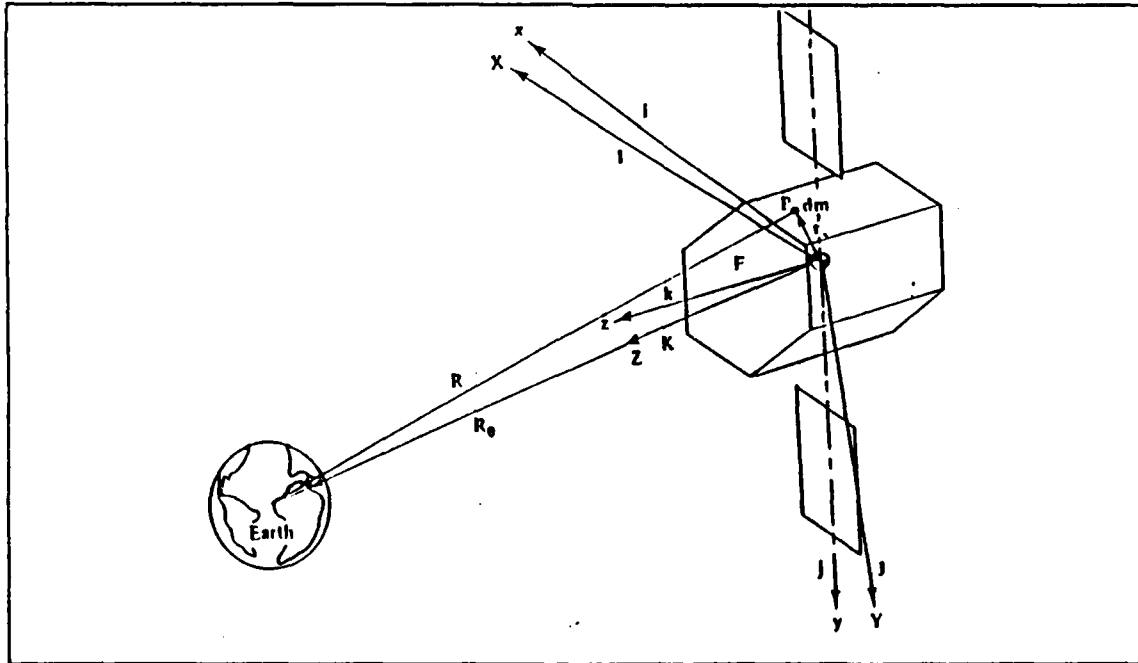


Figure 14. Gravity gradient torque [Ref. 6, p. 113]

Restating the Euler 321 rotation matrix described earlier

$$\begin{aligned}
 \begin{bmatrix} i \\ j \\ k \end{bmatrix} &= \begin{bmatrix} 1 & 0 & 0 \\ 0 & \cos \phi & \sin \phi \\ 0 & -\sin \phi & \cos \phi \end{bmatrix} \begin{bmatrix} \cos \theta & 0 & -\sin \theta \\ 0 & 1 & 0 \\ \sin \theta & 0 & \cos \theta \end{bmatrix} \begin{bmatrix} \cos \psi & \sin \psi & 0 \\ -\sin \psi & \cos \psi & 0 \\ 0 & 0 & 1 \end{bmatrix} \begin{bmatrix} I \\ J \\ K \end{bmatrix} \\
 &= \begin{bmatrix} \cos \theta \cos \psi & \cos \theta \sin \psi & -\sin \theta \\ -\cos \phi \sin \phi + \sin \phi \sin \theta \cos \psi & \cos \phi \cos \psi + \sin \phi \sin \theta \sin \psi & \sin \phi \cos \theta \\ \sin \phi \sin \psi + \cos \phi \sin \theta \cos \psi & -\sin \phi \cos \psi + \cos \phi \sin \theta \sin \psi & \cos \phi \cos \theta \end{bmatrix} \begin{bmatrix} I \\ J \\ K \end{bmatrix} \quad (73)
 \end{aligned}$$

Transforming R_{0r} into the spacecraft's fixed coordinates i, j, and k:

$$R_{0r} = \begin{bmatrix} \cos \theta \cos \psi & \cos \theta \sin \psi & -\sin \theta \\ -\cos \phi \sin \phi + \sin \phi \sin \theta \cos \psi & \cos \phi \cos \psi + \sin \phi \sin \theta \sin \psi & \sin \phi \cos \theta \\ \sin \phi \sin \psi + \cos \phi \sin \theta \cos \psi & -\sin \phi \cos \psi + \cos \phi \sin \theta \sin \psi & \cos \phi \cos \theta \end{bmatrix} \begin{bmatrix} 0 \\ 0 \\ K \end{bmatrix}$$

which reduces to

$$R_{0r} = R_0(-\sin \theta i + \sin \phi \cos \theta j + \cos \phi \cos \theta k) \quad (75)$$

Substituting eq(75) into eq(71) yields the gravity gradient moment equations

$$M_g = \frac{3\mu_e}{R_0^3} \begin{bmatrix} (I_{zz} - I_{yy}) \sin \phi \cos \phi \cos^2 \theta \\ -(I_{xx} - I_{zz}) \sin \theta \cos \theta \cos \phi \\ -(I_{yy} - I_{xx}) \sin \theta \cos \theta \sin \phi \end{bmatrix} \quad (76)$$

Replacing

$$\omega_0^2 = \frac{\mu_e}{R_0^3} \quad (77)$$

where ω_0 is the orbital rate, and making the small angle approximations, the gravity gradient moment equations become

$$M_g = 3\omega_0^2 \begin{bmatrix} (I_{zz} - I_{yy})\phi \\ (I_{zz} - I_{xx})\theta \\ 0 \end{bmatrix} \quad (78)$$

Equation(78) clearly shows that by increasing the moments of inertia for I_x and I_y with respect to I_z , the gravity gradient moments for roll and pitch will increase. By extending a point mass along the z axis, a sizeable increase in the moments of inertia along the x and y axes is realized.

The magnitudes of the gravity gradient torques generated at different altitudes is given by Figure 15.

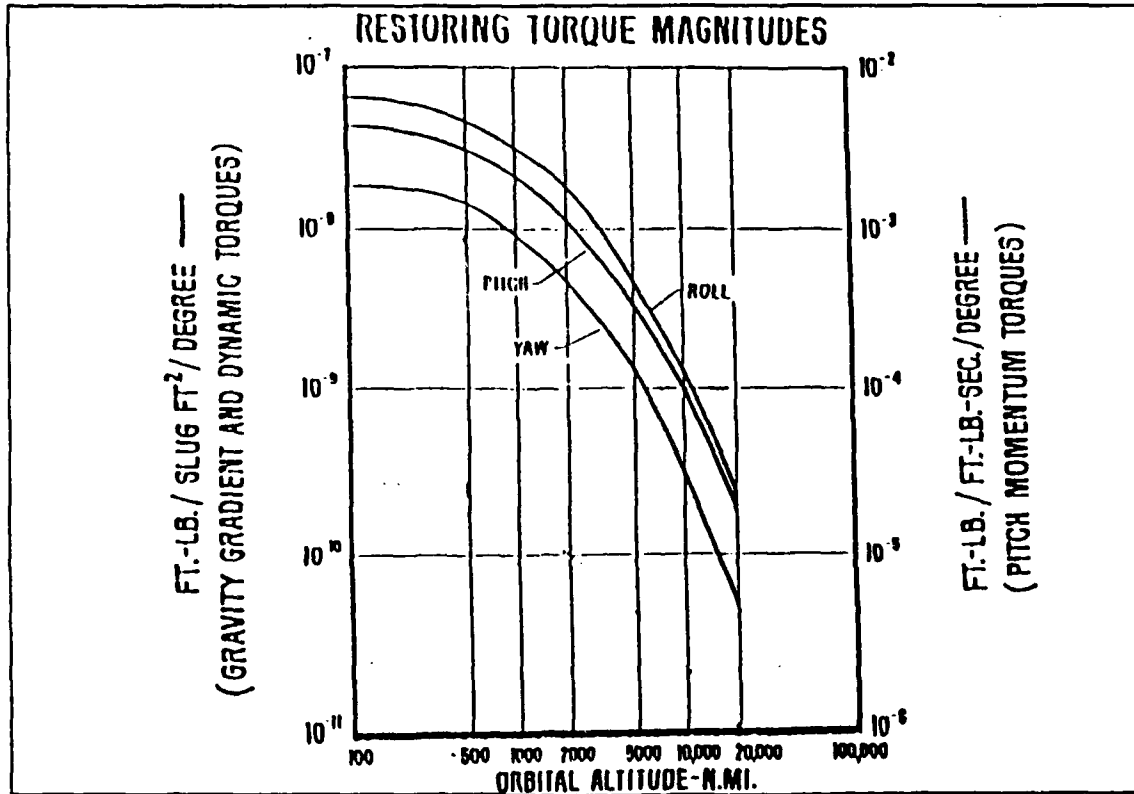


Figure 15. Gravity Gradient torque Magnitudes vs Altitude [Ref. 3, p. 58]

E. DESIGN FOR STABILITY

1. Stability and Frequency Analysis

Combining the rigid body dynamic equations (61-63) with the gravity gradient equation (78) yields the undamped linear dynamic equations for roll, pitch, and yaw:

$$\text{Roll } I_x \ddot{\phi} + 4\omega_0^2(I_y - I_z)\phi - \omega_0(I_x + I_z - I_y)\dot{\psi} = 0 \quad (79)$$

$$\text{Pitch } I_y \ddot{\theta} + 3\omega_0^2(I_x - I_z)\theta = 0 \quad (80)$$

$$Yaw \quad I_z \ddot{\psi} + \omega_0^2(I_y - I_x)\psi + \omega_0(I_x + I_z - I_y)\dot{\phi} = 0 \quad (81)$$

Using Reference 9 notations for simplicity, the following variables are defined:

$$A = \frac{I_y - I_z}{I_x} \quad (82)$$

$$B = \frac{I_x - I_z}{I_y} \quad (83)$$

$$C = \frac{I_y - I_x}{I_z} \quad (84)$$

Substituting eqs(82-84) into eqs(79-81) yields the following second order differential equations

$$\ddot{\phi} + 4A\omega_0^2\phi - (1 - A)\omega_0\dot{\psi} = 0 \quad (85)$$

$$\ddot{\theta} + 3B\omega_0^2\theta = 0 \quad (86)$$

$$\ddot{\psi} + C\omega_0^2\psi + (1 - C)\dot{\phi} = 0 \quad (87)$$

Taking the Laplace transform of eqs(85-87) allows for frequency analysis. The results are put into matrix form:

$$\begin{bmatrix} S^2 + 4A\omega_0^2 & 0 & -(1 - A)\omega_0 S \\ 0 & S^2 + 3B\omega_0^2 & 0 \\ (1 - C)\omega_0^2 S & 0 & S^2 + C\omega_0^2 \end{bmatrix} \begin{bmatrix} \phi \\ \theta \\ \psi \end{bmatrix} = \begin{bmatrix} 0 \\ 0 \\ 0 \end{bmatrix} \quad (88)$$

The determinant of the matrix is the system's characteristic equation. Using the middle row to simplify calculations, the characteristic equation is found to be

$$(S^4 + (1 + 3A + CA)\omega_0^2 S^2 + 4AC\omega_0^4)(S^2 + 3B\omega_0^2) = 0 \quad (89)$$

"Solution of the first term on the left yields the natural frequencies of roll and yaw, respectively; the second term on the left defines the natural frequency of the pitch axis." [Ref. 9, p. 9] Solving for the first term on the left (roll/yaw stability) by the quadratic formula and dividing through by ω_0^2 yields

$$\frac{S_{roll}^2}{\omega_0^2} = \frac{S_{yaw}^2}{\omega_0^2} = \frac{-(1 + 3A + AC) \pm \sqrt{(1 + 3A + AC)^2 - 16AC}}{2} \quad (90)$$

For roll yaw stability the roots of eq(90) must be real and negative; therefore the following stability conditions exist [Ref. 4 p. 611]

$$1 + 3A + AC > 4\sqrt{AC} \quad (91)$$

$$AC > 0 \quad (92)$$

Solving for the second term of Eq(89) and dividing through by ω_0^2 yields

$$\frac{S_{pitch}^2}{\omega_0^2} = 3B = \frac{3(C - A)}{1 - CA} \quad (93)$$

The condition for stability for the pitch axis is

$$A > C \quad (94)$$

Converting A, B, and C back into their respective moment of inertia relationships defined by eqs(82-84), combined with the conditions for stability, yields two possible orientations: $I_y > I_x > I_z$ and $I_x > I_z > I_y$. Figure 16 on page 26 shows a summary of the stability regions based on moment of inertia ratios. [Ref. 10 p. 204]

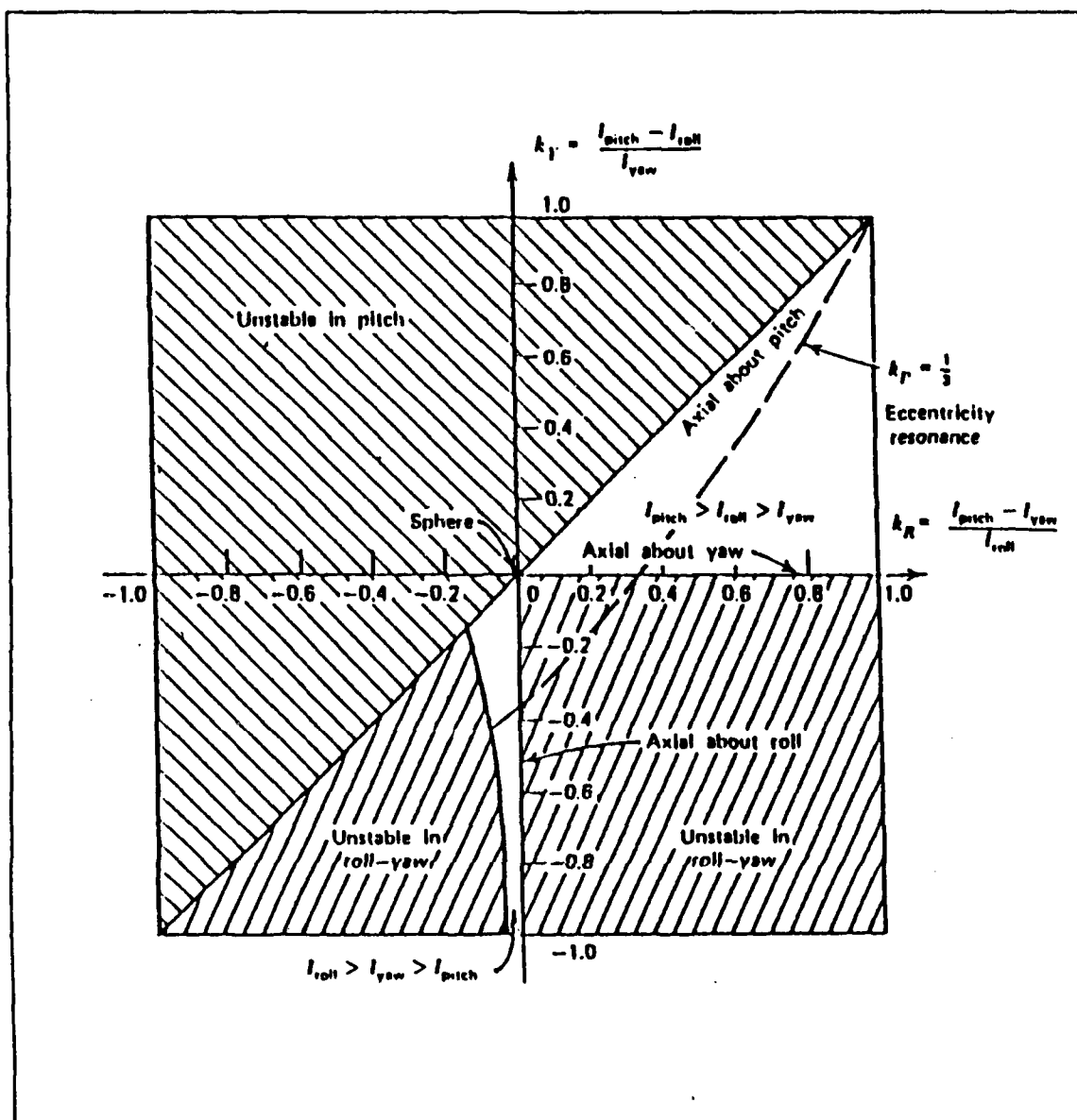


Figure 16. Gravity Gradient Stability Regions

III. ENVIRONMENTAL DISTURBANCES AND RESTORING TORQUES

A. ENVIRONMENTAL DISTURBANCES/TORQUES

There are four major environmental disturbances that affect an orbiting spacecraft: aerodynamic, magnetic, gravity gradient, and solar radiation torque. Figure 17 lists these disturbances and their relative regions of dominance.

SOURCE	DEPENDENCE ON DISTANCE FROM EARTH	REGION OF SPACE WHERE DOMINANT*
AERODYNAMIC	ρ	ALTITUDES BELOW ~ 500 km
MAGNETIC	$1/r^3$	~ 500 km TO ~ 35,000 km;
GRAVITY GRADIENT	$1/r^3$	[I.E., OUT TO ABOUT SYNCHRONOUS ALTITUDE]
SOLAR RADIATION	INDEPENDENT	INTERPLANETARY SPACE ABOVE SYNCHRONOUS ALTITUDE
MICROMETEORITES	LARGELY INDEPENDENT; HIGH CONCENTRATION IN SOME REGIONS OF THE SOLAR SYSTEM	NORMALLY NEGLIGIBLE; MAY BE IMPORTANT IN SOME SMALL REGIONS (INTERIOR OF SATURN'S RINGS)

ALTITUDES LISTED ARE ONLY REPRESENTATIVE; THE SPECIFIC ALTITUDES AT WHICH VARIOUS TORQUES DOMINATE ARE HIGHLY SPACECRAFT DEPENDENT.

Figure 17. Environmental Disturbance Torques [Ref. 4, p. 17]

1. Aerodynamic disturbance

a. Drag

"For satellites near the earth the principle non-gravitational force is aerodynamic drag. Aerodynamic drag is a retarding force due to atmospheric friction and is in the direction opposite the space vehicles velocity vector." [Ref. 4, p. 63]

The drag force is a function of vehicle velocity, air density, and surface area of the satellite. The drag force is given by the following equation:

$$d = \frac{\rho v^2 c_d a}{2} \quad (95)$$

where d is the drag force, ρ is the atmospheric density, v is the velocity of the satellite along its orbital path, c_d is the drag coefficient, and a is the area of the satellite over which the drag acts.

b. Aerodynamic torque

The collisions of air molecules of the upper atmosphere with the satellite surface produces a torque about its center of mass. Aerodynamic disturbances are a

function of the satellite's altitude, velocity, and symmetry. A satellite with a relatively low earth orbit may be significantly affected by aerodynamic torques.

Shown in Figure 18 is a cylindrical satellite with its center of mass (cm) and center of pressure (cp). The offset between the center of mass (cm) and the center of pressure (cp) is denoted by L_x , L_y , and L_z , respectively. The simplified aerodynamic disturbance torques from Ref 8 may be computed by the following expression:

$$T_a = P_a l_a A_a \sin \alpha \quad (96)$$

where T_a is the torque due to aerodynamic pressure (ft-lbs), P_a is the aerodynamic pressure (lbs/ft²), l_a is the distance between the center of mass and the center of pressure (ft), A_a is the exposed surface area (ft²) and α is the angle of attack (radians). For practical purposes, the aerodynamic torque in the x direction is zero ($\sin \alpha = 0$ when $\alpha \approx 0$). The conversion factor from ft-lbs to N-m is approximately 1.356. Figure 19 on page 29 shows aerodynamic pressure as a function of altitude.

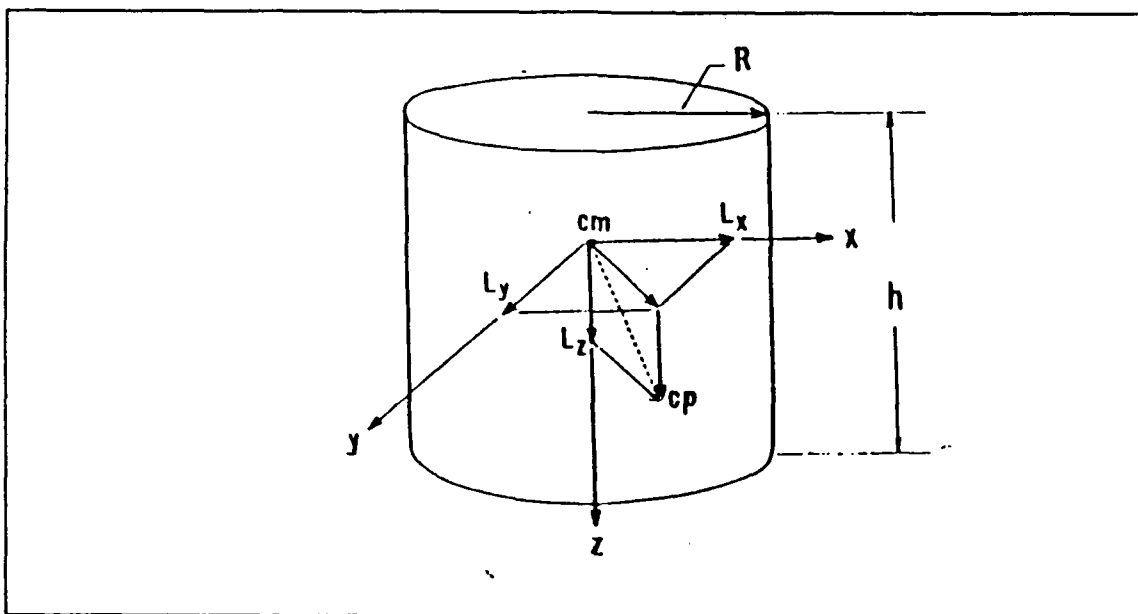


Figure 18. Aerodynamic effects for cylindrical satellite [Ref. 3, p. 58]

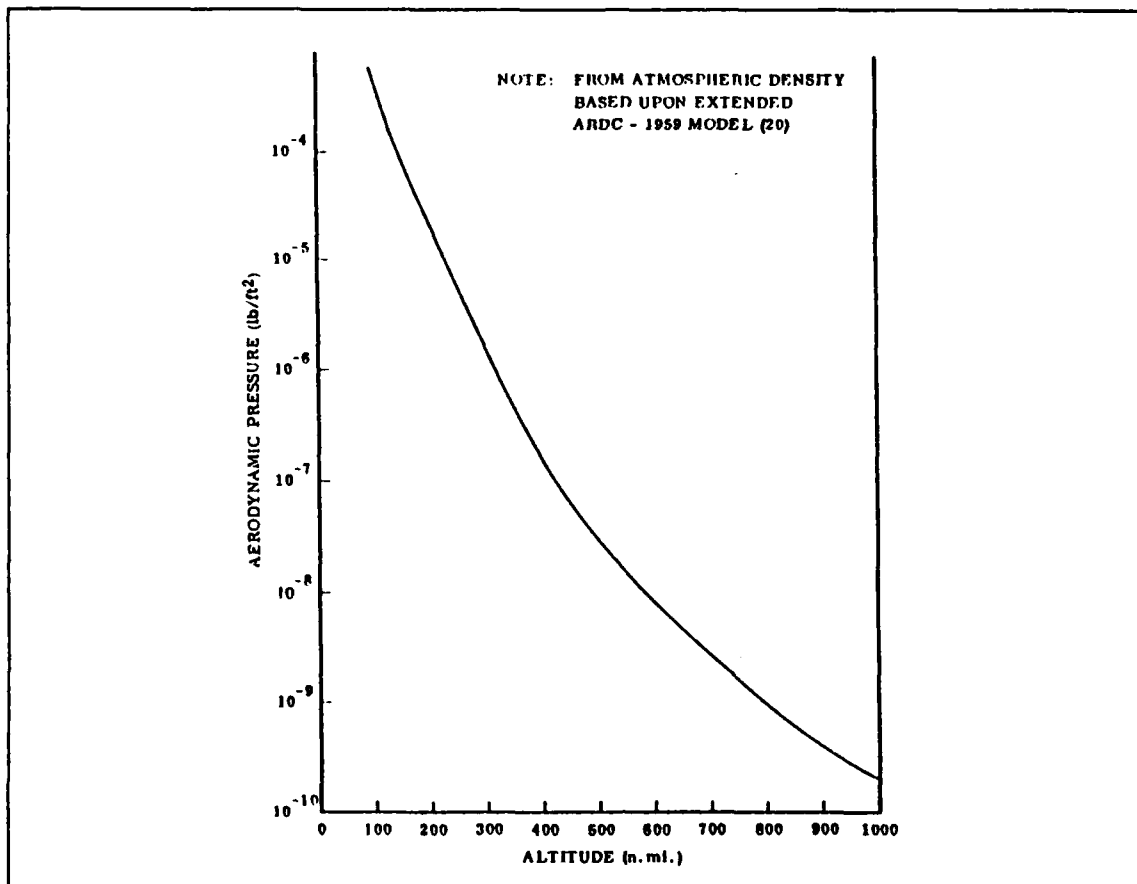


Figure 19. Aerodynamic pressure as a function of altitude [Ref. 8, p. 456]

The magnitude of the pitch and yaw aerodynamic disturbances for a one inch cm-cp offset are shown in Figure 20 on page 30 for various altitudes. The magnitude of these torques decrease significantly with increases in altitude. "Proper control of the satellites inertias to enhance gravity gradient torques can make aerodynamic disturbances essentially insignificant for orbital altitudes above 300 nautical miles (480km). On the other hand, in the 100 to 200 nautical mile (160-320km) altitudes aerodynamic disturbances are 3 to 4 orders of magnitude greater than the gravity gradient torque from a 1 slug-ft² inertia difference and 1 degree attitude error. In the lower regions, very large inertia differences are required for accuracy. [This leads to design considerations] where proper configuration can make these aerodynamic torques work as restoring torques instead of disturbance torques" [Ref. 3, p. 57].

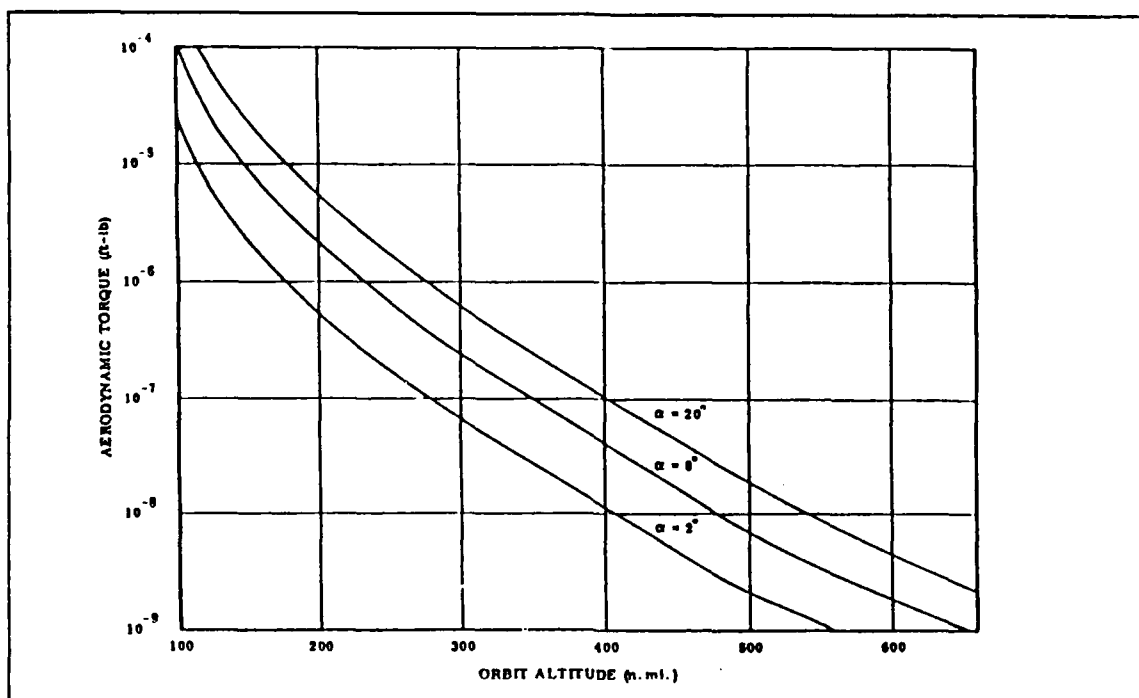


Figure 20. Aerodynamic torque for a 1 inch offset as a function of altitude.

2. Rigid Body Solar Pressure Torque

"The major factors determining the radiation torque on a spacecraft are the intensity and spectral distribution of the incident radiation, the geometry of the surface and its optical properties, and the orientation of the sun vector relative to the spacecraft" [Ref. 4, p. 570].

Solar pressure torques are the disturbances produced by solar radiation pressure and is a function of the offset of the center of pressure (cp) and the center of mass (cm). Referring to Figure 21 on page 31, the center of mass-center of pressure offsets are designated as L_x , L_y , and L_z , respectively. The torques generated due to solar pressure are given by [Ref. 8, p. 454] as:

$$T_s = P_s L_s A_s \cos \epsilon \quad (97)$$

$$T_s = 2P_s L_s A_s \cos^2 \epsilon \quad (98)$$

where T_s = torque due to solar radiation (ft-lbs), P_s = radiation pressure (lb/ft²) and is \approx constant at 9.65×10^{-8} lb/ft² for an earth orbiting vehicle, L_s = center of mass center of pressure offset (ft), A_s = surface area of satellite normal to sun(ft²), and ϵ = angle

of incidence (degrees). Note, equation (97) is for an *absorbent satellite body* and equation (98) is for a *reflective body*.

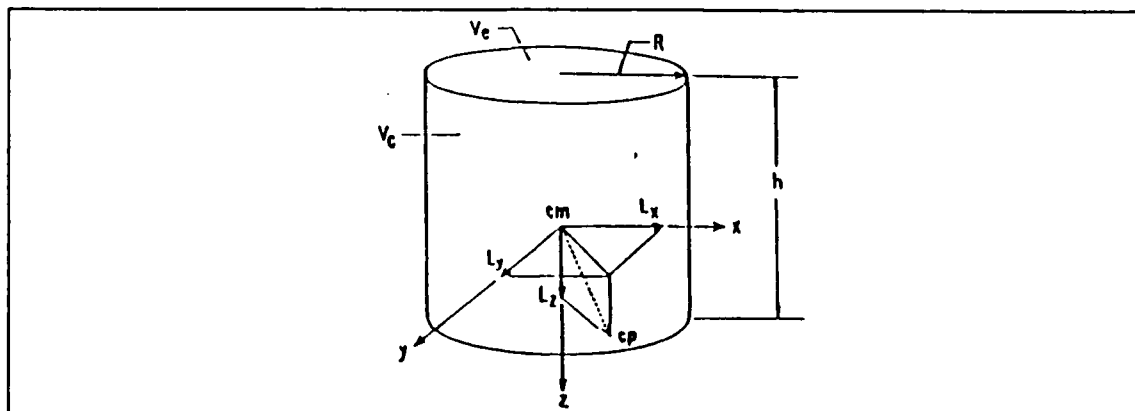


Figure 21. Rigid body solar pressure torques [Ref. 3, p. 61]

B. RESTORING TORQUES

As seen from chapter 2, the restoring torques of the undamped rigid body combined with the gravity gradient effects are considerably smaller for the yaw axis than for either the pitch or roll axes. This is due to the necessity of large moments of inertia along the pitch and roll axes, as compared to the yaw axis, for gravity gradient stabilization to occur. The lack of adequate yaw restoring torque requires that additional yaw restoring torque be provided for accurate 3-axis stabilization. A discussion of yaw restoring torque methods follows.

1. Thrusters

Thrusters are an effective torque generating device; however, for the purpose of this thesis, thrusters will not be considered for attitude control. Thrusters are necessary for orbit maintenance and orbital transfer. Due to the physical size constraints imposed by the GAS cannister, ORION is severely limited in its fuel storage capacity to approximately 71 lbs of hydrazine fuel [Ref 1]. An assumption that the launch platform will place ORION in its final orbit is optimistic. Figure 22 on page 32 shows the fuel required to go from one orbital altitude to another. Saving the onboard fuel for orbit maintenance and transfer and not for attitude control allows more fuel to be devoted towards supporting the mission either by allowing greater orbital flexibility and/or a longer lifetime.

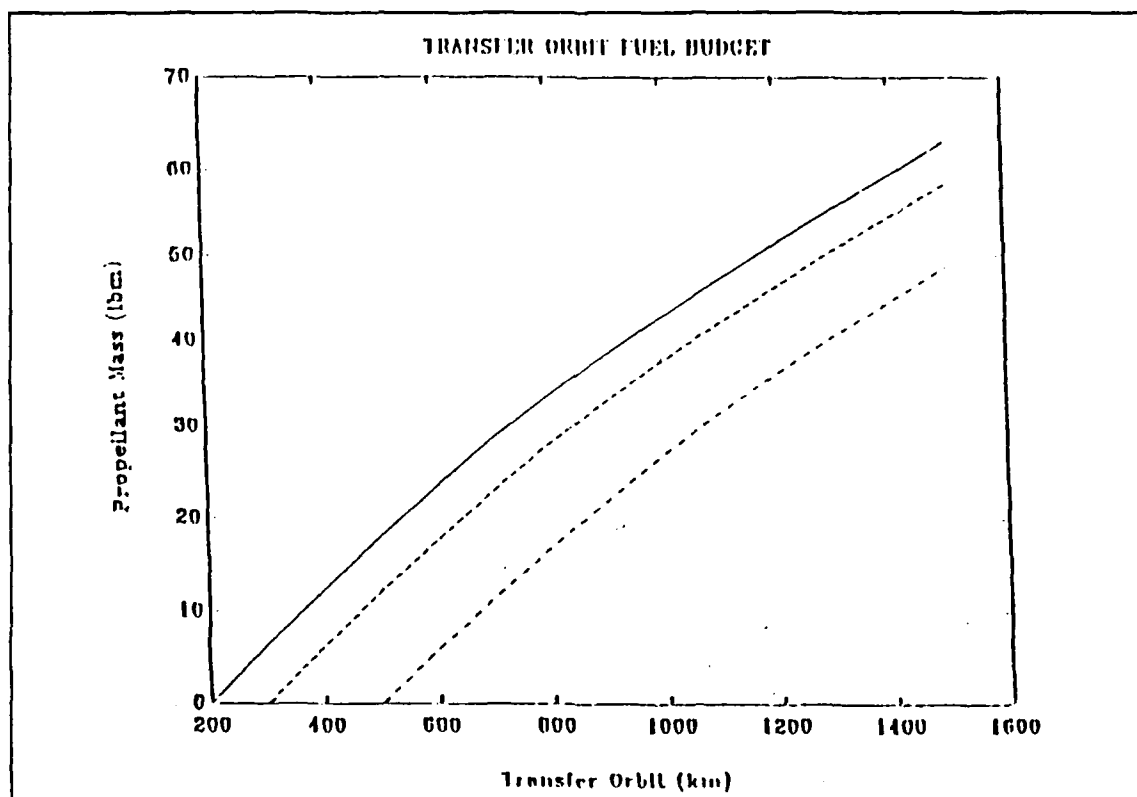


Figure 22. Fuel required for orbit transfer based on a 250lb satellite. [Ref 2, p. 23]

2. Momentum Exchange Devices

The principle behind momentum exchange devices is that by changing the angular momentum of the control device, the angular momentum of the vehicle will be changed an equal and opposite amount. Recall that the rate of change of angular momentum is equal to the torque that is generated. The two basic types of momentum exchange devices are reaction wheels and control moment gyros (CMG). The basic difference between the two is the method by which the change in angular momentum is accomplished. The reaction wheel axis is fixed (generally along one of the axes of the vehicle) so that the change in angular momentum is accomplished by varying the speed of rotation of the flywheel. The CMG creates the change in angular momentum by tilting the constant speed flywheel with respect to the vehicle.

a. Reaction wheels

"An axis may be controlled by varying the speed of the reaction wheel in response to an attitude error [Ref. 6, p.149]. The momentum of a system with a reaction wheel is

$$H = H_w + H_c \quad (99)$$

where H_c is the angular momentum of the system and

$$H_w = \begin{bmatrix} H_{wx} \\ H_{wy} \\ H_{wz} \end{bmatrix}$$

is the angular momentum of the reaction wheel. Aligning the reaction wheels along each axis, and substituting eq(99) into eq(48) and adding the gravity gradient moments of eq(78) yields

$$\begin{aligned} I_x \ddot{\phi} + 4\omega_0^2(I_y - I_z)\phi - \omega_0(I_x + I_z - I_y)\dot{\psi} + (\dot{\theta} - \omega_0)H_{wz} - (\dot{\psi} + \omega_0\phi)H_{wy} + \dot{H}_{wx} &= \sum T_x \\ I_y \ddot{\theta} + 3\omega_0^2(I_x - I_z)\theta + (-\dot{\phi} + \omega_0\psi)H_{wz} + (\dot{\psi} + \omega_0\phi)H_{wx} + \dot{H}_{wy} &= \sum T_y \\ I_z \ddot{\psi} + \omega_0^2(I_y - I_x)\psi + \omega_0(I_x + I_z - I_y)\dot{\phi} + (\dot{\phi} - \omega_0\psi) + (-\dot{\phi} + \omega_0\psi)H_{wx} + \dot{H}_{wz} &= \sum T_z \end{aligned} \quad (101)$$

"Because H_{wx}, H_{wy}, H_{wz} , and ω_0 are small, the coupling terms are small. If the coupling terms are neglected, the equations of motion about the roll, pitch, and yaw axes become independent, and hence, they can be controlled independently" [Ref. 6, pp. 149-150]. Dropping the coupled terms, the motion equations become

$$I_x \ddot{\phi} + 4\omega_0^2(I_y - I_z)\phi - \omega_0(I_x + I_z - I_y)\dot{\psi} + \dot{H}_{wx} = \sum T_x \quad (102)$$

$$I_y \ddot{\theta} + 3\omega_0^2(I_x - I_z)\theta + \dot{H}_{wy} = \sum T_y \quad (103)$$

$$I_z \ddot{\psi} + \omega_0^2(I_y - I_x)\psi + \omega_0(I_x + I_z - I_y)\dot{\phi} + \dot{H}_{wz} = \sum T_z \quad (104)$$

Allowing the momentum of the reaction wheel to be proportional to the attitude error, then by differentiation, the reaction wheel control torques are equal to

$$T_{xrw} = -K_x(\tau_x \dot{\phi} + \phi) \quad (105)$$

$$T_{yrw} = -K_y(\tau_y \dot{\theta} + \theta) \quad (106)$$

$$T_{zrw} = -K_z(\tau_z \dot{\psi} + \psi) \quad (107)$$

and the control scheme would be as shown in Figure 23.

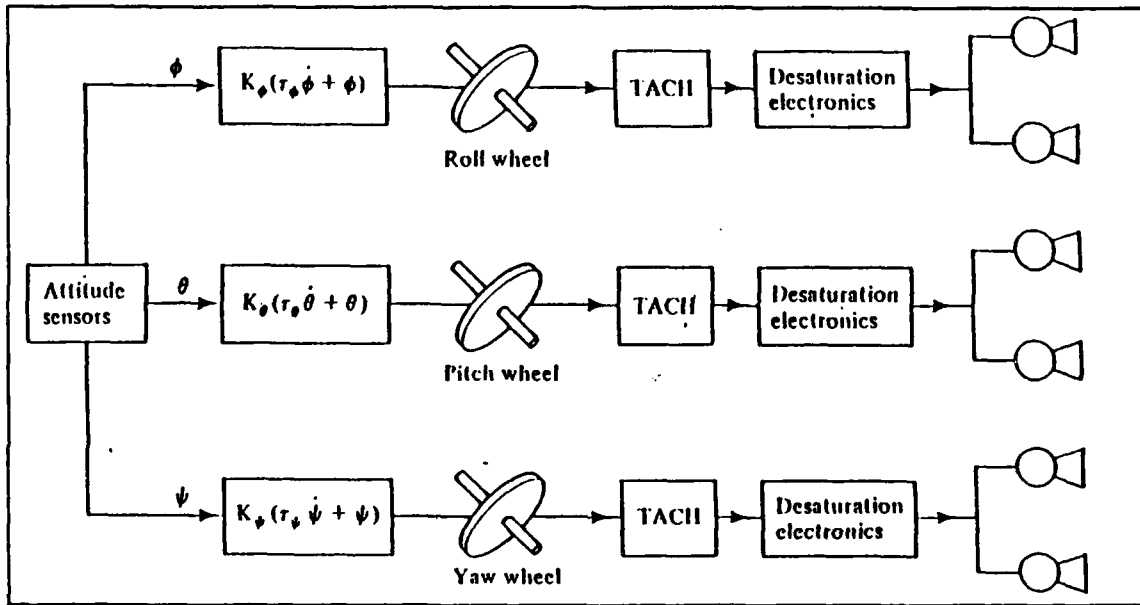


Figure 23. 3 axis reaction wheel control scheme [Ref. 6, p. 149]

The torque generated by the reaction wheel is a function of the wheel's angular velocity and its moment of inertia. This means that a small lightweight wheel at a high rate of speed generates the same amount of torque that a large wheel at a low rate of speed. Since *ORION* is designed for a relatively short lifespan, wear and tear on spinning parts is not an overriding concern. It should be noted that continuous disturbance torques that are not cyclical in nature will eventually saturate the reaction wheel, whereby, the reaction wheel rotational speed will reach a maximum. Thrusters or some other method of momentum removal must be used to reduce wheel speed. Disturbance torques that

are cyclical in nature are easily offset by the reaction wheel as long as the disturbance torque is such that it does not saturate the reaction wheel speed.

3. CMG(s)

"A control moment gyro's (either single or double gimbaled) angular momentum is due to the rotor which is spinning about the spin axis with a constant angular rate. Because the spin axis is gimbaled, a commanded gimbal rotation causes the direction of the angular momentum vector to change, thus creating a control torque parallel to the output axis. The magnitude of this torque depends on the speed of the rotor and the gimbal rotation rate." [Ref. 4, p. 200]

A control moment gyro scheme is shown in Figure 24.

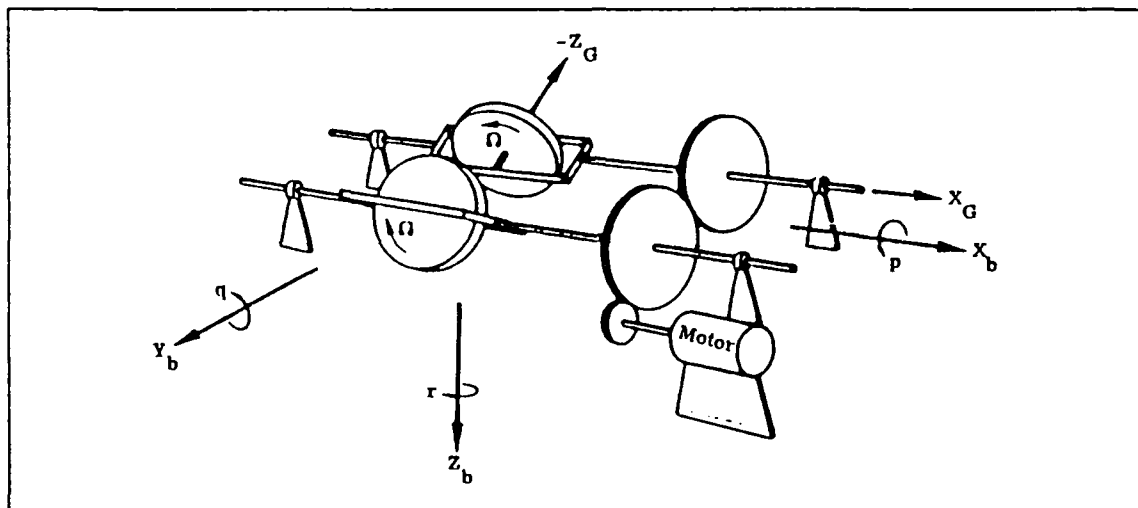


Figure 24. Twin gyro controller with one drive motor [Ref. 8, p. 415]

Because of their expense and weight, CMG's are only used on large spacecraft [Ref. 4]. For this reason, control moment gyros will not be addressed.

4. Magnetic torquers

Magnetic torquers may be used to dampen the kinetic energy of the libration motion as well as correcting attitude errors in any direction. The magnetic torquers consist of three wire coil sets arranged perpendicularly to each other. This configuration allows magnetic torque to be generated along any axis or in any direction as a result of adding two or three different orthogonal torques. As shown in Figure 25 on page 36, when a current is applied around the loop of a coil, it produces a magnetic dipole that is normal to the plane of the coil and a magnitude which is proportional to the coil's enclosed area and ampere-turns.

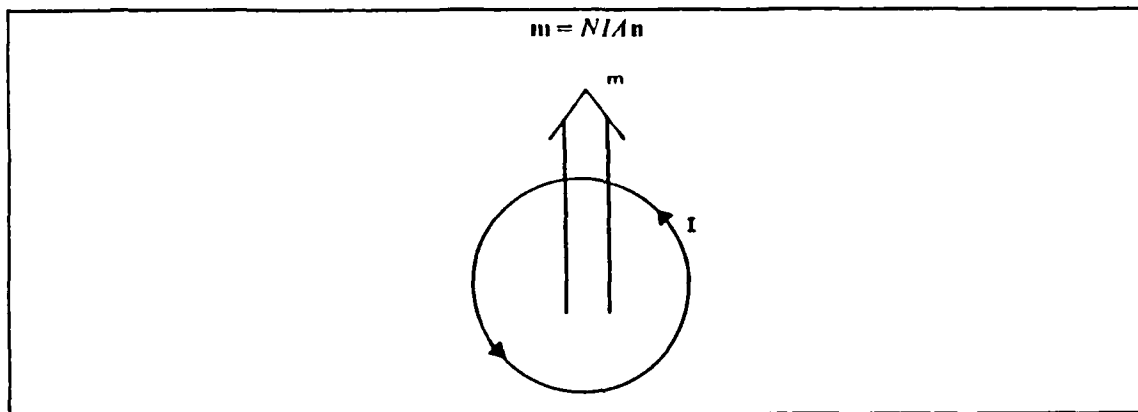


Figure 25. Magnetic Moment Due to a Current Loop [Ref. 4, p. 204]

The magnetic moment M is defined as

$$M = NIA\hat{n} \quad (108)$$

where N is the the number of turns around the coil, I is the current in amperes, A is the area enclosed by the loop, and \hat{n} is the unit vector normal to the plane of the loop. Because of the relationship between N , I , and A , many different combinations are available to produce the desired magnitude of the magnetic moment. Figure 26 on page 37 shows three existing spacecraft with various combinations of number of turns and current drawn. The torque generated by the magnetic torquer is

$$T_{mag} = M \times B \quad (109)$$

where M is the magnetic dipole and B is the earth's magnetic field. The earth's magnetic field for an equatorial orbit can be approximately modeled as a tilted dipole located at 78.3° north latitude and 69° west longitude as shown in Figure 27 on page 37.

SPACECRAFT	REMARKS
SAS-3	COIL CONSISTS OF 260 TURNS. MAXIMUM CURRENT IS 0.6 A AND MAXIMUM POWER CONSUMPTION IS 10 W
OSO-8	COIL CONSISTS OF 360 TURNS. MAXIMUM CURRENT IS 0.075 A
AE-3	TWO COILS; EACH HAS 500 TURNS. MAXIMUM POWER CONSUMPTION IS 12 W

Figure 26. Some existing magnetic moment schemes [Ref. 3, p. 205]

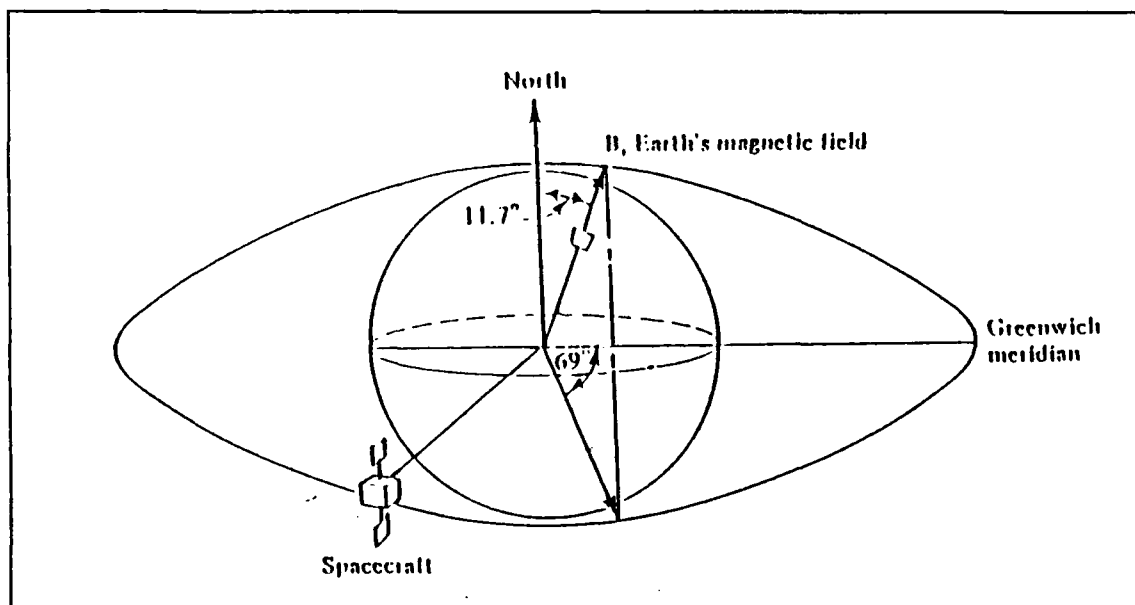


Figure 27. Earth's magnetic field modeled as a tilted dipole [Ref. 6, p. 148]

The strength of the earth's magnetic field for a circular equatorial orbit in component form can be approximated by

$$B_x = -\frac{M_g}{R^3} \sin(11.7) \sin(281 - lam_s) \quad (110)$$

$$B_y = -\frac{M_g}{R^3} \cos(11.7) \quad (111)$$

$$B_z = \frac{M_g}{R^3} \sin(11.7) \cos(281 - lam_s) \quad (112)$$

where lam_s is measured in degrees of right ascension from Grenich, M_g is the strength at the earth's center which is approximately 8×10^{15} Wb-m, and R is the distance in meters from the earth's center to the orbital altitude. With respect to the satellite, the earth's magnetic field is changing continuously as the vehicle moves along its orbital path. Putting into component form both M and B , eq(109) becomes

$$T_{mag-x} = M_z B_y - M_y B_z \quad (113)$$

$$T_{mag-y} = M_x B_z - M_z B_x \quad (114)$$

$$T_{mag-z} = M_y B_x - M_x B_y \quad (115)$$

It should be noted that the earth's magnetic field is not uniform and varies in direction based on the satellite's position. For accurate attitude control, the vehicle must be able to exactly know both its position and the earth's magnetic field at that position. For low earth orbits, the magnetic field is well mapped and may be easily programmed into the attitude control computer. For the purpose of this thesis, magnetic field approximations will suffice to demonstrate magnetic torquing as a viable attitude control capability.

IV. CHAPTER 4

A. GRAVITY GRADIENT STABILIZATION RESULTS

1. Attitude Control

There are three general attitude control phases with respect to gravity gradient systems: gravity gradient capture, transition period, and steady state. Gravity gradient from a tumbling mode occurs when angular velocity slows to one rotation per orbit or less, allowing the minimum moment of inertia axis to align with the local vertical. The transition period is the time from gravity gradient capture until a steady state has been achieved. This period of oscillations will vary depending on the dampening scheme used to reduce the amplitude of oscillations. Predominant throughout the satellite's lifetime, the steady state phase is the period in which the satellite's errors are confined within operationally acceptable amplitudes. Maintenance of the desired steady state requires minimization of external disturbances and control of those which cannot be eliminated.

The following group of simulations assumes that a steady state phase has been achieved and that the small angle approximations are in effect. For each of the simulations, the following initial conditions are in effect: ϕ , θ , and ψ position error = 5° , and $\dot{\phi}$, $\dot{\theta}$, and $\dot{\psi} = 0$.

2. Various results based on different configurations

a. *Effects of extending booms*

For Figure 28 on page 40, a 10 kg point mass is used and the mass of the boom is assumed to be negligible. Extension of the boom increases the moment of inertia in the x and y directions. This increases the restoring torque along the roll and pitch axes although it does little to dampen the libration motion.

b. *Gravity gradient effect alone*

The following figures show the gravity gradient effect on a satellite at an altitude of 1000 km having moments of inertias as shown. As shown by Figure 29 on page 41 and Figure 30 on page 42, stabilization along the roll and pitch axes would take a prohibitively long time while the yaw direction would not stabilize. It is clear that gravity gradient stabilization alone is incapable of acceptable three axis stabilization.

MOMENT OF INERTIA VS BOOM LENGTH

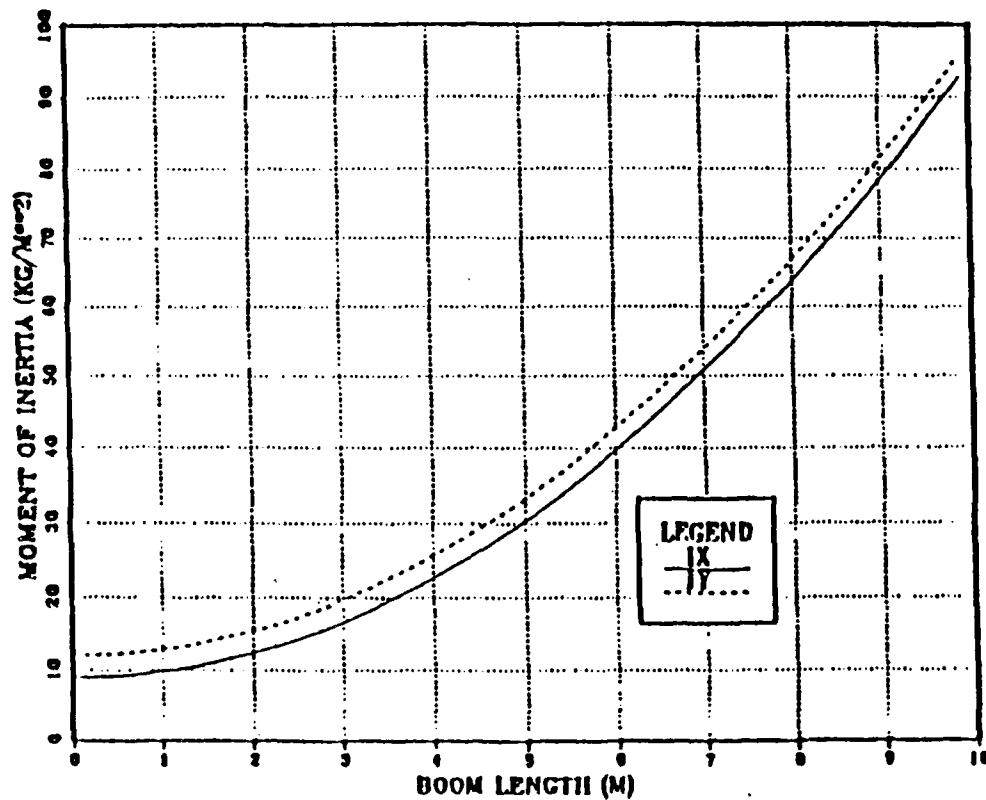


Figure 28. Effect of extending boom on moments of inertia

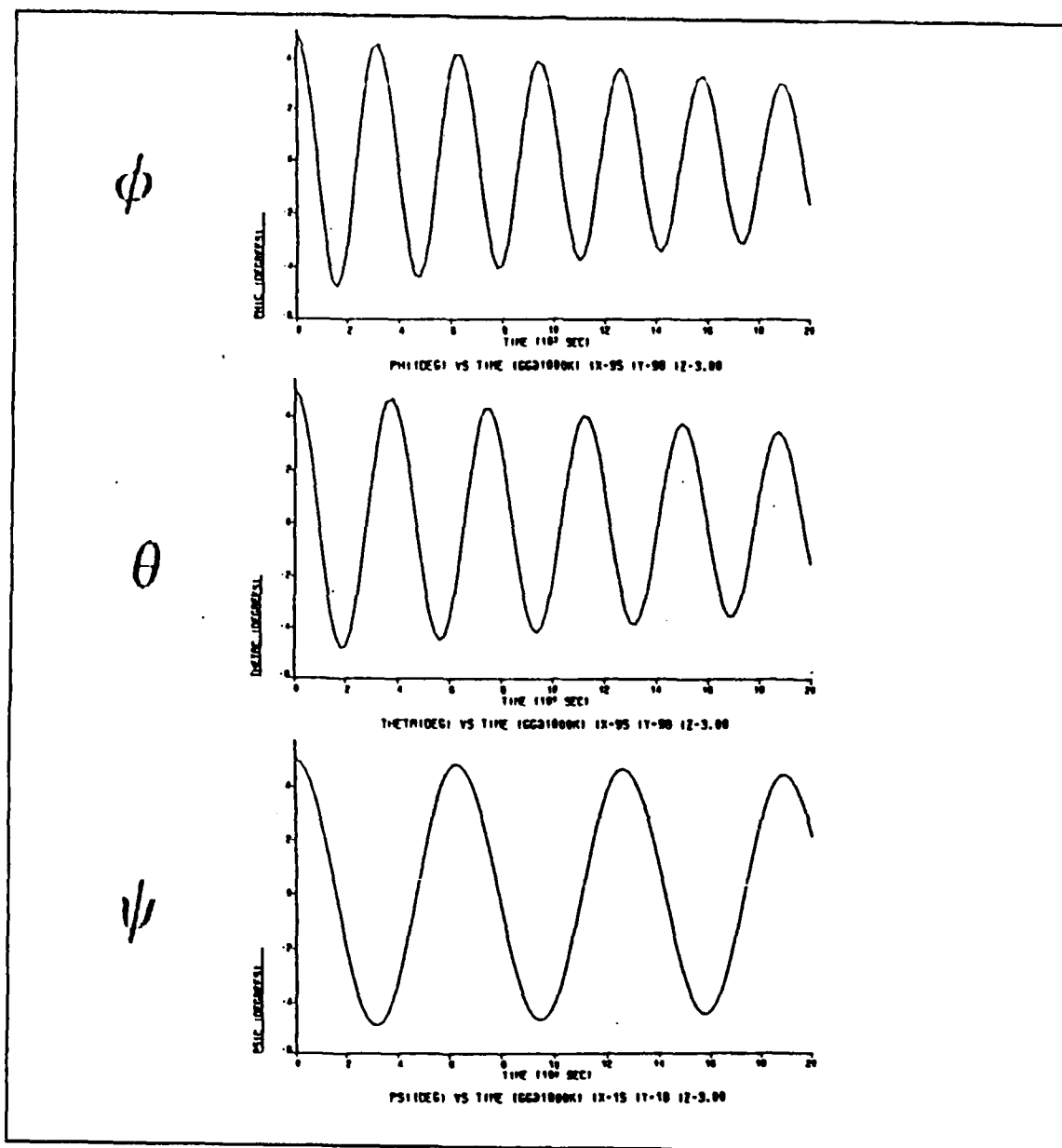


Figure 29. Gravity gradient effect only $I_x = 15$, $I_y = 18$, $I_z = 3$

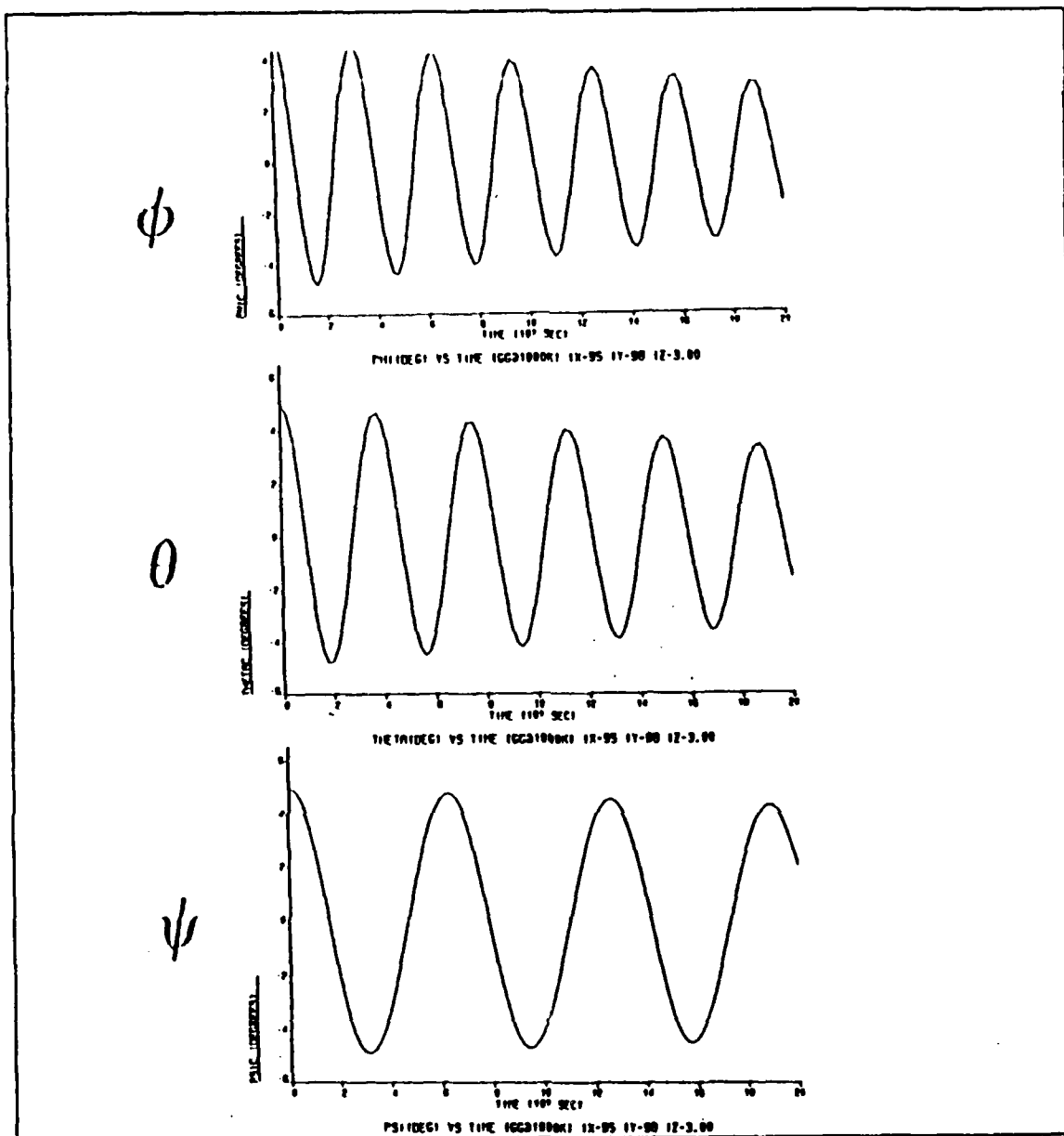


Figure 30. Gravity gradient effect only $I_x=95$, $I_y=98$, $I_z=3$

c. *Effects of Reaction Wheel(s)*

One method of augmenting gravity gradient stabilization is through the use of reaction wheels. Teldrix reaction wheel classes and corresponding technical data are presented in Figure 31 on page 43.

Wheel diameter	cm	20	26	35	50	60")
Angular momentum range	Nms	1.8...6.5	5.0...20	14...80	50...300	200...1000
Max. reaction torque	Nm	0.2	0.2	0.2	0.3	0.3-0.6
Speed**)	min ⁻¹	6000	6000	6000	6000	6000
Loss torque at max. speed**)	Nm	≤ 0.012	≤ 0.013	≤ 0.015	≤ 0.022	≤ 0.07
Power consumption:						
- steady state (depending on speed)	W	2...7	2...8	2...10	3...15	10...50
- max. power rating	W	≤ 60	≤ 80	≤ 100	≤ 150	≤ 500
Dimensions:						
- diameter A	mm	203	260	350	500	600
- height B	mm	75	85	120	150	180
Weight	kg	2.7...3.4	3.5...6.0	5.0...8.0	7.5...12	20...37
Environmental conditions:		suitable for satellites compatible with launchers such as ARIANE or Space Shuttle				
- operating temperature						
- vibration (sinusoidal)						
- vibration (random)						
- linear acceleration						

Figure 31. Teldrix Reaction Wheel Technical Data

Of the five diameter classes, the 20 cm diameter wheel is the most appropriate of the classes listed for ORION. Reaction wheels also come in diameters smaller than 20 cm diameter. Bendix Aerospace SP reaction wheel of Figure 32 on page 44 has a diameter of 6 inches.

As illustrated in Figure 31 and Figure 32 on page 44, power consumption values differ with different reaction wheels. For the 20 cm Teldrix reaction wheel, steady state requires 2-7 watts with a maximum less than 60 watts. The Bendix SP reaction wheel requires 2.5 watts at steady state with a maximum power consumption of 6.5 watts. Due to weight and power consumption values, the Bendix reaction wheel appears to be the superior choice of the two.

The following figures were generated by setting the reaction wheel torques equal to eqs(107-109). The initial conditions are ϕ , θ , and ψ position errors = 5° , and $\dot{\phi} = \dot{\theta} = \dot{\psi} = 0$. For simulation purposes, the maximum reaction torque value of .2 N-m from Figure 31 will be in effect.

Figures 33-35 have moment of inertias $I_x = 15$, $I_y = 18$, and $I_z = 3$, with $K_x = K_y = 2.0$, $K_z = 1.0$, and $\tau_x = \tau_y = \tau_z = 1.0$. Figure 33 on page 45 shows ϕ (position error), $\dot{\phi}$ (velocity), and the restoring torque ($T_{rw\phi}$) generated by the reaction wheel with respect to time. Figures 34 and 35 show θ , $\dot{\theta}$, $T_{rw\theta}$, and ψ , $\dot{\psi}$, $T_{rw\psi}$, respectively. With the relatively small moments of inertias, stabilization of all axes within the $\pm 1^\circ$ criteria

occurs within 40 seconds. Increasing the moments of inertias to $I_x = 95$, $I_y = 98$, and $I_z = 3$ while holding K_x , K_y at 2.0, K_z at 1.0, and τ_x , τ_y , and τ_z constant at 1.0, yields Figures 36-38. As expected, the ϕ and θ axes take longer to stabilize (approximately 160 seconds) than the above case with the smaller moments of inertia. The ψ axis of Figure 38 stabilizes much faster than either the ϕ or θ axes. This is due to the relatively small moment of inertia (I_z) compared to the restoring torque generated by the reaction wheel.

PROGRAM/UNIT NAME	:	SF Reaction Wheel
UNIT TYPE NO. (REF)	:	3890003
MOMENTUM (FT-LB-SBC)	:	0.4 @ 1250 RPM
WEIGHT (LBS.)	:	4.9
SIZE	:	6.0" DIA. MAX x 3.9" HIGH (excluding mounting feet projection)
STALL TORQUE (OZ-IN)	:	2.2
PEAK POWER (WATTS)	:	6.5
MAX SPEED (RPM)	:	1350
MOTOR EXCITATION	:	28V, 0-peak, Squarewave, 400 Hz, 2 Phase
STEADY STATE POWER(WATTS):	:	2.5 @ 1350 RPM
TACHOMETER TYPE	:	P.M. Rotor, 2 Phase Wound Stator, Sinusoidal Output, 1 Cycle/Rev/Phase, Amplitude varies with speed.
QUANTITY BUILT	:	42
COMMENTS	:	AC Squirrel Cage Induction Motor
FLIGHT HISTORY	:	More than 20 of these units have flown. Units with operating time greater than 5 years are presently functioning in-orbit.

Figure 32. Bendix Aerospace Reaction Wheel Technical Data.

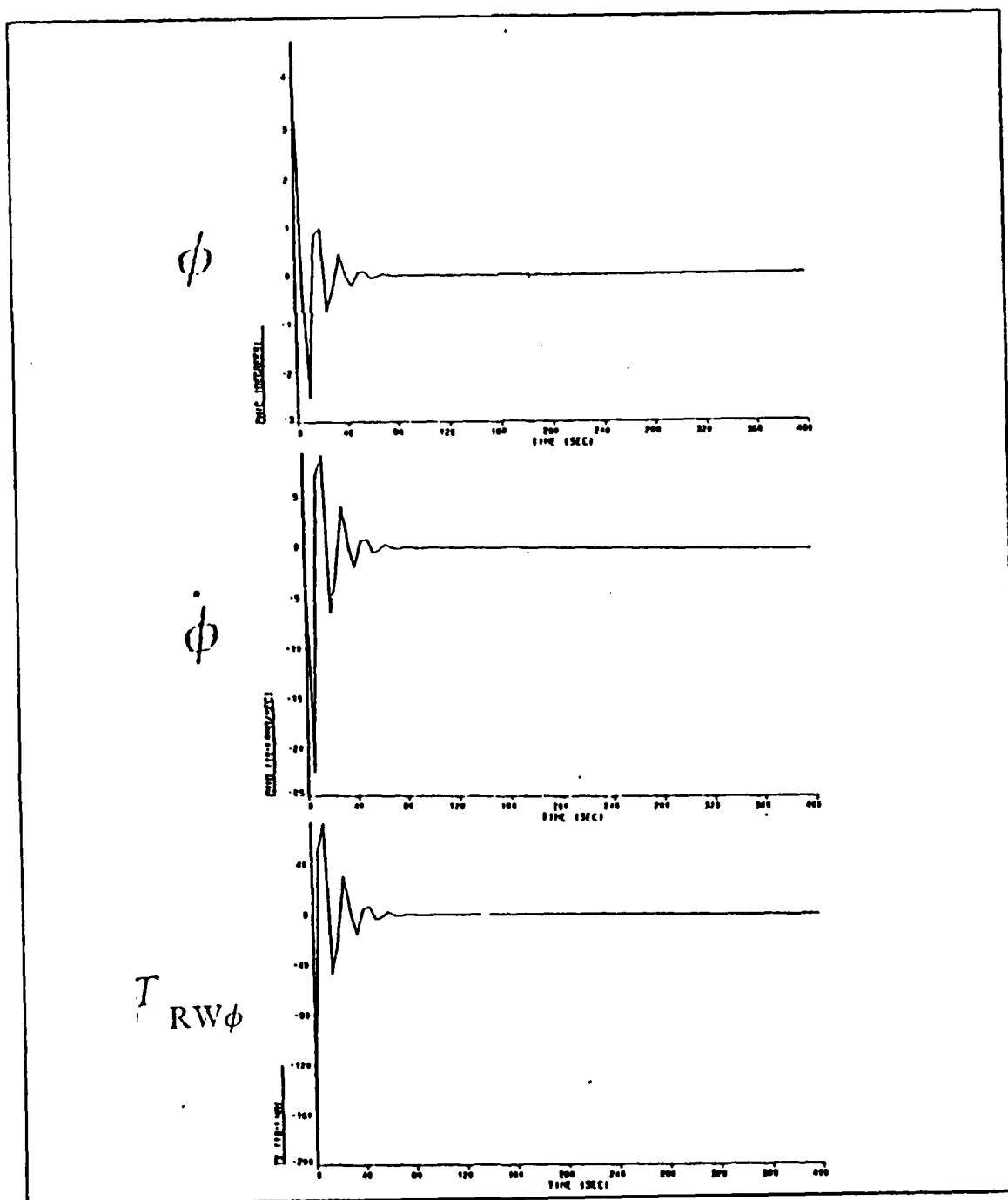


Figure 33. Gravity gradient effect with 3 RW (X axis) $I_x=15$, $I_y=18$, $I_z=3$
 $K_x=2.0$, $\tau_x=1.0$

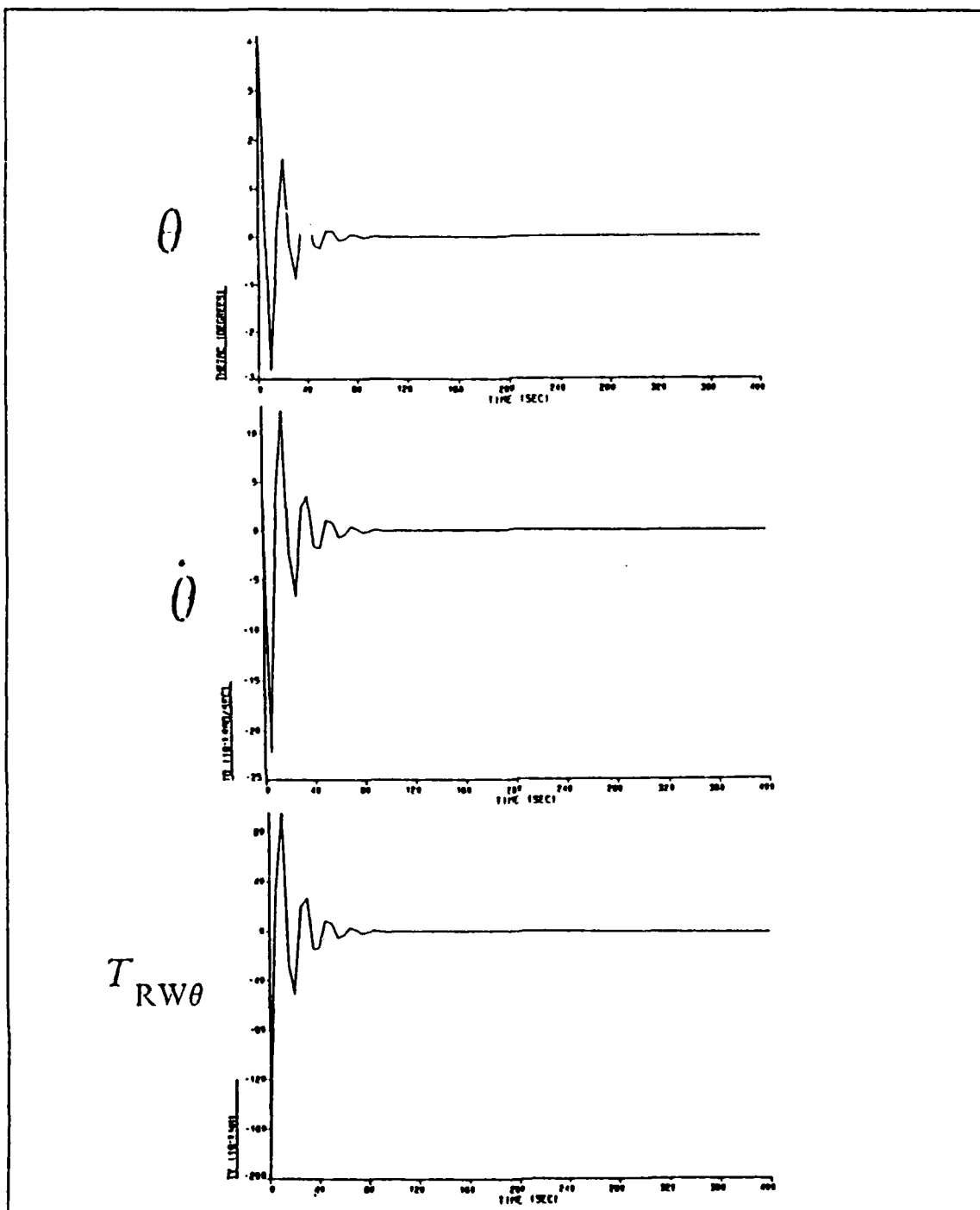


Figure 34. Gravity gradient effect with 3 RW (Y axis) $I_x = 15$, $I_y = 18$, $I_z = 3$
 $K_y = 2.0$, $\tau_y = 1.0$

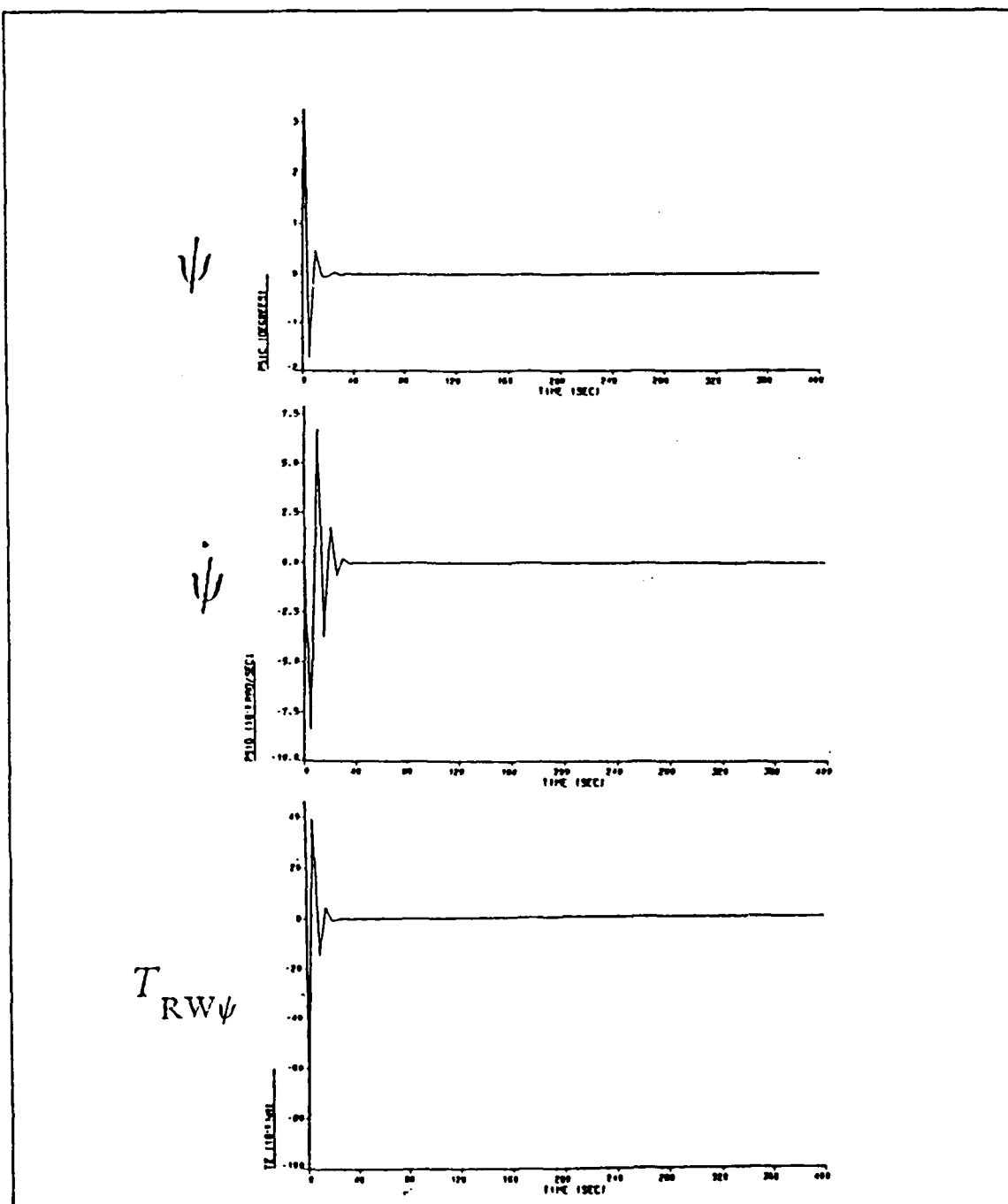


Figure 35. Gravity gradient effect with 3 RW (Z axis) $I_x = 15$, $I_y = 18$, $I_z = 3$
 $K_z = 2.0$, $\tau_z = 1.0$

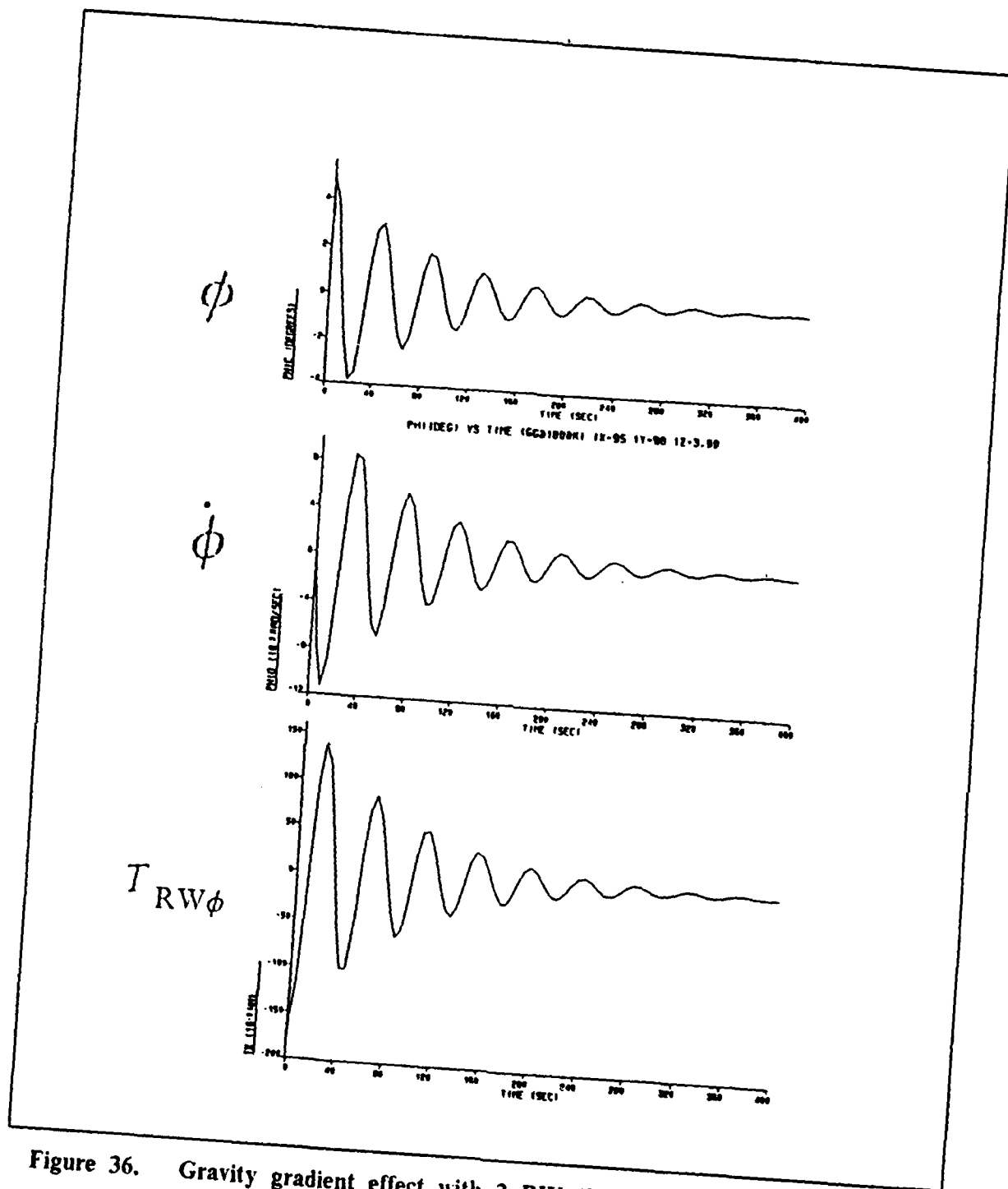


Figure 36. Gravity gradient effect with 3 RW (X axis) $I_x=95$, $I_y=98$, $I_z=3$
 $K_r = 2.0$, $\tau_r = 1.0$

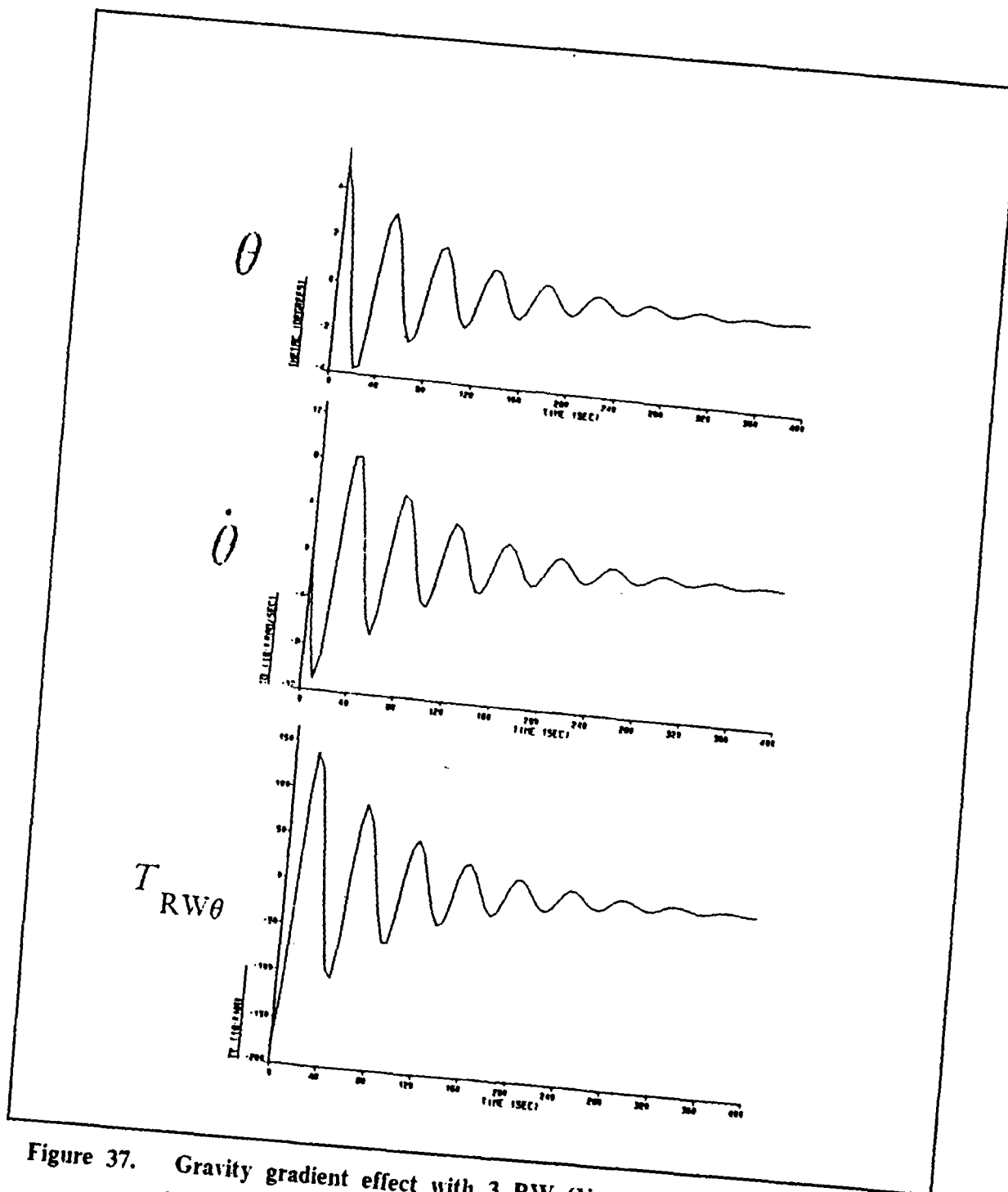


Figure 37. Gravity gradient effect with 3 RW (Y axis) $I_x=95$, $I_y=98$, $I_z=3$
 $K_y=2.0$, $\tau_y=1.0$

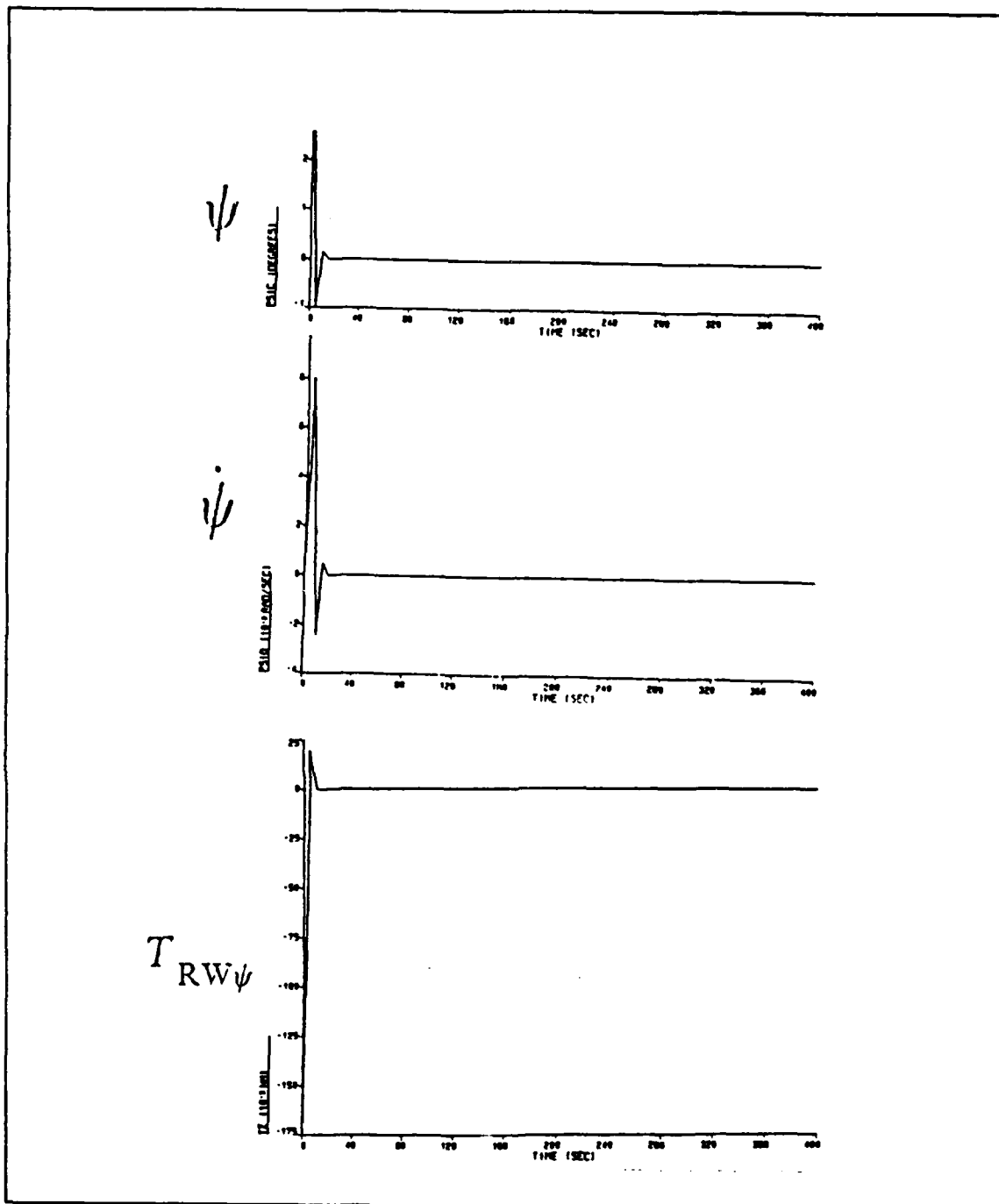


Figure 38. Gravity gradient effect with 3 RW (Z axis) $I_x=95$, $I_y=98$, $I_z=3$
 $K_z = 1.0$, $\tau_z = 1.0$

Figures 39-41 have moments of inertia of $I_x = 15$, $I_y = 18$, and $I_z = 3$ with $K_x = K_y = .2$, $K_z = .1$, and $\tau_x = \tau_y = \tau_z = 1.0$. The reduction of K_x , K_y and K_z reduces the reaction wheel torque generated.

Figure 39 shows ϕ (position), $\dot{\phi}$ (velocity), and reaction wheel torque ($T_{rw\phi}$) with respect to time. Figures 40 and 41 show θ , $\dot{\theta}$, $T_{rw\theta}$, and ψ , $\dot{\psi}$, $T_{rw\psi}$, respectively. Stabilization, within the $\pm 1^\circ$ criteria, occurs for all axes in under 200 seconds. Comparison of the magnitudes of the torque values of Figures 33-35 and Figures 39-41 for the same moment of inertia values shows a decrease of roughly a factor of five.

Increasing the moments of inertia to $I_x = 95$, $I_y = 98$ and $I_z = 3$, while holding $K_x = K_y = .2$, $K_z = .1$, and $\tau_x = \tau_y = \tau_z = 1.0$, produces Figures 42-44. This last group of reaction wheel figures shows that ≈ 650 seconds are required to dampen the system to the $\pm 1^\circ$ stabilization criteria. The tradeoffs between the different reaction wheel combinations are essentially time response against torque/power. The faster the desired response, the greater the magnitude of the restoring torque, and ultimately, the more power that will be consumed in achieving this response.

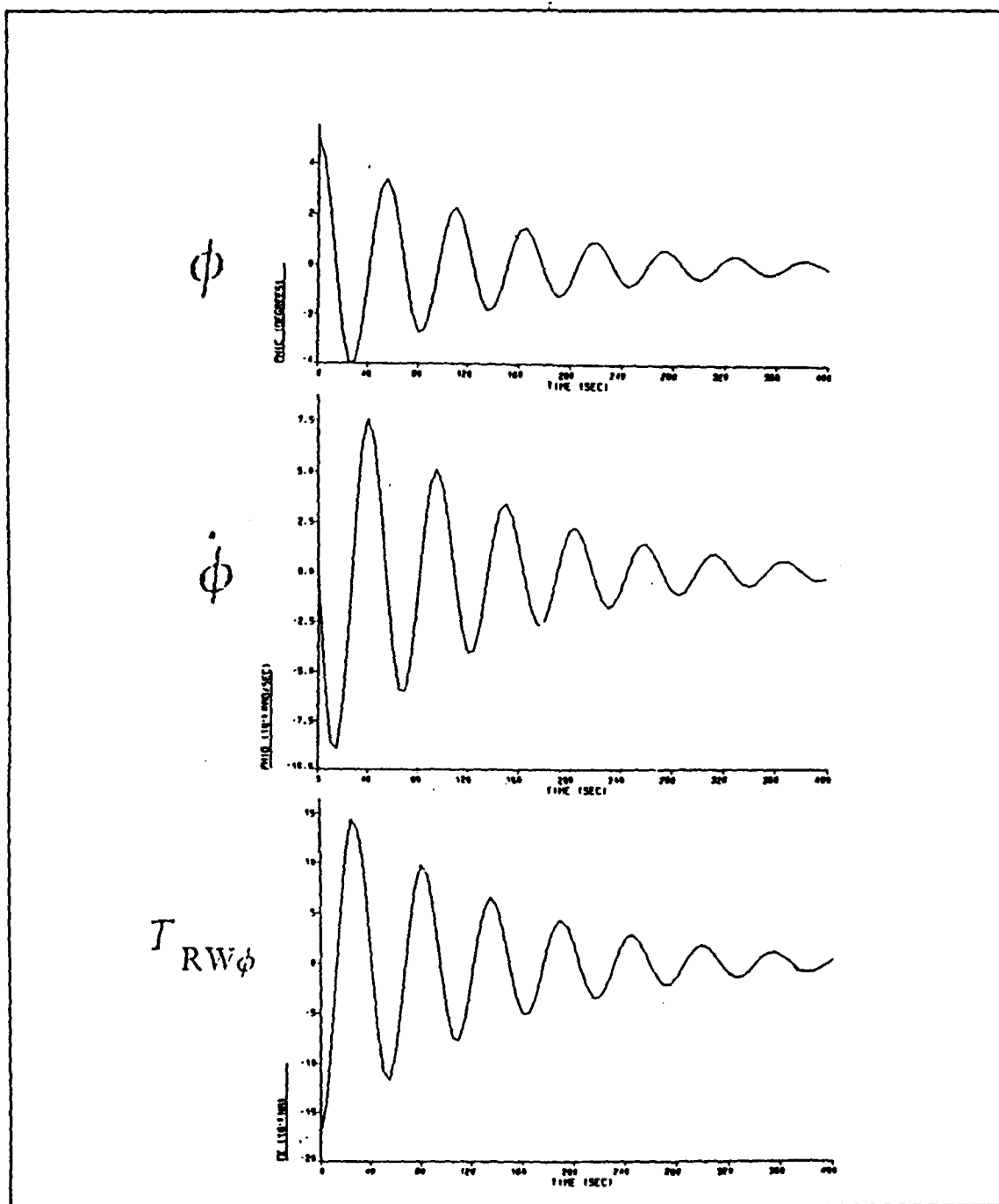


Figure 39. Gravity gradient effect with 3 RW (X axis) $I_x=15$, $I_y=18$, $I_z=3$
 $K_x=.2$, $\tau_x=1.0$

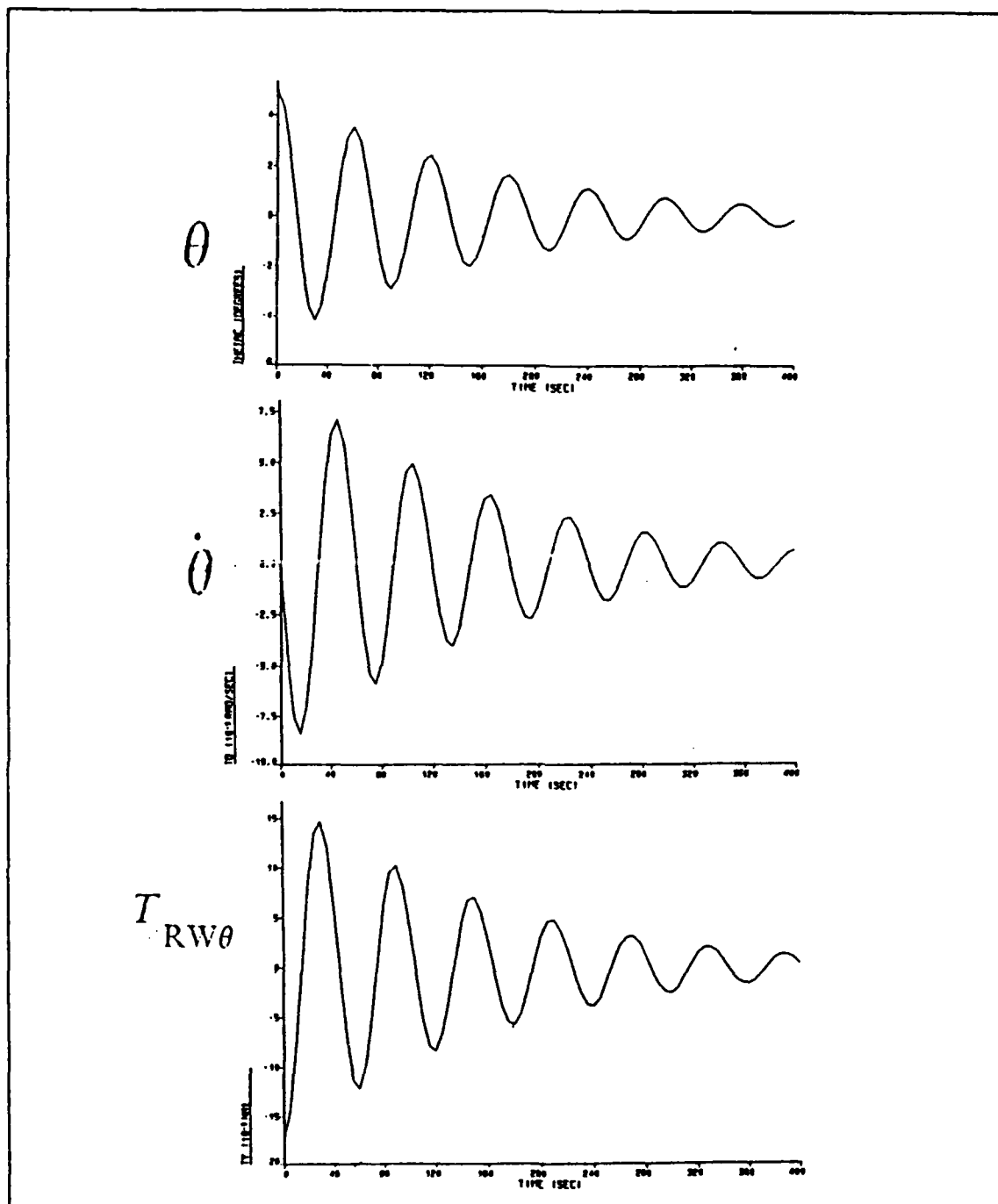


Figure 40. Gravity gradient effect with 3 RW (Y axis) $I_x=15$, $I_y=18$, $I_z=3$
 $K_y=.2$, $\tau_y=1.0$

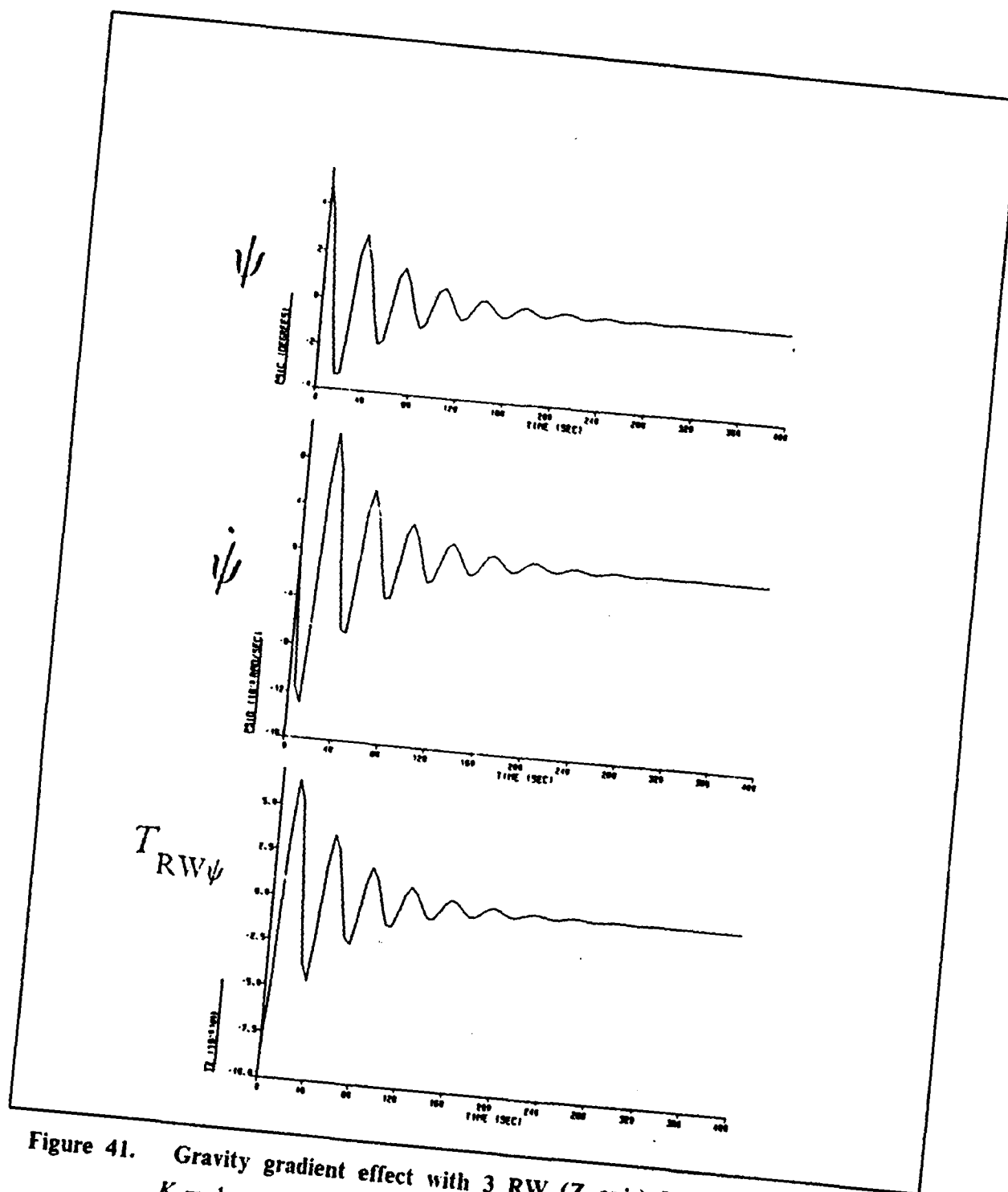


Figure 41. Gravity gradient effect with 3 RW (Z axis) $I_x=15$, $I_y=18$, $I_z=3$
 $K_z = .1$, $\tau_z = 1.0$

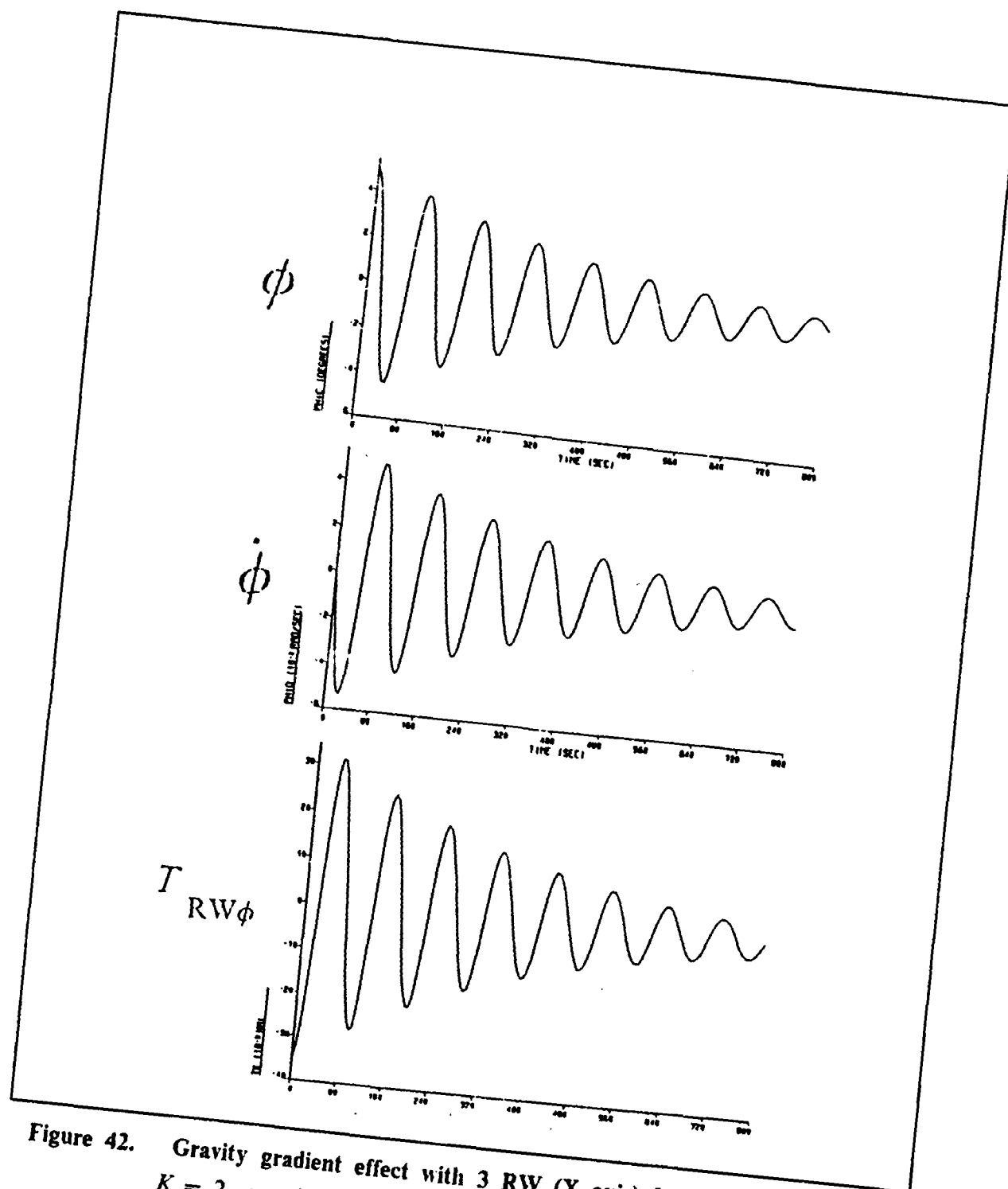


Figure 42. Gravity gradient effect with 3 RW (X axis) $I_x=95$, $I_y=98$, $I_z=3$
 $K_r = .2$, $\tau_r = 1.0$

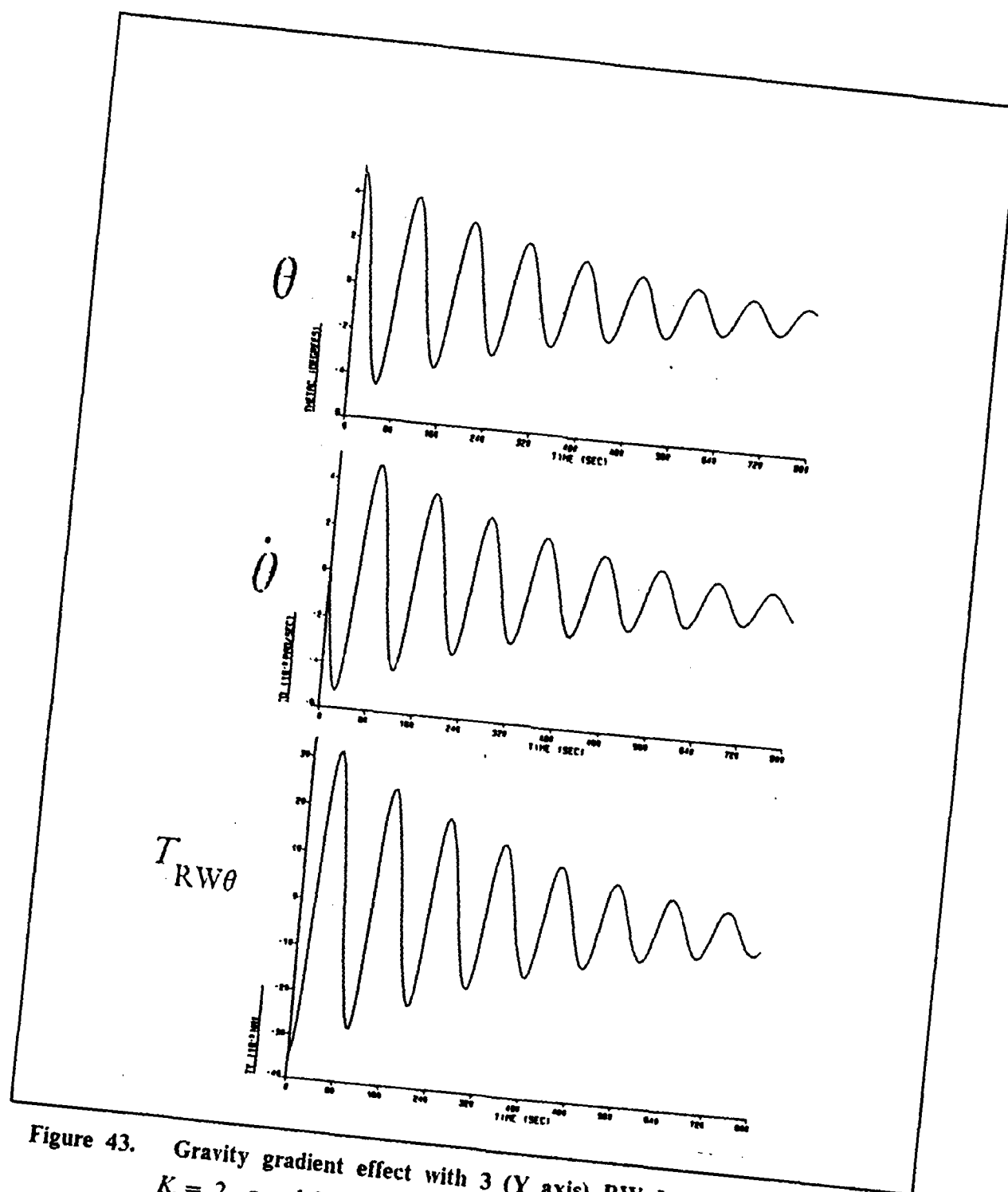


Figure 43. Gravity gradient effect with 3 (Y axis) RW $I_x=95$, $I_y=98$, $I_z=3$
 $K_y=.2$, $\tau_y=1.0$

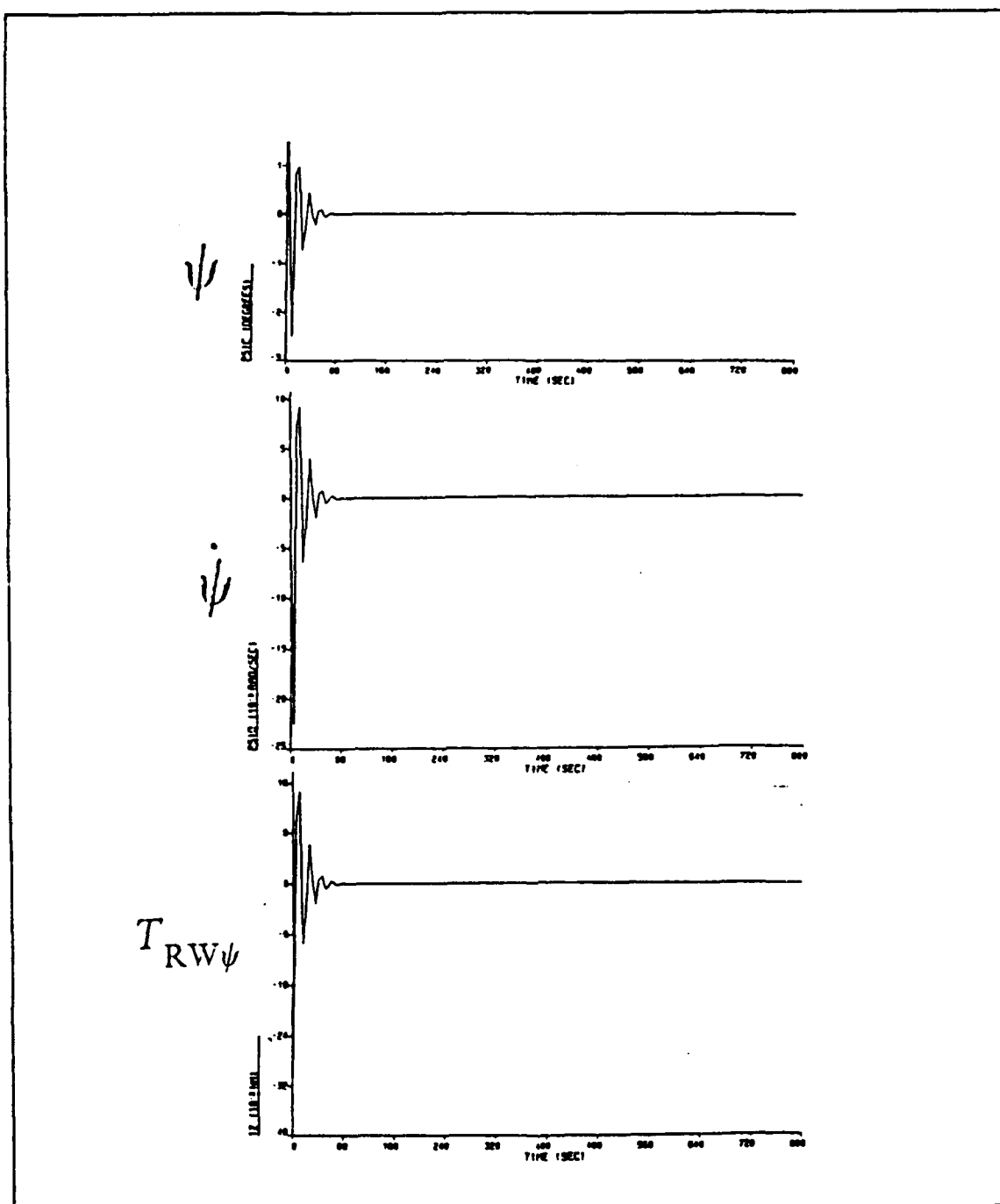


Figure 44. Gravity gradient effect with 3 RW (Z axis) $l_x=95$, $l_y=98$, $l_z=3$
 $K_z = .1$, $\tau_z = 1.0$

d. Effects of Magnetic torquers

For the magnetic torquing simulations, the initial conditions are ϕ , θ , and ψ position errors = 5° , and $\dot{\phi}$, $\dot{\theta}$, and $\dot{\psi}$ = 0. The initial restoring torque is provided by the gravity gradient effect combined with the rigid body dynamics. For the following simulations, one of the two conditions must exist prior to energizing the magnetic coils to generate magnetic torque:

1) position greater than $.5^\circ$ and velocity greater than 0, or

2) position less than $-.5^\circ$ and velocity less than 0. For the following figures, the magnetic moment varies from 9.0427 to .5 Wb-m. At the maximum value of 9.0427W-m, $N=400$ turns, $I=.5$ amp, and $A=\pi r^2$ where r is the radius at .12m. Subsequent values are obtained by reducing the current drawn.

The magnetic field in component form for an equatorial orbit can be approximated by eqs(110-112). Since the earth's magnetic field is highly dependent on the satellite's position, ORION must have the capability to determine its position in order to effectively utilize magnetic torquing. For simulation purposes, the satellite is assumed to be directly over Greenwich at time $t=0$. The magnetic coils are turned on and off at the specified strength as needed. Varying the strengths of the magnetic moments generated would enhance performance, but is beyond the scope of this thesis. The assumption that magnetic torque may be generated in any direction due to vector addition is not always valid; magnetic torque may not be generated in the direction of the magnetic field.

Figures 45-47 utilized magnetic moments of $m_x = m_y = m_z = 9.0427$ with moments of inertias $I_x = 15$, $I_y = 18$, and $I_z = 3$. For Figure 45 on page 60, the gravity gradient restoring torque takes approximately 800 seconds before meeting a condition necessary for energizing the magnetic coils. Due to the small moments of inertia, the ϕ restoring torque is needed for only a short time. Figures 46 and 47 show the θ and ψ axes essentially stabilized within the $\pm 1^\circ$ criteria after the initial magnetic torque pulse. For the θ axis, this pulse occurs at the 1200 seconds and lasts for approximately 300 seconds. The θ axis has a lower frequency response and, therefore, takes longer to meet the condition necessary to energize the magnetic coils. Due to its relatively small moment of inertia, the ψ axis chatters slightly before stabilizing. A smaller magnitude of restoring torque eliminates this problem.

Increasing the moments of inertia to $I_x = 95$, $I_y = 98$, and $I_z = 3$ while leaving the magnetic moments m_x , m_y , and m_z constant at 9.0427wb-m, produces Figures 48-50. As expected, more restoring torque is needed to stabilize the ϕ and θ axes forc-

ing the magnetic coils to remain energized for a longer period of time. The time needed for all axes to be within the $\pm 1^\circ$ criteria is limited by the θ axis. Stabilization occurs within 2800 seconds while for the case with the smaller moments of inertias, stabilization occurs at approximately 2100 seconds.

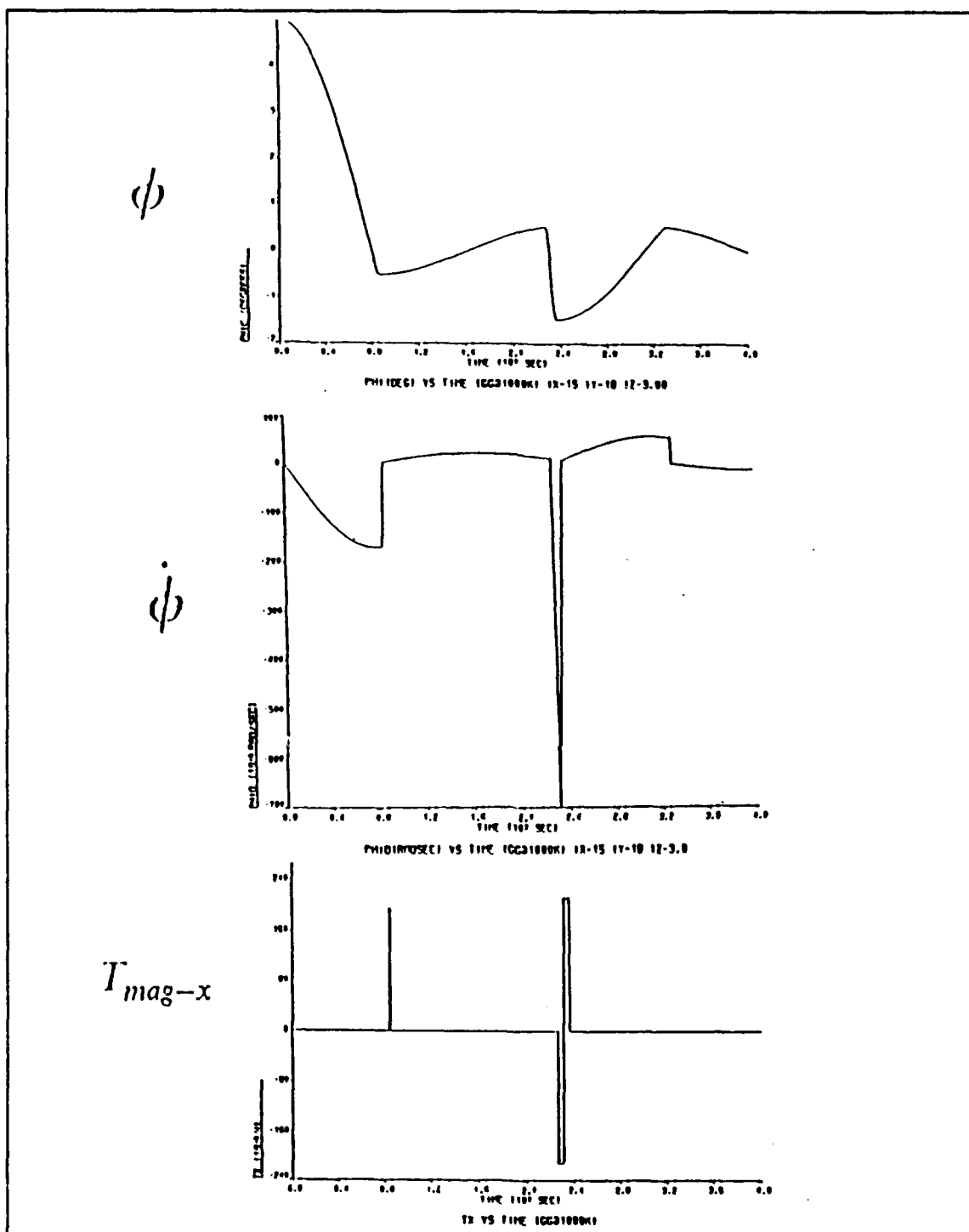


Figure 45. Gravity gradient with magnetic torquing (X axis): Magnetic moment = 9.0427 W-m $I_x = 15$, $I_y = 18$, $I_z = 3$.

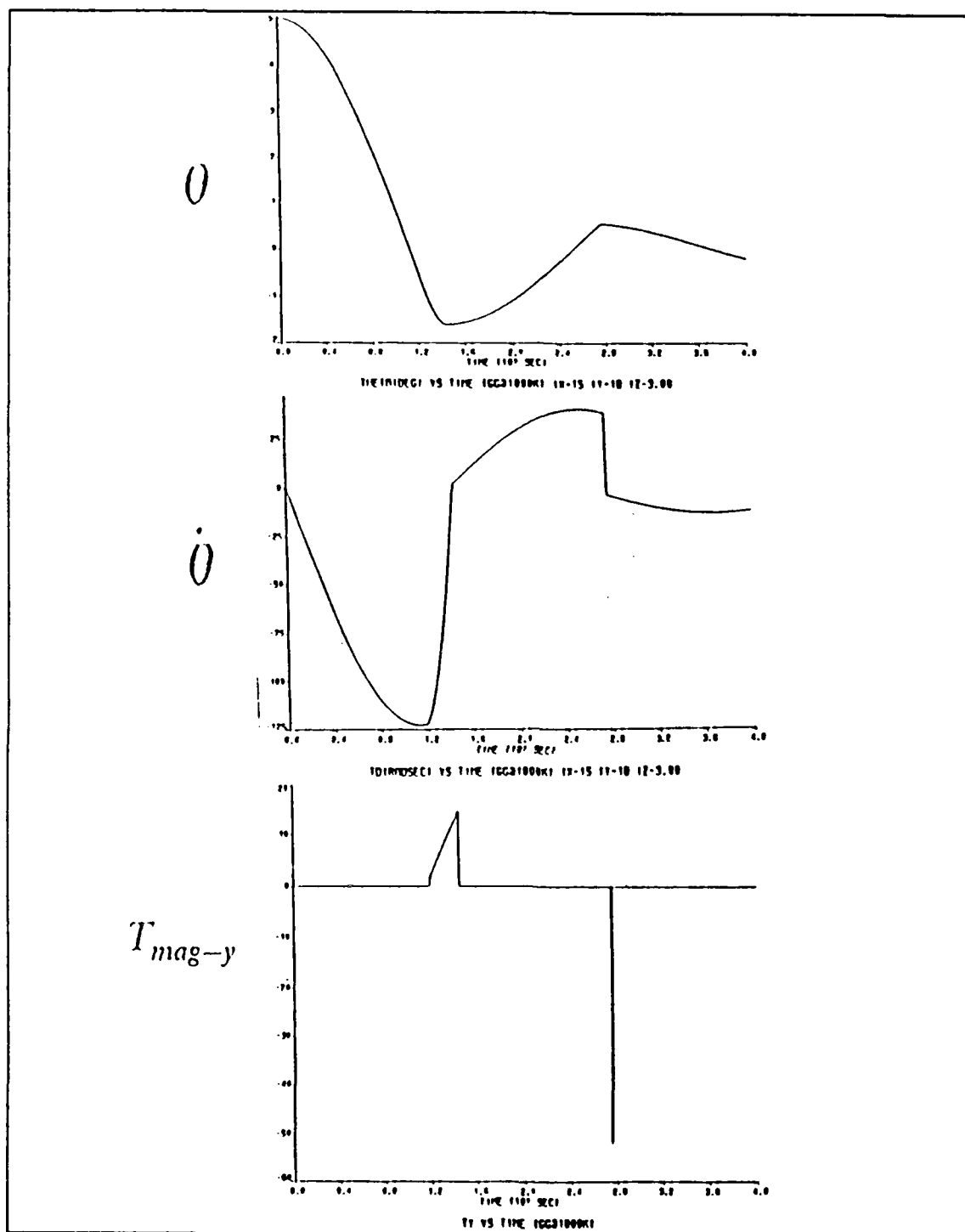


Figure 46. Gravity gradient with magnetic torquing (Y axis): Magnetic moment = 9.0427W-m $I_x = 15$, $I_y = 18$, $I_z = 3$.

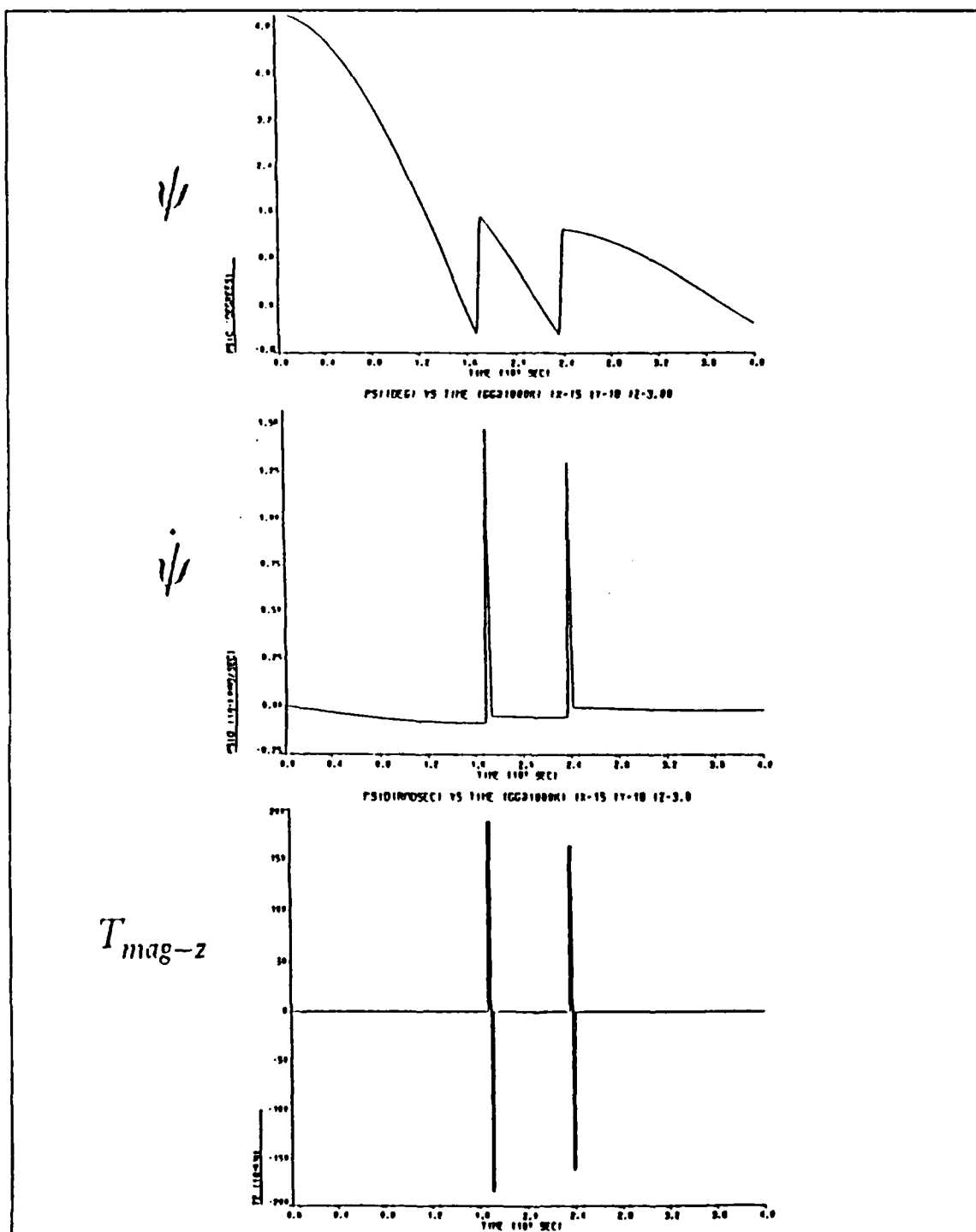


Figure 47. Gravity gradient with magnetic torquing (Z axis): Magnetic moment = 9.0427W-m $I_x = 15$, $I_y = 18$, $I_z = 3$.

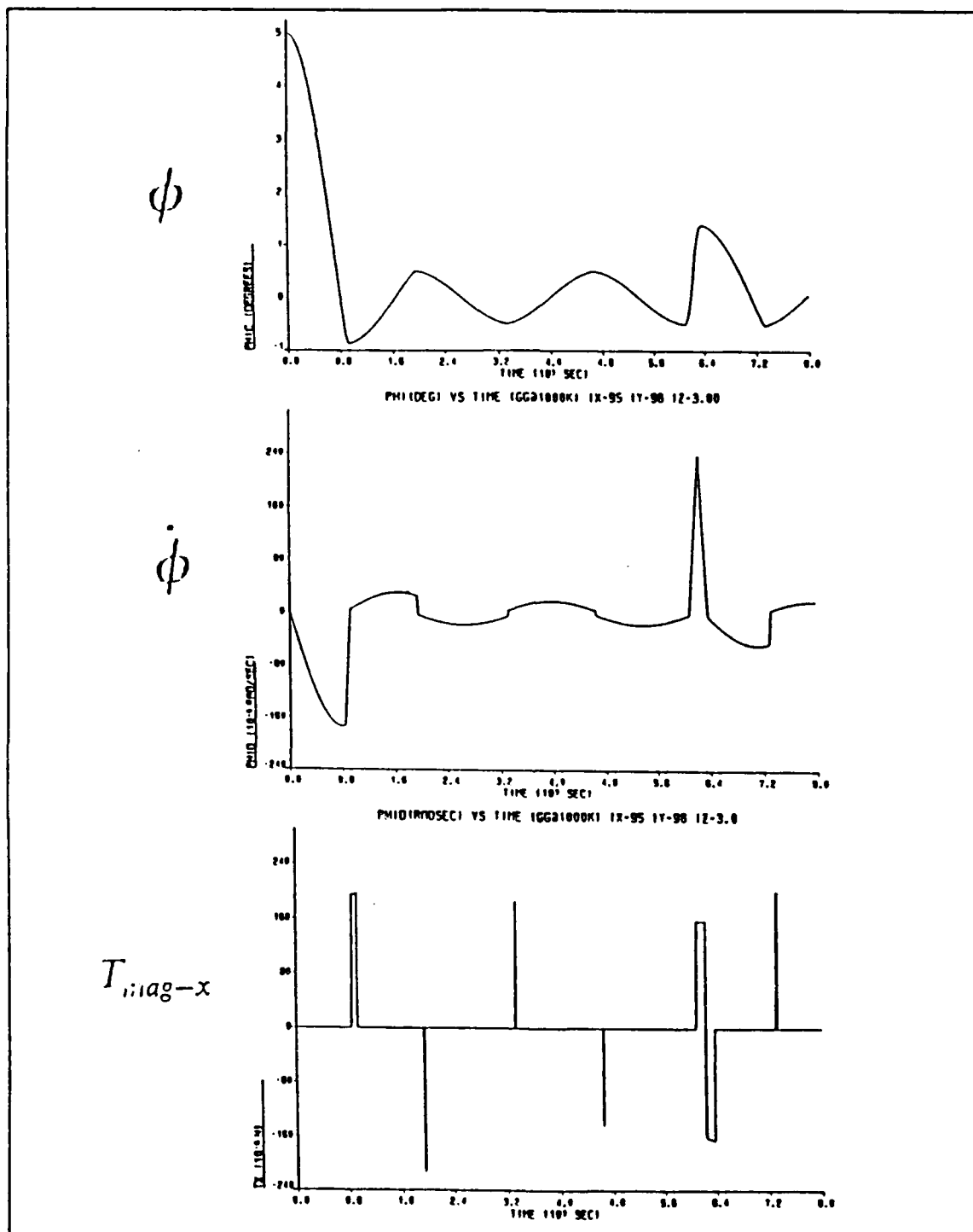


Figure 48. Gravity gradient with magnetic torquing (X axis): Magnetic moment = 9.0427W-m Ix = 95, Iy = 98, Iz = 3.

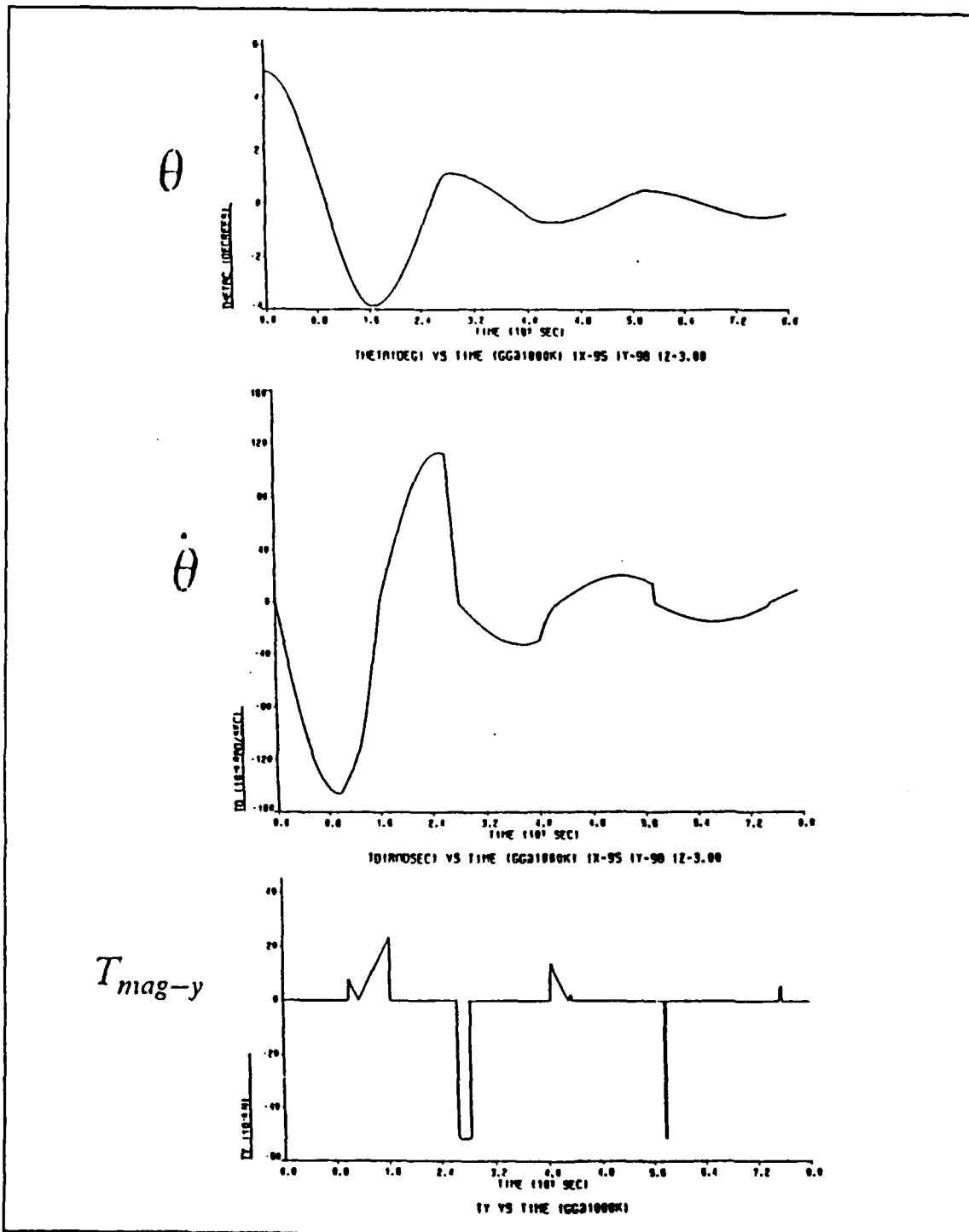


Figure 49. Gravity gradient with magnetic torquing (Y axis): Magnetic moment = 9.0427W-m $I_x = 95$, $I_y = 98$, $I_z = 3$.

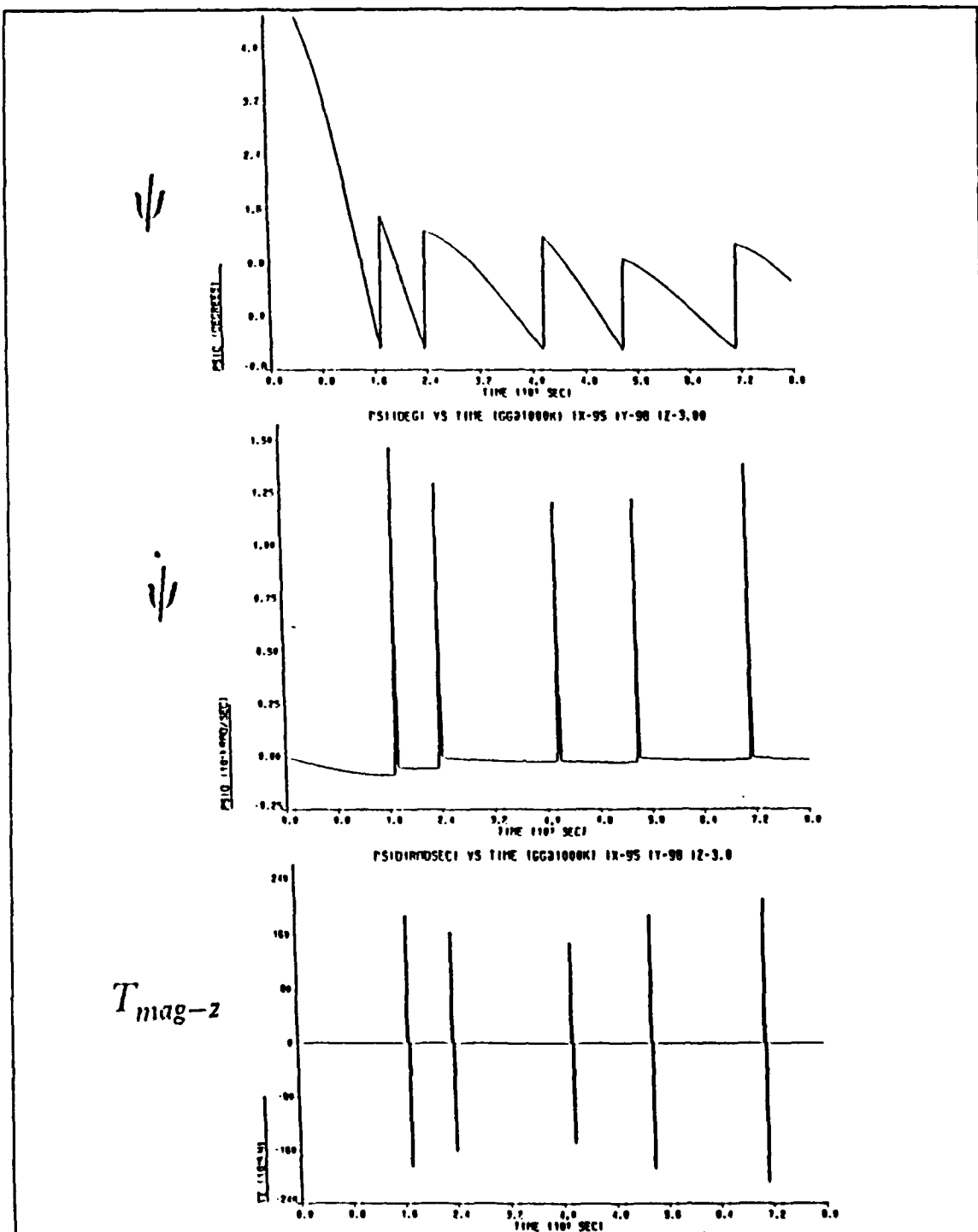


Figure 50. Gravity gradient with magnetic torquing (Z axis): Magnetic moment = 9.0427W-m $I_x=95$, $I_y=98$, $I_z=3$.

Reducing the strength of the magnetic moments reduces the torque that is generated and, thereby, slows the response time to stabilization. For Figures 51-56, the magnetic moments $m_x = m_y = m_z = 1.0$. Figures 51-53 have moments of inertia $I_x = 15$, $I_y = 18$, and $I_z = 3$. Stabilization for the θ axis occurs within approximately 3600 seconds. Increasing the moments of inertia to $I_x = 95$, $I_y = 98$, and $I_z = 3$ produces Figures 54-56. Stabilization within the $\pm 1^\circ$ criteria for the θ axis occurs at approximately 11000 seconds. The length of time that the magnetic torquers are energized increases as the strength of the moment decreases. Figures 57-62 show the effects of magnetic torquing using a maximum magnetic moment of .5Wb-m for each coil. Figures 57-59 show that for low moments of inertia ($I_x = 15$, $I_y = 18$, and $I_z = 3$), stabilization occurs within the $\pm 1^\circ$ within 4800 seconds. Increasing the moments of inertia to $I_x = 95$, $I_y = 98$, and $I_z = 3$ holding the maximum magnetic moment = .5Wb-m, produces Figures 60-62. In Figure 61, the θ axis may take a prohibitively long time.

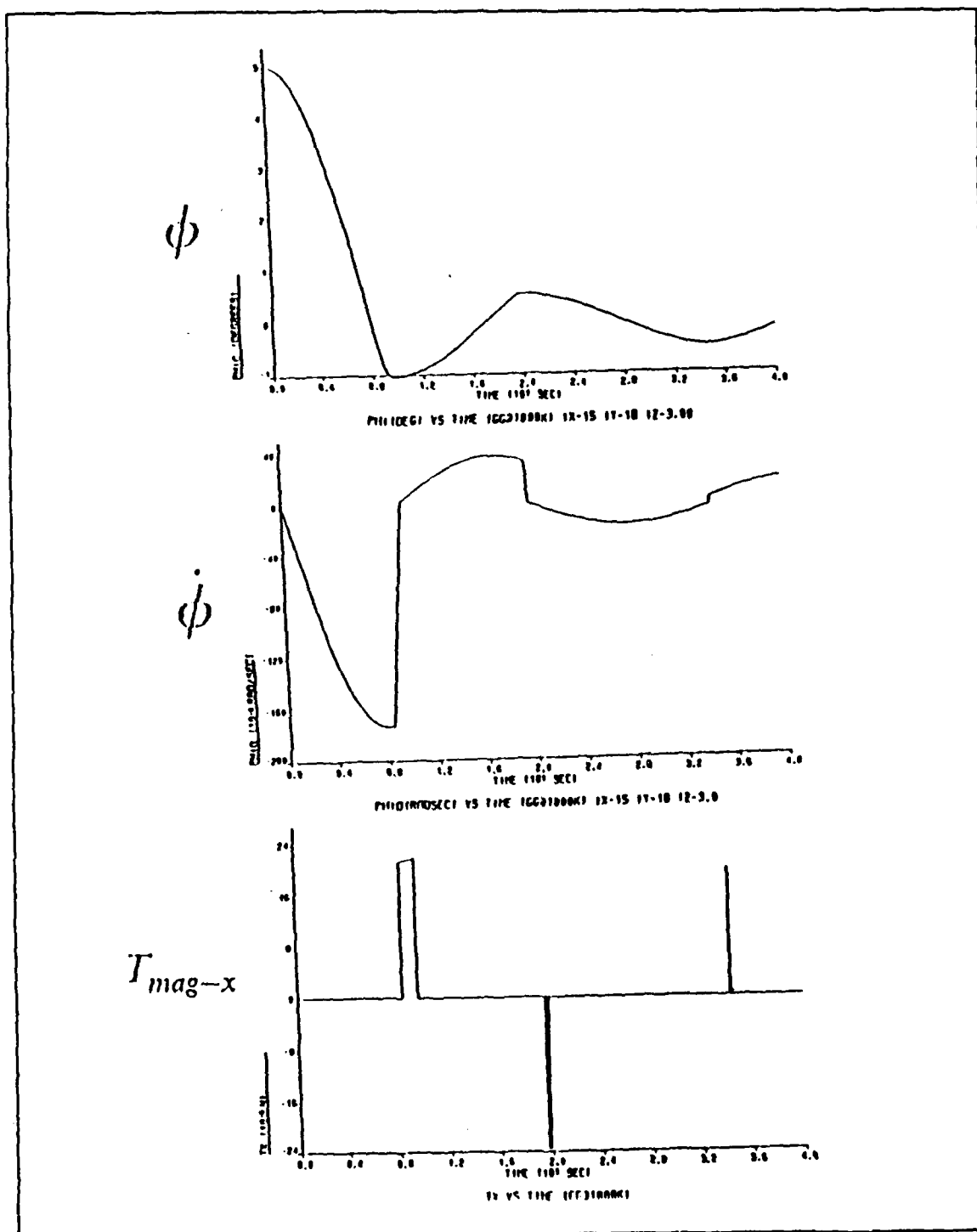


Figure 51. Gravity gradient with magnetic torquing (X axis): Magnetic moment = 1.0W-m $I_x = 15$, $I_y = 18$, $I_z = 3$.

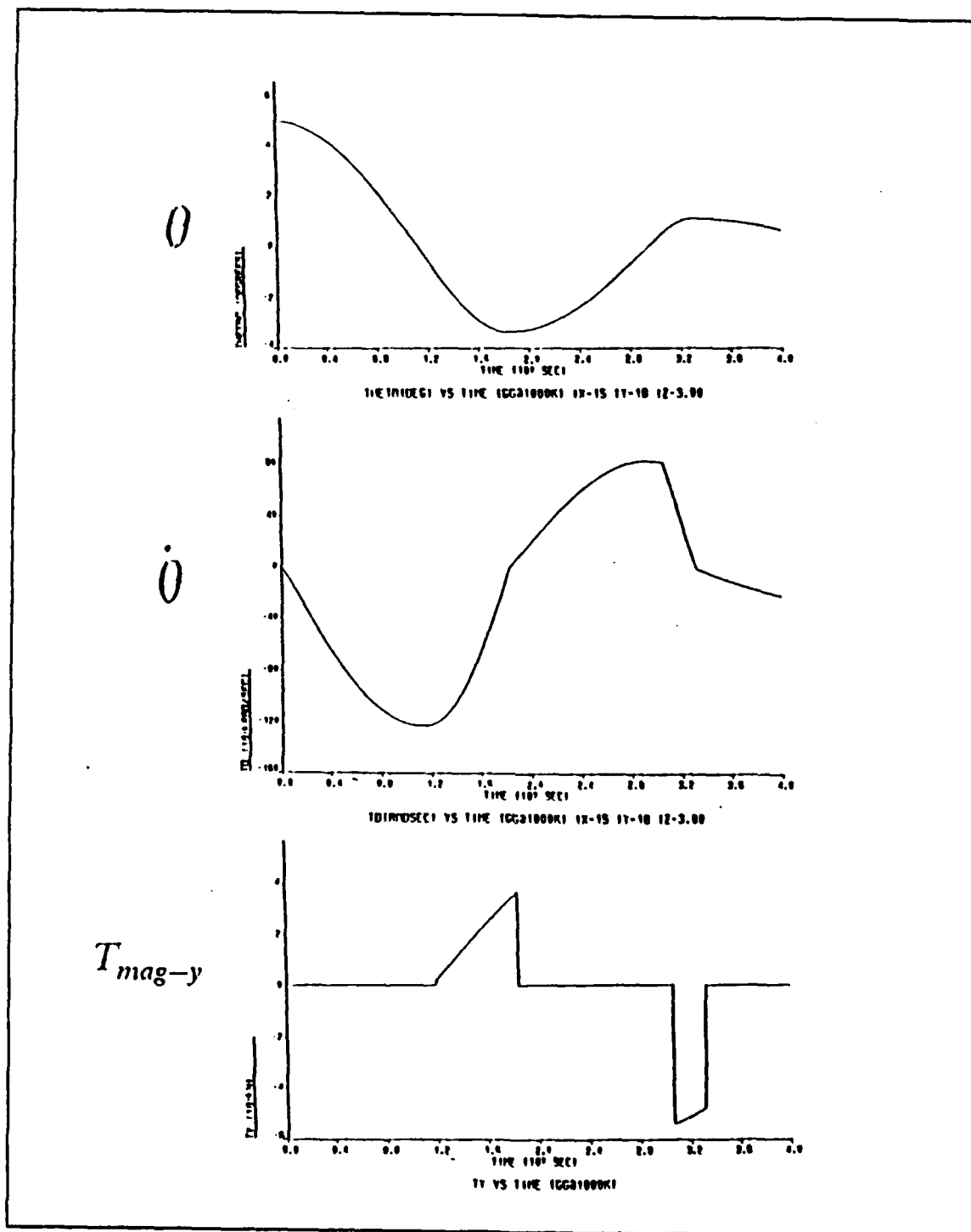


Figure 52. Gravity gradient with magnetic torquing (Y axis): Magnetic moment = 1.0W-m $I_x = 15$, $I_y = 18$, $I_z = 3$.

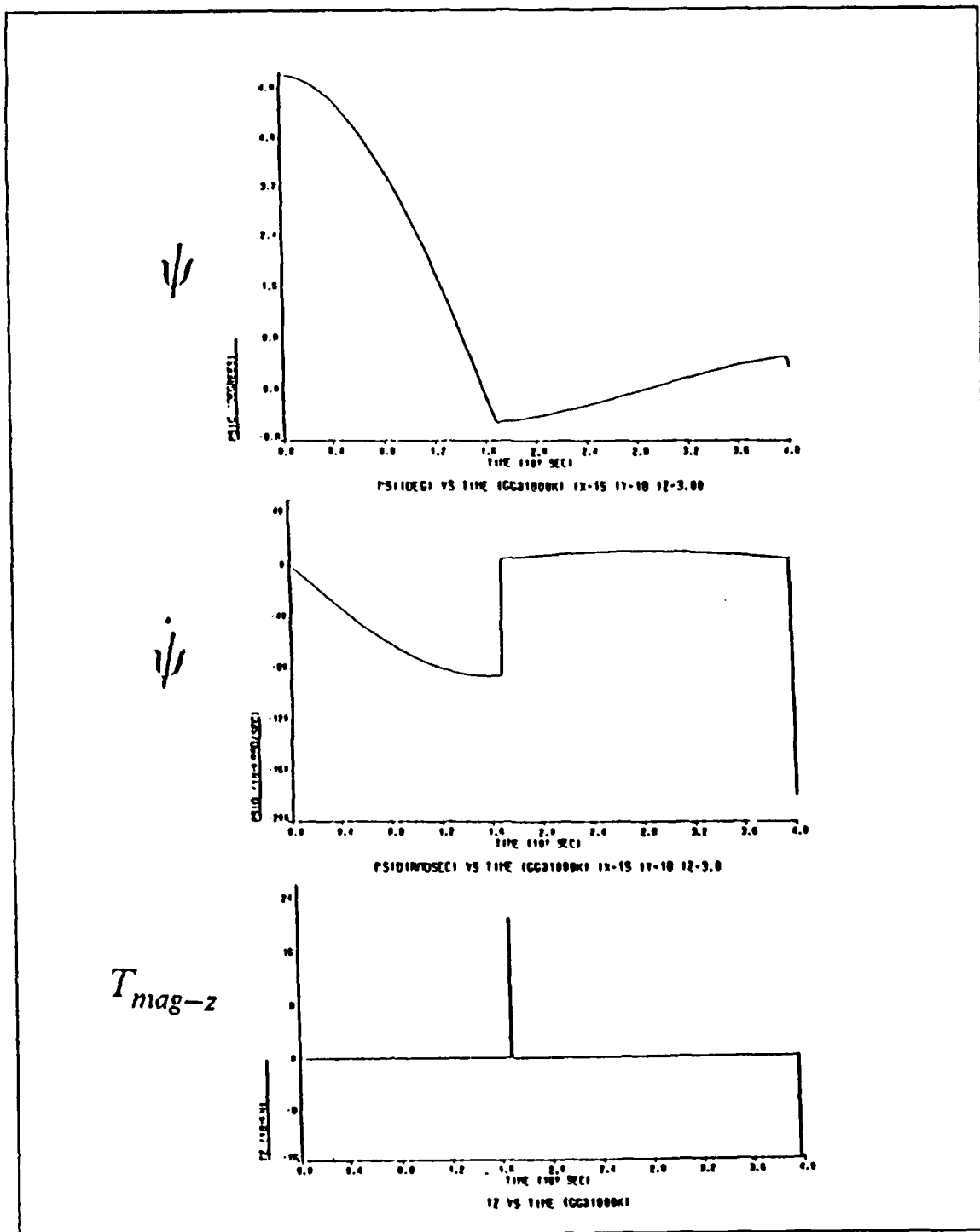


Figure 53. Gravity gradient with magnetic torquing (Z axis): Magnetic moment = 1.0W-m $I_x = 15$, $I_y = 18$, $I_z = 3$.

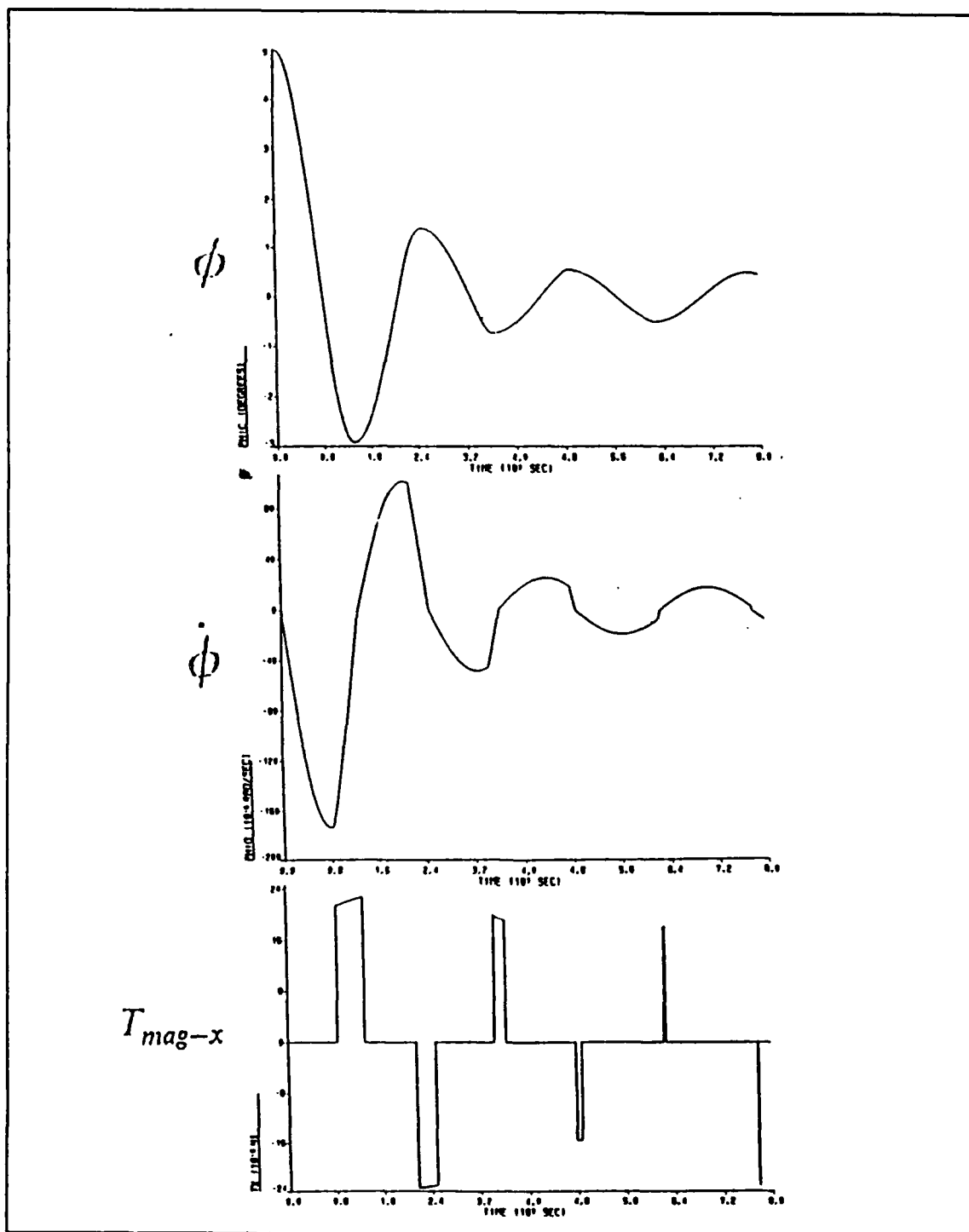


Figure 54. Gravity gradient with magnetic torquing (X axis): Magnetic moment = 1.0W-m $I_x = 95$, $I_y = 98$, $I_z = 3$.

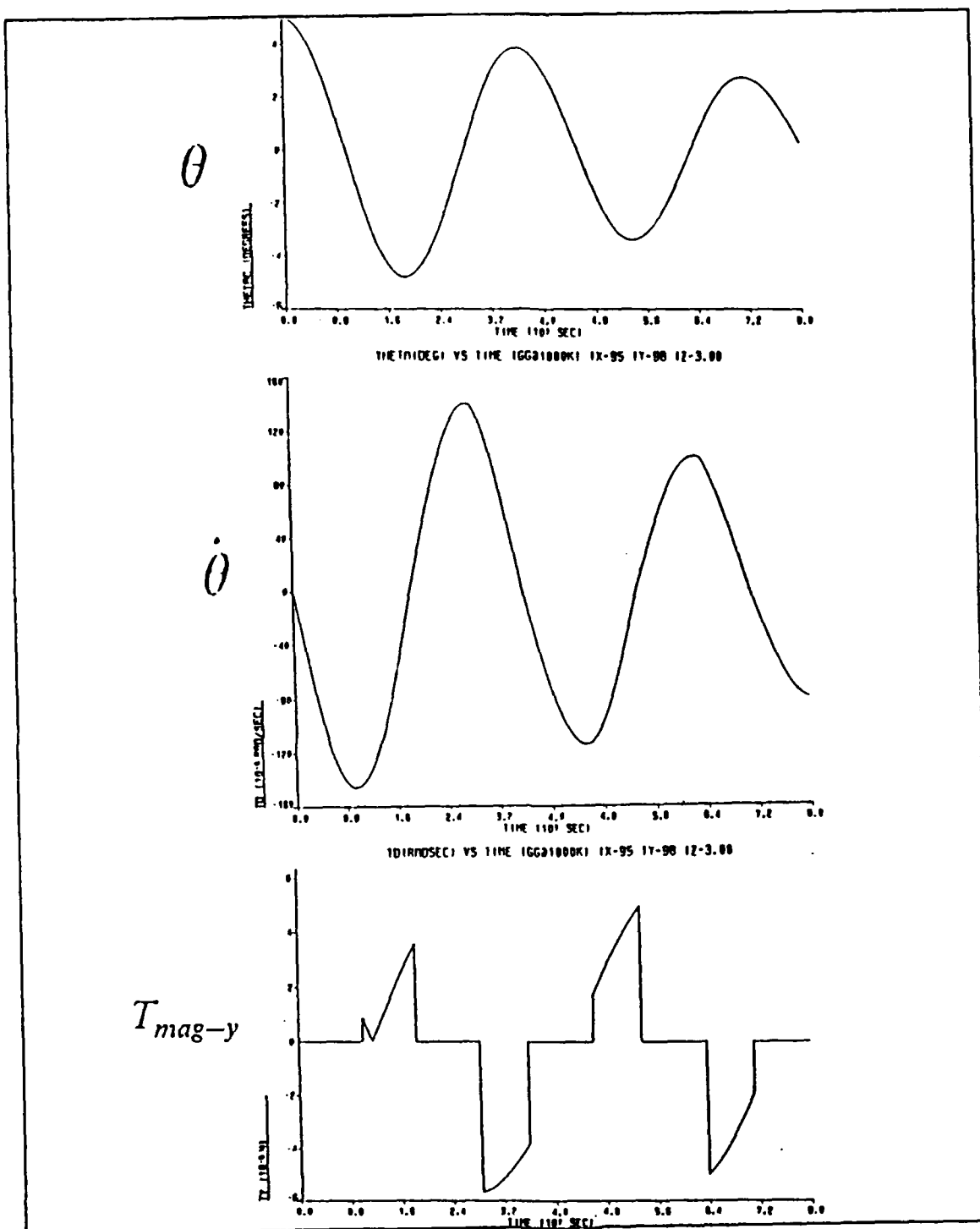


Figure 55. Gravity gradient with magnetic torquing (Y axis): Magnetic moment = 1.0W-m $I_x = 95$, $I_y = 98$, $I_z = 3$.

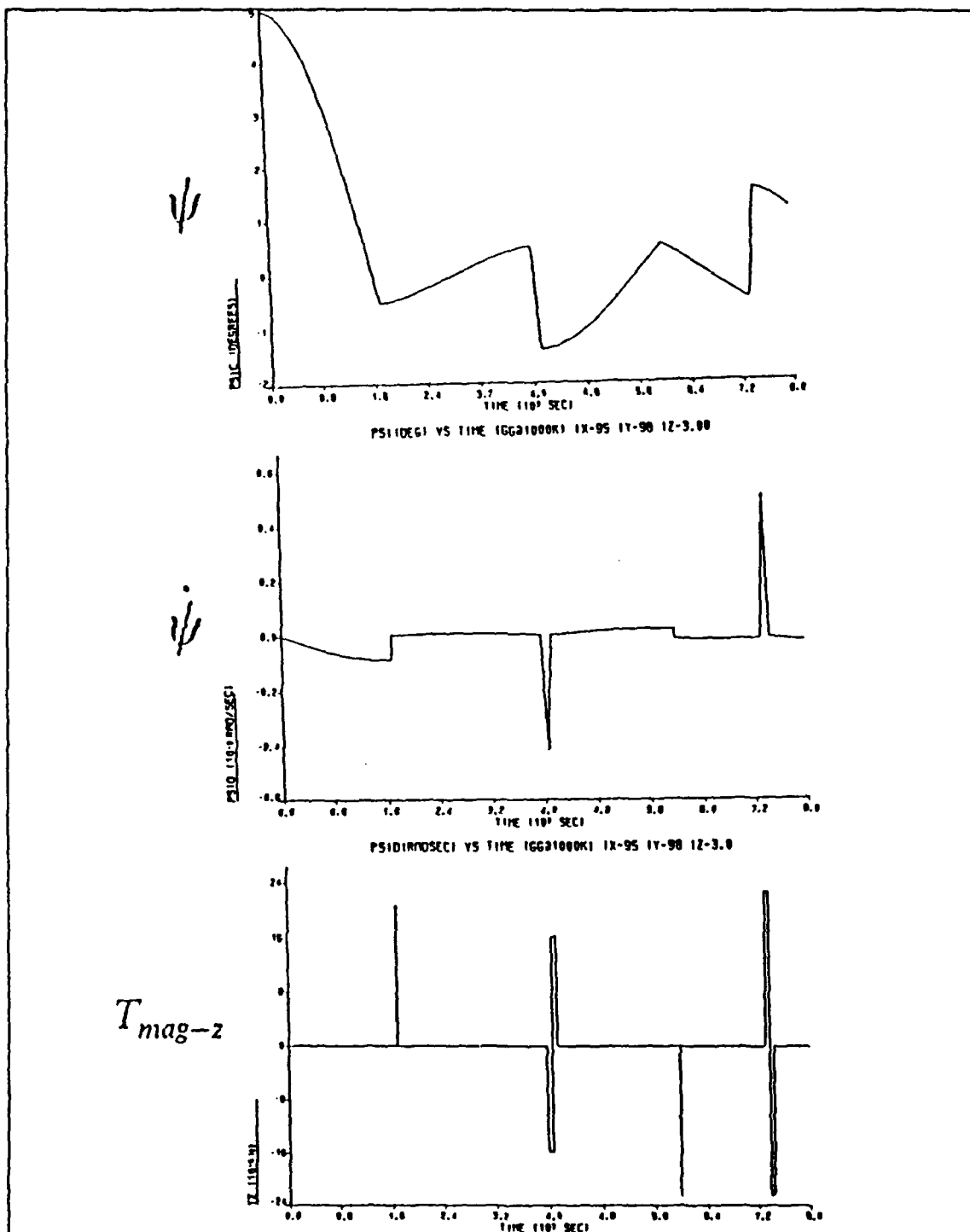


Figure 56. Gravity gradient with magnetic torquing (Z axis): Magnetic moment = 1.0W-m $I_x=95$, $I_y=98$, $I_z=3$.

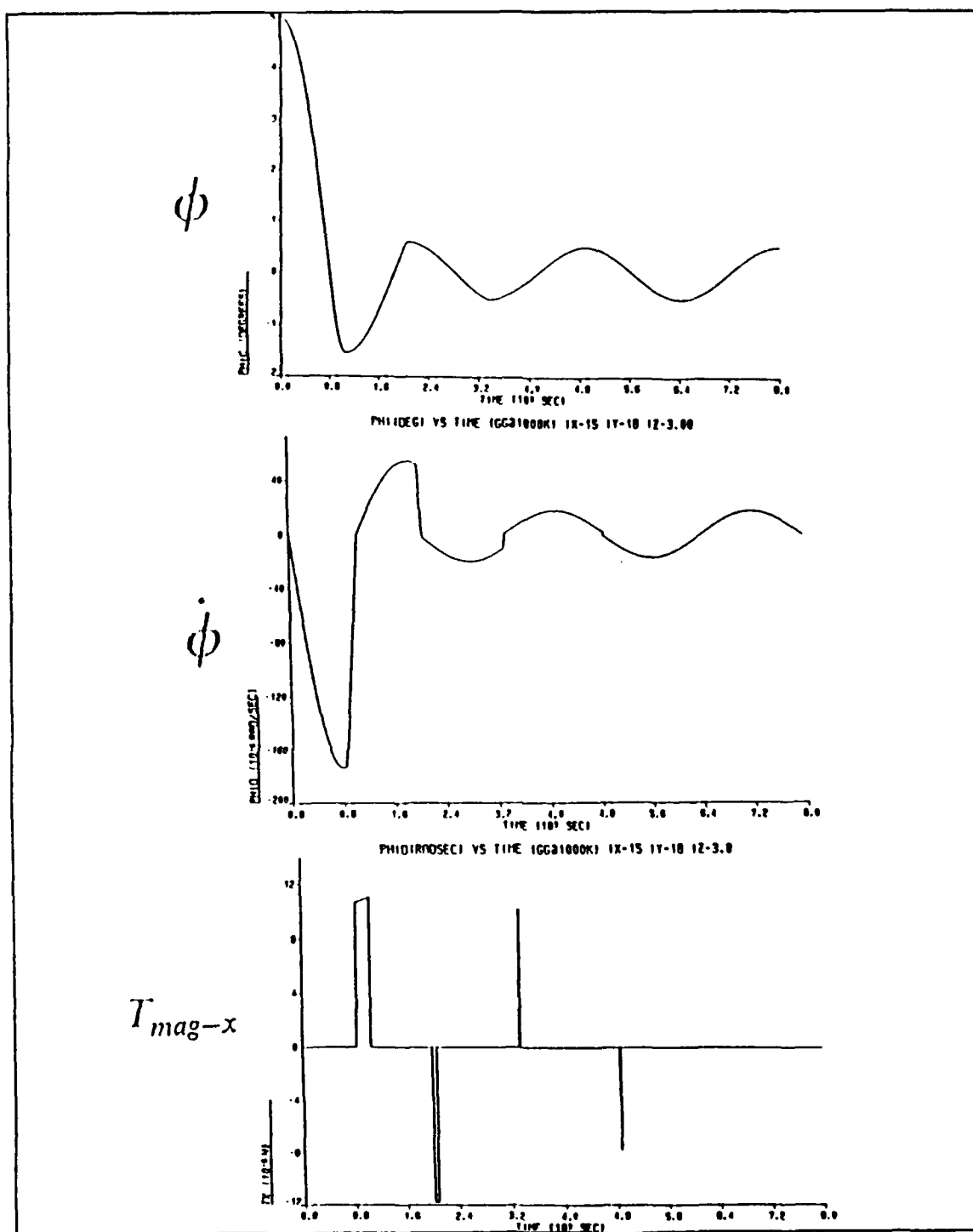


Figure 57. Gravity gradient with magnetic torquing (X axis): Magnetic moment = .50W-m $I_x = 15$, $I_y = 18$, $I_z = 3$.

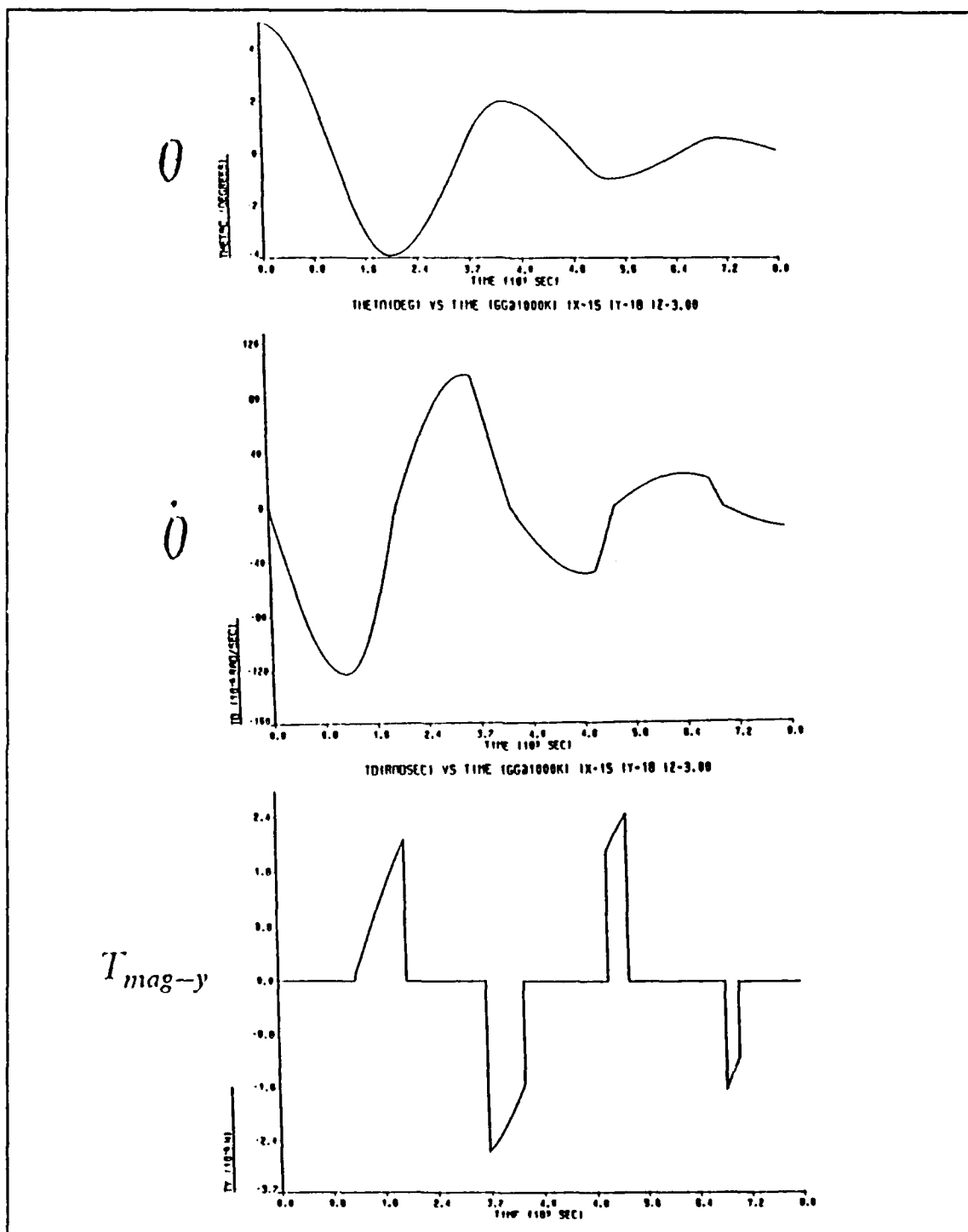


Figure 58. Gravity gradient with magnetic torquing (Y axis): Magnetic moment = .50W-m $I_x = 15$, $I_y = 18$, $I_z = 3$.

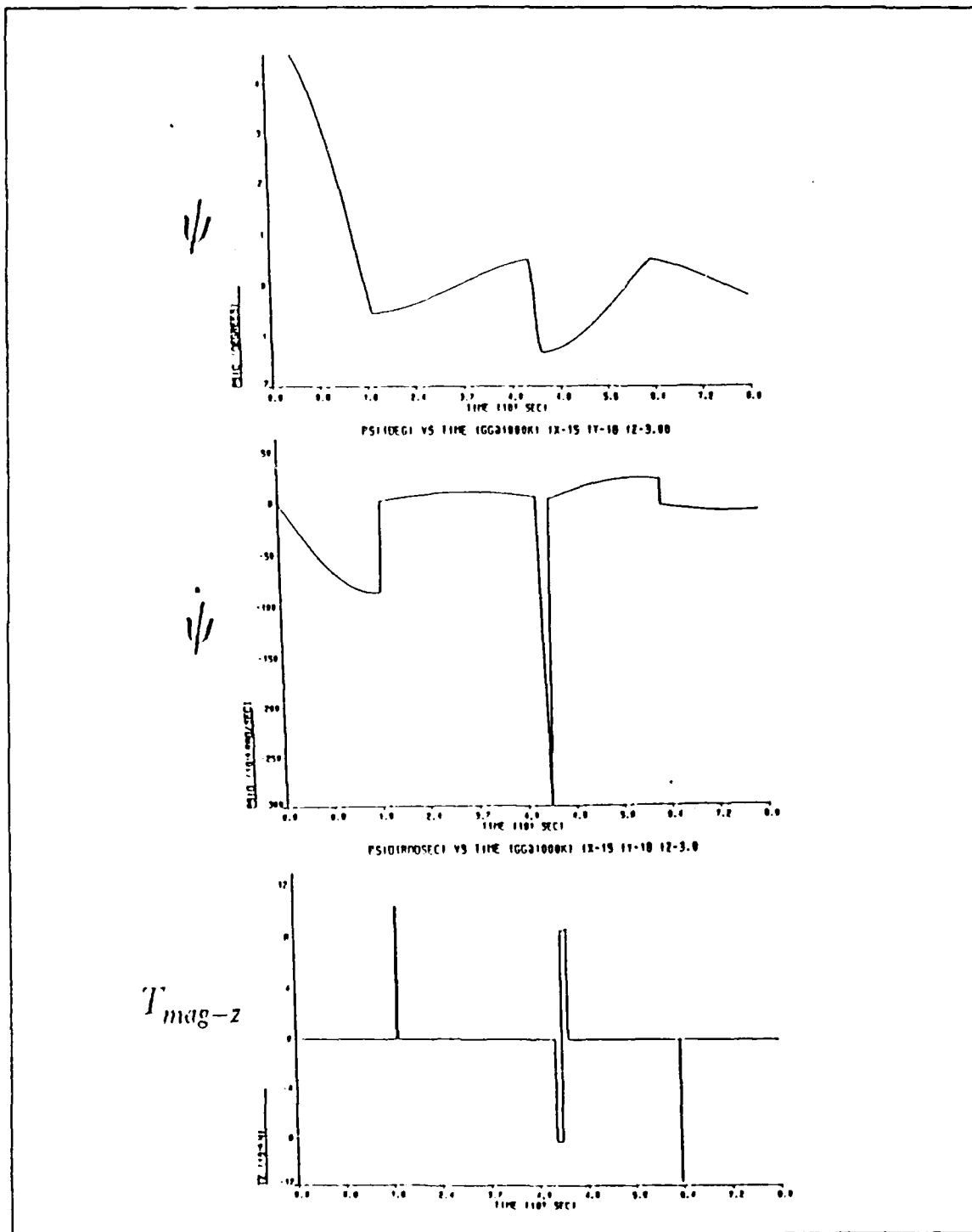


Figure 59. Gravity gradient with magnetic torquing (Z axis): Magnetic moment = .50W-m $I_x = 15$, $I_y = 18$, $I_z = 3$.

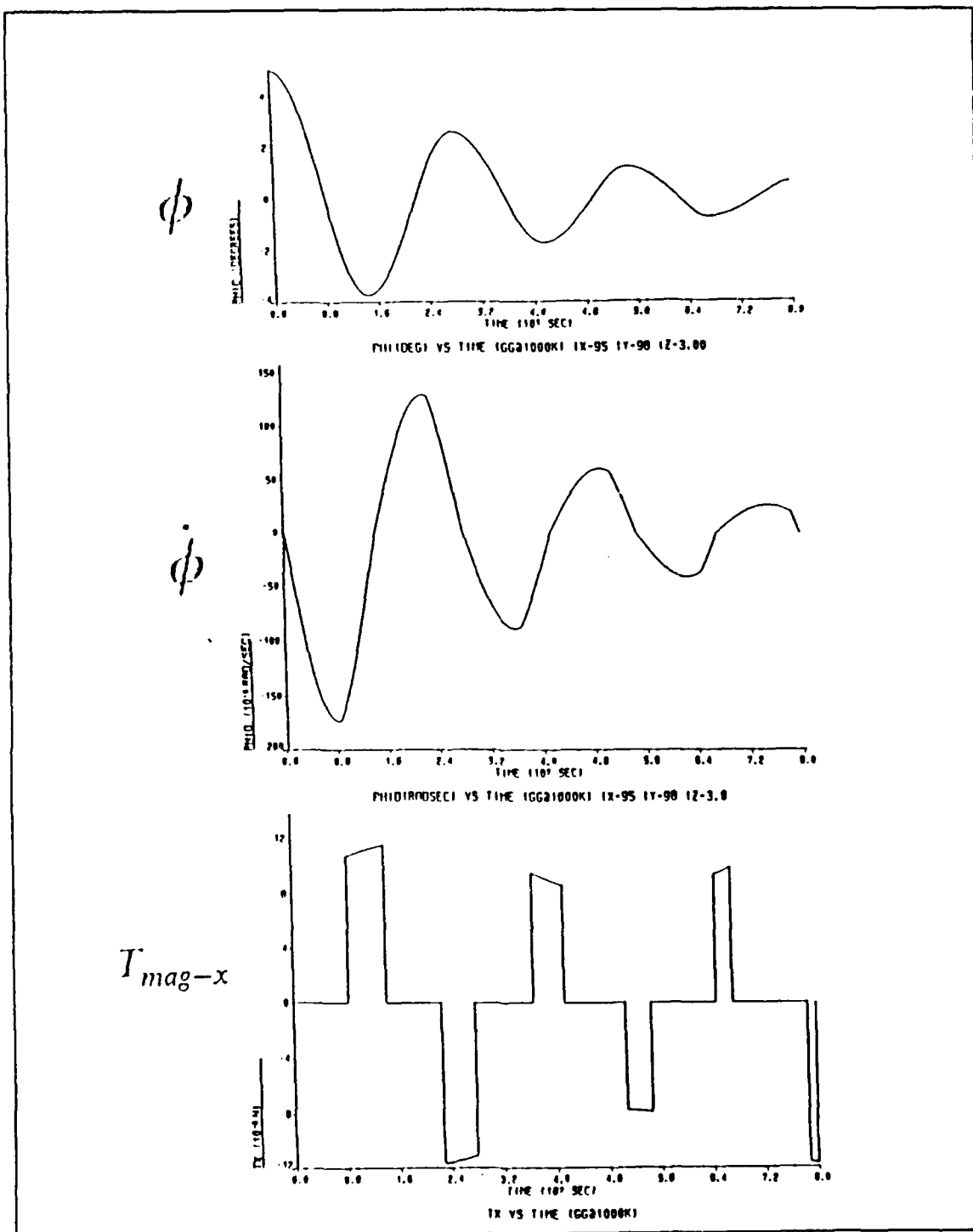


Figure 60. Gravity gradient with magnetic torquing (X AXIS): Magnetic moment = .50W-m $I_x = 95$, $I_y = 98$, $I_z = 3$.

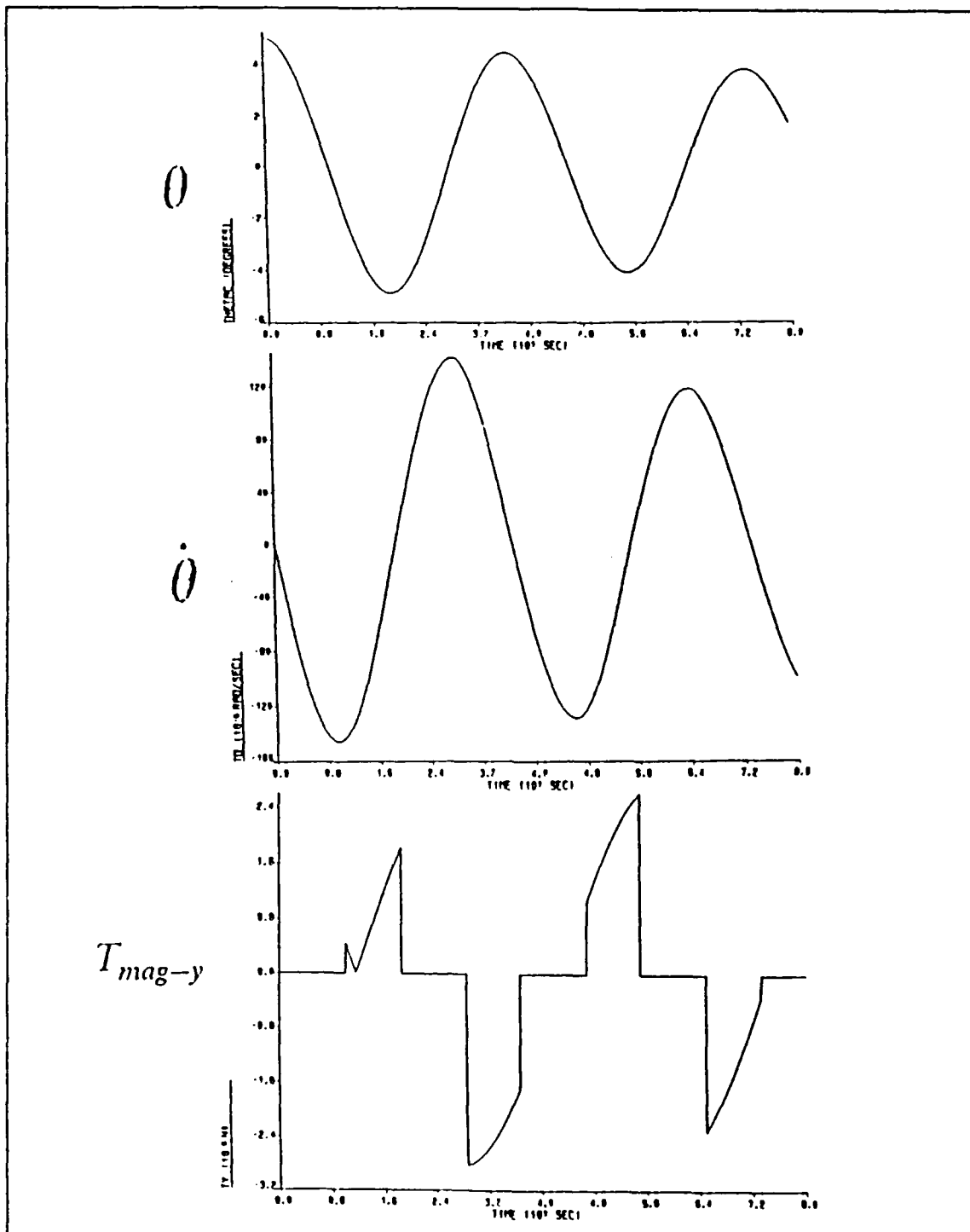


Figure 61. Gravity gradient with magnetic torquing (Y AXIS): Magnetic moment = .50W-m $I_x = 95$, $I_y = 98$, $I_z = 3$.

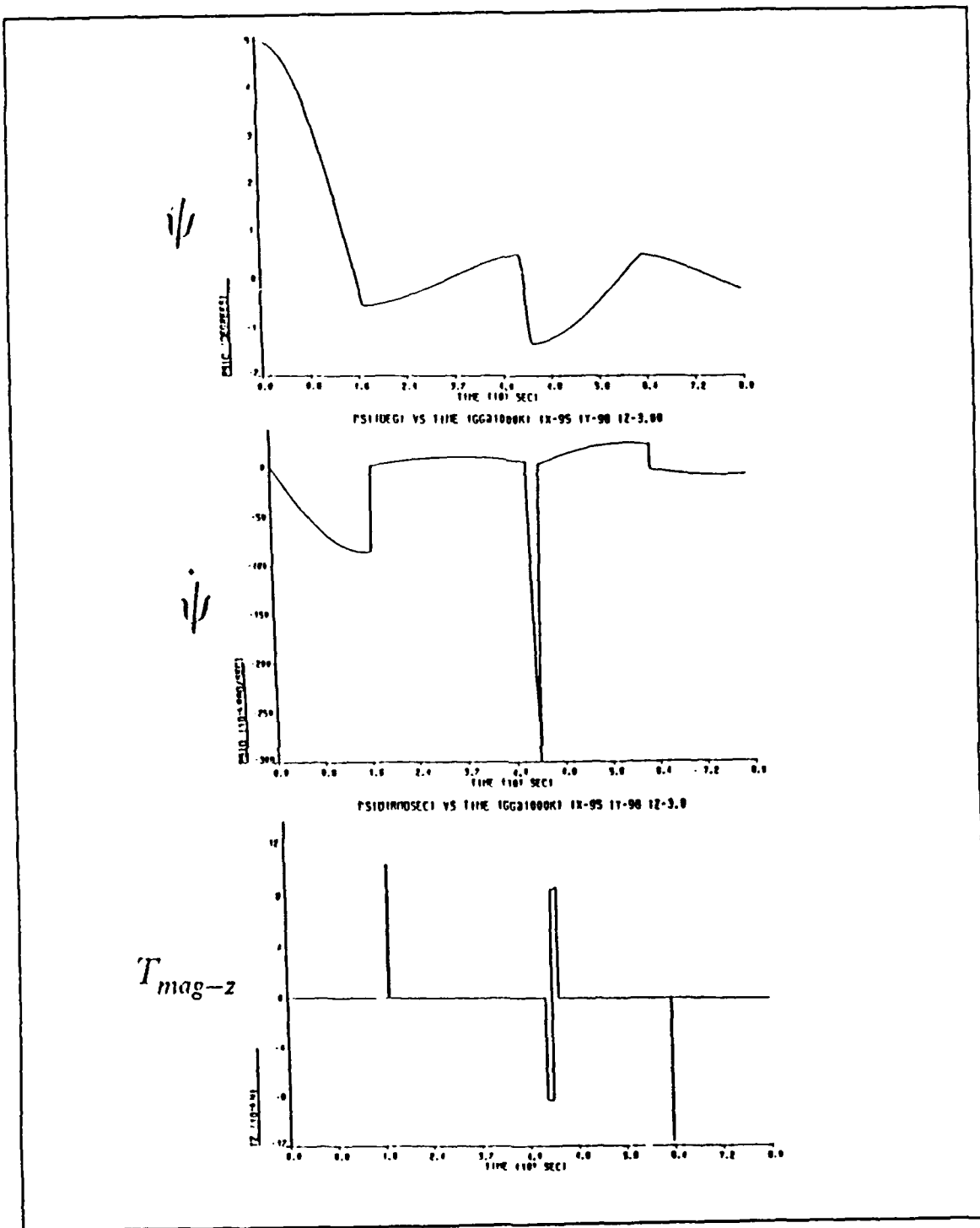
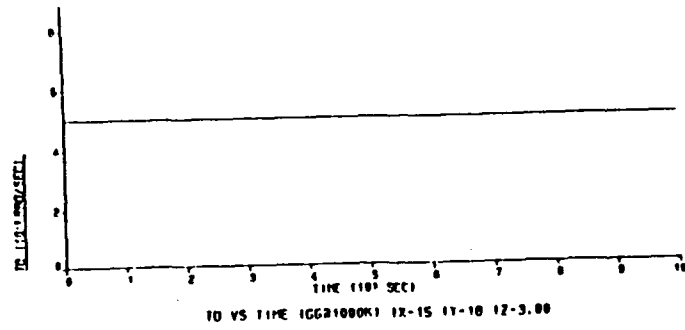


Figure 62. Gravity gradient with magnetic torquing (Z AXIS): Magnetic moment = .50W-m $I_x = 95$, $I_y = 98$, $I_z = 3$.

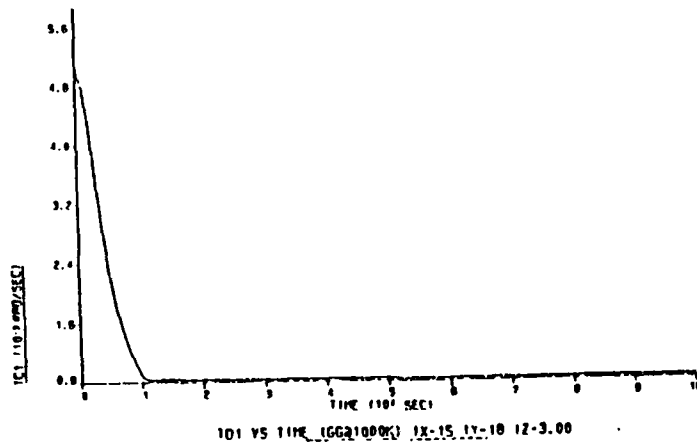
3. Gravity Gradient capture (from tumbling mode)

Increasing the inertia will reduce the tumbling rate by conforming to the conservation of angular momentum, $I_0\omega_0 = I_1\omega_1$. As the inertia increases, a corresponding decrease in angular rate must be realized. This is useful in obtaining the initial gravity gradient capture from a tumbling mode. Figure 63 on page 80 shows that for a slow tumbling satellite, the change in the moment of inertia by extending the boom may be sufficient to allow gravity gradient capture. The satellite is initially tumbling at a rate of 5 rotations per orbit about the pitch axis. The extension of the boom increases the moment of inertia about the y axis by a factor of 6; therefore, by the conservation of angular momentum, the angular rate must decrease by a factor of 6. This reduces the rotations per orbit to approximately 5/6 per orbit well below the one rotation per orbit rate necessary to achieve gravity gradient capture. Figure 63a shows the initial tumbling rate of 5 rotations per orbit. Figure 63b shows the corresponding decrease in the tumbling rate as the moment of inertia is increased. Figure 63c shows the increase in moment of inertia as the boom is extended with respect to time.

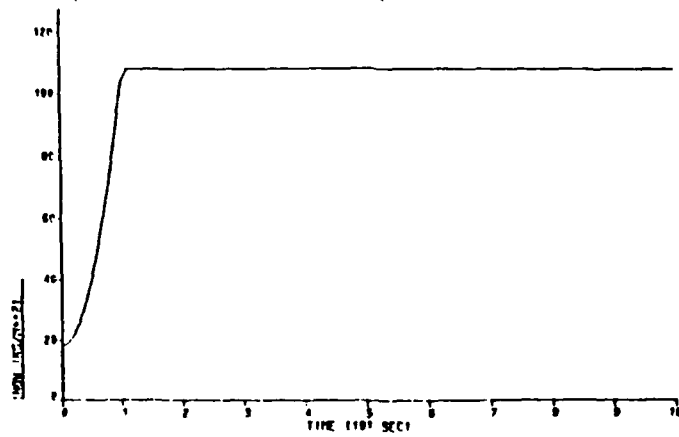
When an initial tumbling rate is higher than the rate that can be captured solely through the extension of the boom, magnetic torquing may aid in gravity gradient capture. By creating torque in the direction opposite to that of the angular velocity, magnetic torquing can be used to slow the rate of the tumbling vehicle.



(A)



(B)



(C)

Figure 63. Gravity gradient capture by extension of boom

V. CHAPTER 5

A. CONCLUSIONS

1. Gravity gradient stabilization (only)

Gravity gradient stabilization alone is not a viable attitude control method for ORION. This is due to gravity gradient effect providing little yaw restoring torque. In addition, gravity gradient stabilization provides little dampening effect on the roll and pitch axes. When augmented by other control schemes, gravity gradient stabilization provides sufficient passive restoring torque to warrant its use.

2. Gravity gradient with 3 reaction wheels

a. *Advantages*

Gravity gradient stabilization augmented by three reaction wheels, each aligned along the body's axes, provides excellent attitude control results both in time response and accuracy.

b. *Disadvantages*

Power consumption may be prohibitively high for this method. At steady state, each reaction may use up to 6 watts while drawing considerably more during the acceleration or deceleration phase. If a steady state drain of 18 watts (6 for each reaction wheel) is acceptable, then this method should be considered. The projected end-of-life power budget for ORION is 60 watts [Ref. 1, p. 132]. Using this figure as an estimate, a steady state draw of 18 watts leaves 42 watts available for mission support. From Figure 3 on page 3, an average of 34 watts is required for mission support. The size and weight of three reaction wheels may be prohibitively high as well. Another disadvantage is that thrusters must be used to remove momentum when the reaction wheel(s) become saturated.

3. Control moment gyro (CMG)

a. *Advantages*

Although not discussed in detail, control moment gyros are capable of generating large restoring torques.

b. *Disadvantages*

The weight requirements for a control moment gyro are prohibitively high when compared to reaction wheels when relatively small torques are involved. As a small

multi-purpose satellite, ORION does not need the magnitude of restoring torque necessary to warrant the use of control moment gyros.

4. Gravity gradient with three magnetic torquers

a. Advantages

Three orthogonally oriented magnetic torquers have the advantage of generating restoring torque in almost any direction based on vector addition. In this manner, the corrective torque may be produced to counter any disturbance from any direction as long as it is small enough not to tumble the vehicle. Another advantage for magnetic torquing is that the torquers only draw power while providing restoring torque. This amounts to a considerable power savings when compared to the reaction wheel. The power drawn by the magnetic torquers during operations is based on the amperes used. This allows for flexibility of design since doubling the number of turns and halving the current drawn still provides the same magnitude of the magnetic moment.

b. Disadvantages

Magnetic torquers are altitude dependent. The magnitude of the earth's magnetic field is a function of $\frac{1}{R^3}$. At high altitudes, magnetic torquing is not effective. In addition, magnetic torquing is not always available in all directions. Recalling that magnetic torque is $T_{mag} = M \times B$, magnetic torque may not be generated in the direction of the B field due to vector cross product relationships. Due to the continuously changing B field with respect to the satellite, this is a minor disadvantage. The desired restoring torque can soon be generated as soon as the B field direction changes.

5. Thrusters

a. Advantages

At high altitudes, thrusters and momentum exchange devices are the only control methods available for accurate stabilization. In addition, thrusters are the most effective method for stabilizing a vehicle with a high tumbling rate.

b. Disadvantages

Thrusters are necessary for satellites; however, any fuel used for attitude control or momentum removal is less fuel available for orbit transfer and maintainance. For a small, lightweight satellite with limited fuel storage capacity, fuel resources must be economized.

6. Overview

In the final analysis, the attitude control system employed will be based on specific mission requirements. Only when the ORION mission is known can proper

weights be given to each of the attitude control system design factors, most noticeably, power consumption, pointing accuracy, altitude, and desired lifetime.

APPENDIX GRADIENT STABILIZATION PROGRAM

TITLE 3 AXIS STABILIZATION WITH GRAVITY GRADIENT EFFECT

* DEFINITION OF TERMS

*

* ALT=ALTITUDE OF SATELLITE (METERS)

* R1=RADIUS OF EARTH (METERS)

* R=RADIUS OF EARTH + SATELLITE ALT (METERS)

* RO=DENSITY OF AIR AT THE ORBITAL ALTITUDE

* W0=ANGULAR RATE OF SATELLITE WITH RESPECT TO EARTH

* D=DRAG FORCE=1.7E+14*(RO/R)

* PSI,THETA,PHI ARE ANGLES ABOUT THE X,Y,Z, AXES (RADIAN)

* PSIC,THETAC,PHIC ARE ANGLES ABOUT THE X,Y,Z AXES (DEGREES)

* PSID,TD,PHID ARE ANGULAR VELOCITIES ABOUT THE X,Y,Z AXES (RADS/SEC)

* (B1),B(2),B(3) ARE THE ANGULAR ACCELERATION ABOUT THE

* X,Y,Z AXES (RADS/SEC**2)

* IX,IY,IZ ARE THE MOMENTS OF INERTIA ABOUT THE X,Y,Z AXES (KG-M**2)

* TX,TY,TZ ARE THE SUMMATION OF THE DISTURBANCE TORQUES AND

* RESTORING TORQUES EXCLUDING GRAVITY GRADIENT EFFECTS

* TMX,TMY,TMZ ARE MAGNETIC TORQUES ABOUT THE X,Y,Z AXES

* TRWX,TRWY,TRWZ ARE REACTION WHEEL TORQUES ABOUT THE X,Y,Z AXES

* TSX,TSY,TSZ ARE SOLAR PRESSURE TORQUES ABOUT THE X,Y,Z AXES

* TAX,TAY,TAZ ARE AERODYNAMIC TORQUES ABOUT THE X,Y,Z AXES

* LX,LY,LZ IS THE DISTANCE BETWEEN THE CENTER OF PRESSURE AND

* CENTER OF MASS (M)

* MX,MY,MZ=SPACECRAFT'S GENERATED MAGNETIC MOMENT WITH RESPECT TO

* THE X,Y,Z AXES (WB-M) M=NIA WHERE M=MAGNETIC MOMENT,

* N=# OF TURNS, I=CURRENT (AMPS), AND A=AREA (M**2). FOR

* THE MAXIMUM VALUE OF M=9.0427, N=400, I=.5A, RADIUS=.12M.

* MG=STRENGTH OF EARTH'S MAGNETIC DIPOLE=8.0E15 WB-M AT R=0

* BX,BY,BZ=EARTH'S MAG FIELD WITH RESPECT TO X,Y,Z(WB/M**2)

* LAMS=RIGHT ASCENSION FROM GREENWICH @ TIME=0, IN DEGREES(LONGITUDE)

ARRAY B(3)

CONST ALT=1000E+03,RO=7.0E-10,R1=6378.E+03,...

IX=95., IY=98., IZ=03.00, LAMS0=0,...

MX=9.0478, MY=9.0427, MZ=9.0427, MG=8.0E+15,...

KX=2., KY=2., KZ=1., TAU1=1., TAU2=1., TAU3=1.,...

TSX=0., TSY=0., TSZ=0., TAX=0., TAY=0., TAZ=0.

*

* PHI,THETA,AND PSI ARE INIT 5 DEGREES = .08725 RADIAN OF ERROR*

INCON ITHETA=.08725,IPHI=.08725,IPSI=.08725,ILAMS=0,PHIC=5.,...

THETAC=5.,PSIC=5.

*

DERIVATIVE

R=R1+ALT

D=1.7E+14*(RO/R)

```

      W0=SQRT(3.987E+14/(R**3))

NOSORT      LAMS=LAMS0+W0*TIME*(57.3)
10      IF (LAMS.GE.360) THEN
      LAMS=LAMS-360.
      GO TO 10
      ENDIF

*
*
*****
* THIS SECTION ADDS THE REACTION WHEEL EQUATIONS *
*****
*      TRWX=-KX*(TAU1*PHID + PHI)
*      TRWY=-KY*(TAU2*TD + THETA)
*      TRWZ=-KZ*(TAU3*PSID + PSI)
*****END REACTION WHEEL*****
*****
* THIS SECTION ADDS THE MAGNETIC TORQUE EQUATIONS *
* AND SOLVES AN EXAMPLE FOR THE EARTH'S MAGNETIC *
* FIELD (EQUATORIAL ORBIT ASSUMED) *
*****
      BX=(MG/(R**3))*SIN(.2042)*SIN(((LAMS*PI)/180)-5.0789)
      BY=-(MG/(R**3))*COS(.2042)
      BZ=-(MG/(R**3))*SIN(.2042)*COS(((LAMS*PI)/180)-5.0789)

*
      TMAGX=(MZ*BY)-(MY*BZ)
      TMAGY=(MX*BZ)-(MZ*BX)
      TMAGZ=(MY*BX)-(MX*BY)

*****
* CONDITIONS FOR TORQUE GENERATION MET?
*****
      IF(PHIC.GT..5) THEN
      IF(PHID.GT.0) THEN
      TMX=-(ABS(TMAGX))
      ELSE
      TMX=0
      ENDIF
      ENDIF
      IF(PHIC.LT.-.5) THEN
      IF(PHID.LT.0) THEN
      TMX=ABS(TMAGX)
      ELSE
      TMX=0
      ENDIF
      ENDIF
      IF(THETAC.GT..5) THEN
      IF(TD.GT.0) THEN
      TMY=-(ABS(TMAGY))
      ELSE
      TMY=0
      ENDIF
      ENDIF
      IF(THETAC.LT.-.5) THEN

```

```

        IF(TD.LT.0) THEN
          TMY=ABS(TMAGY)
        ELSE
          TMY=0
        ENDIF
      ENDIF
    IF(PSIC.GT..5) THEN
      IF(PSID.GT.0) THEN
        TMZ=-(ABS(TMAGZ))
      ELSE
        TMZ=0
      ENDIF
    ENDIF
    IF(PSIC.LT.-.5) THEN
      IF(PSID.LT.0) THEN
        TMZ=ABS(TMAGZ)
      ELSE
        TMZ=0
      ENDIF
    ENDIF
    IF(PSID.LT.0) THEN
      TMZ=ABS(TMAGZ)
    ELSE
      TMZ=0
    ENDIF
  ENDIF
  IF(PSID.LT.0) THEN
    TMZ=ABS(TMAGZ)
  ELSE
    TMZ=0
  ENDIF
ENDIF
*****END MAGNETIC TORQING SECTION*****

TX=TMX+TRWX+TSX+TAX
TY=TMY+TRWY+TSY+TAY
TZ=TMZ+TRWZ+TSZ+TAZ

*****FOR GRAVITY GRADIENT EFFECT ONLY SET TX=TY=TZ=0*****

B(1)=-4*(W0**2)*((IY-IX)/IZ)*PHI+W0*((IX+IZ-IY)/IX)*PSID+(TX/IX)
B(2)=-3*(W0**2)*((IX-IZ)/IY)*THETA+TY/IY
B(3)=- (W0**2)*((IY-IX)/IZ)*PSI-W0*((IX+IZ-IY)/IZ)*PHID+(TZ/IZ)
*
*
PHID=INTGRL(0.,B(1))
TD=INTGRL(0.,B(2))
PSID=INTGRL(0.,B(3))
*
*
CPHI=INTGRL(0.,PHID)
CTHETA=INTGRL(0.,TD)
CPSI=INTGRL(0.,PSID)
*
PHI=IPHI+CPHI
THETA=ITHETA+CTHETA
PSI=IPSI+CPSI
*****
*PHI,THETA,PSI ARE = TO INITIAL CONDITIONS AS ANNOTATED WITH AN "I"
*PRECEDING VARIABLE+CALCULATED VALUES AS ANNOTATED WITH THE "C" IN FRONT
*****
*
PHIC=PHI*57.3
THETAC=THETA*57.3
PSIC=PSI*57.3
*
*****
* USE FOLLOWING IF GRAVITY GRADIENT EFFECT ONLY
*
```

```

*****
*ONTRL FINTIM=20000,DELT=200.
*RINT 200., PHIC, THETAC, PSIC, PHIDC, TDC, PSIDC
*AVE 200., PHIC, THETAC, PSIC, PHIDC, TDC, PSIDC
*RAPH (G1,DE=TEK618) TIME(UN=SEC),PHIC(UN=DEGREES)
*ABEL (G1,DE=TEK618) PHI(DEG) VS TIME (GG@1000K) IX=95 IY=98 IZ=3.00
*RAPH (G2,DE=TEK618) TIME(UN=SEC),THETAC(UN=DEGREES)
*ABEL (G2,DE=TEK618) THETA(DEG) VS TIME (GG@1000K) IX=95 IY=98 IZ=3.00
*RAPH (G3,DE=TEK618) TIME(UN=SEC),PSIC(UN=DEGREES)
*ABEL (G3,DE=TEK618) PSI(DEG) VS TIME (GG@1000K) IX=95 IY=98 IZ=3.00
*RAPH (G4,DE=TEK618) TIME(UN=SEC),PHIDC(UN='DEG/SEC')
*ABEL (G4,DE=TEK618) PHID VS TIME (GG@1000K) IX=95 IY=98 IZ=3.00
*RAPH (G5,DE=TEK618) TIME(UN=SEC),TDC(UN='DEG/SEC')
*ABEL (G5,DE=TEK618) TDC VS TIME (GG@1000K) IX=95 IY=98 IZ=3.00
*RAPH (G6,DE=TEK618) TIME(UN=SEC),PSIDC(UN='DEG/SEC')
*ABEL (G6,DE=TEK618) PSIDC VS TIME (GG@1000K) IX=95 IY=98 IZ=3.00
*****END GRAVITY GRADIENT ONLY GRAPHS *****
*
*****
* USE THE FOLLOWING IF REACTION WHEELS ARE USED *
*****
*ONTRL FINTIM=400,DELT=5.
*RINT 100., PHIC, THETAC, PSIC, TX, TY, TZ
*AVE 5., PHIC, THETAC, PSIC, TX, TY, TZ, PHID, TD, PSID
*RAPH (G1,DE=TEK618) TIME(UN=SEC),PHIC(UN=DEGREES)
*ABEL (G1,DE=TEK618) PHI(DEG) VS TIME (GG@1000K) IX=95 IY=98 IZ=3.00
*RAPH (G2,DE=TEK618) TIME(UN=SEC),THETAC(UN=DEGREES)
*ABEL (G2,DE=TEK618) THETA(DEG) VS TIME (GG@1000K) IX=95 IY=98 IZ=3.00
*RAPH (G3,DE=TEK618) TIME(UN=SEC),PSIC(UN=DEGREES)
*ABEL (G3,DE=TEK618) PSI(DEG) VS TIME (GG@1000K) IX=95 IY=98 IZ=3.00
*RAPH (G4,DE=TEK618) TIME(UN=SEC),TX(UN=NM)
*ABEL (G4,DE=TEK618) TXRW VS TIME (GG@1000K) IX=95 IY=98 IZ=3.00
*RAPH (G5,DE=TEK618) TIME(UN=SEC),TY(UN=NM)
*ABEL (G5,DE=TEK618) TYRW VS TIME (GG@1000K) IX=95 IY=98 IZ=3.00
*RAPH (G6,DE=TEK618) TIME(UN=SEC),TZ(UN=NM)
*ABEL (G6,DE=TEK618) TZRW VS TIME (GG@1000K) IX=95 IY=98 IZ=3.00
*RAPH (G7,DE=TEK618) TIME(UN=SEC),PHID(UN='RAD/SEC')
*ABEL (G7,DE=TEK618) PHID VS TIME (GG@1000K) IX=95 IY=98 IZ=3.00
*RAPH (G8,DE=TEK618) TIME(UN=SEC),TD(UN='RAD/SEC')
*ABEL (G8,DE=TEK618) TD VS TIME (GG@1000K) IX=95 IY=98 IZ=3.00
*RAPH (G9,DE=TEK618) TIME(UN=SEC),PSID(UN='RAD/SEC')
*ABEL (G9,DE=TEK618) PSID VS TIME (GG@1000K) IX=95 IY=98 IZ=3.00
*****END REACTION WHEEL GRAPHS*****
*
*****
* USE FOLLOWING GRAPHS IF MAGNETIC TORQUING IS UTILIZED *
*****
*ONTRL FINTIM=4000.,DELT=5.
*RINT 100., PHIC, THETAC, PSIC, W0,B(1),B(2),B(3),LAMS
*AVE 5., PHIC, THETAC, PSIC, LAMS, TX,TY,TZ,BX,BY,BZ,PHID,TD,PSID
*RAPH (G1,DE=TEK618) TIME(UN=SEC),PHIC(UN=DEGREES)
*ABEL (G1,DE=TEK618) PHI(DEG) VS TIME (GG@1000K) IX=95 IY=98 IZ=3.00
*RAPH (G2,DE=TEK618) TIME(UN=SEC),THETAC(UN=DEGREES)
*ABEL (G2,DE=TEK618) THETA(DEG) VS TIME (GG@1000K) IX=95 IY=98 IZ=3.00
*RAPH (G3,DE=TEK618) TIME(UN=SEC),PSIC(UN=DEGREES)
*ABEL (G3,DE=TEK618) PSI(DEG) VS TIME (GG@1000K) IX=95 IY=98 IZ=3.00

```

```

*RAPH (G4,DE=TEK618) TIME(UN=SEC),LAMS(UN=DEGREES)
*ABEL (G4,DE=TEK618) LAMS(DEG) VS TIME (GG@1000K) IX=95 IY=98 IZ=3.00
*RAPH (G5,DE=TEK618) TIME(UN=SEC),TX(UN=N-M)
*ABEL (G5,DE=TEK618) TX VS TIME (GG@1000K)
*RAPH (G6,DE=TEK618) TIME(UN=SEC),TY(UN=N-M)
*ABEL (G6,DE=TEK618) TY VS TIME (GG@1000K)
*RAPH (G7,DE=TEK618) TIME(UN=SEC),TZ(UN=N-M)
*ABEL (G7,DE=TEK618) TZ VS TIME (GG@1000K)
*RAPH (G8,DE=TEK618) TIME(UN=SEC),BX(UN=W-M)
*ABEL (G8,DE=TEK618) BX VS TIME (GG@1000K)
*RAPH (G9,DE=TEK618) TIME(UN=SEC),BY(UN=W-M)
*ABEL (G9,DE=TEK618) BY VS TIME (GG@1000K)
*RAPH (G10,DE=TEK618) TIME(UN=SEC),BZ(UN=W-M)
*ABEL (G10,DE=TEK618) BZ VS TIME (GG@1000K)
*RAPH (G11,DE=TEK618) TIME(UN=SEC),PHID(UN='RAD/SEC')
*ABEL (G11,DE=TEK618) PHID(RADSEC) VS TIME (GG@1000K) IX=95 IY=98 IZ=3.00
*RAPH (G12,DE=TEK618) TIME(UN=SEC),TD(UN='RAD/SEC')
*ABEL (G12,DE=TEK618) TD(RADSEC) VS TIME (GG@1000K) IX=95 IY=98 IZ=3.00
*RAPH (G13,DE=TEK618) TIME(UN=SEC),PSID(UN='RAD/SEC')
*ABEL (G13,DE=TEK618) PSID(RADSEC) VS TIME (GG@1000K) IX=95 IY=98 IZ=3.00
END
STOP

```


LIST OF REFERENCES

1. Boyd, Austin W., *Design Considerations for the ORION Satellite: Structure, Propulsion, and Attitude Control Subsystems for a Small, General Purpose Spacecraft*, Master's Thesis, Naval Postgraduate School, Monterey, California, March 1988.
2. Dee, Suzanne M., *Design of a Three-Axis Stabilized ORION Satellite Using an All-Thruster Control System*, Master's Thesis, Naval Postgraduate School, Monterey, California, December 1988.
3. *Gravity Gradient Stabilization Principles*, TRW Space Technology Laboratories, 1965.
4. Wertz, James R., *Spacecraft Attitude Determination and Control*, Reidel Publishing Company, Dordrecht, Holland, 1986.
5. Ickes, B. P., *A New Method for Performing Digital Control System Attitude Computations Using Quaternions*, AIAA Journal, vol.8, n.1, pp. 13-17, January 1970.
6. Agrawal, Brij N., *Design of Geosynchronous Spacecraft*, Prentice-Hall, Inc., Englewood Cliffs, New Jersey, 1986.
7. Thomson, W. T., *Introduction to Space Dynamics*, John Wiley and Sons, New York, 1961.
8. Greensite, Arther L., *Analysis and Design of Space Vehicle Flight Control Systems*, Spartan Books, New York, 1970.
9. Siahpush, Ali, *A Study for Semi-Passive Gravity Gradient Stabilization of Small Satellites*, Utah State University Conference on Small Satellites, October 7-9, 1987.
10. Kaplan, Marshall H., *Modern Spacecraft Dynamics and Design*, John Wiley and Sons, Inc., New York, 1976.

VIII. INITIAL DISTRIBUTION LIST

	No. Copies
1. Defense Technical Information Center Cameron Station Alexandria, VA 22304-6145	2
2. Library, Code 0142 Naval Postgraduate School Monterey, CA 93943-5002	2
3. Dr. H. A. Titus Code 62Ts Dept. of Electrical & Computer Engineering Naval Postgraduate School Monterey, CA 93943-5002	2
4. Professor J. B. Burl Code 62BI Dept. of Electrical & Computer Engineering Naval Postgraduate School Monterey, CA 93943-5000	1
5. Chairman, Dept. of Electrical & Computer Engineering Code 62 Naval Postgraduate School Monterey, CA 93943-5000	1
6. Navy Space Command Code N3 Dahlgren, VA 22448	1
7. Director, Navy Space Systems Division Chief of Naval Operations OP-943 Washington, DC 20305-2006	1
8. LT F. W. Boyd 1172 El Alameda Palm Springs, CA 92262	2